Western Australian School of Mines

Minerals, Energy and Chemical Engineering

Water Treatment Methods for Mineral Processing Operations

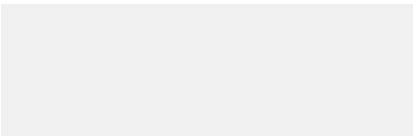**Hugo Alejandro Guerra Rodriguez**

0000-0003-1465-039X

This thesis is presented for the Degree of

Master of Philosophy (Mining and Metallurgy)

of

Curtin University

August 2023

DECLARATION

To the best of my knowledge and belief this thesis contains no material previously published by any other person except where due acknowledgment has been made.

This thesis contains no material which has been accepted for the award of any other degree or diploma in any university.

Signature: …   ….

11/08/2023

Date: ………………………...

ACKNOWLEDGEMENTS

TABLE OF CONTENTS

LIST OF FIGURES

LIST OF TABLES

THESIS RELATED PUBLICATIONS

Conference paper

Guerra, H., Tadesse, B., Albijanic, B., Dyer, L. (2022). Title Fit-for-purpose water treatment methods for. mineral processing operations. *IMPC Asia Pacific, Conference proceedings*, (pp. 1468-1474). 22-24 of August 2022. Melbourne Australia

Journal paper

Guerra, H., Tadesse, B., Albijanic, B., Dyer, L. (2023). Nanofiltration for treatment of Western Australian bore water for mineral processing operations: A pilot scale study. *Journal of water process Engineering*, 52, 103484. https://doi.org/10.1016/j.jwpe.2023.103484

Guerra, H., Tadesse, B., Albijanic, B., Dyer, L. (2023). A comparative study of nanofiltration and electrodialysis for treatment of bore water in mineral processing operations. *Journal of Environmental Chemical Engineering* (Manuscript on peer review)

Guerra, H., Tadesse, B., Albijanic, B., Dyer, L.(2023). The ultra-high lime aluminium process as potential method to treat bore water for mineral processing operations. (*Manuscript on review)*

ABSTRACT

Limited freshwater availability, increasing competition for water among multiple users, cost of purification, corporate sustainability goals, etc., are the main factors driving the minerals industry to focus on water quality and usage. Increasing water re-use and accessing alternative sources to freshwater for mineral processing, particularly in flotation, are potential strategies being implemented to improve water efficiency. In flotation, good water quality is needed to develop an appropriate reagent scheme and optimise operating conditions to maximise performance. High concentrations of dissolved ions in groundwater, seawater, or recycled water may alter the water structure, particle surface wettability, and colloidal interactions between bubbles and particles, negatively affecting mineral flotation. Currently, several treatment options involve physical, electro, and chemical processes that remove salts through a membrane or an ion exchange resin inducted by a specific current or precipitation of the ions as an insoluble salt. Membrane separation methods such as reverse osmosis (RO) have been implemented in several processes because this method provides rates high ion rejection. Many mineral processing operations do not require ultra-high-quality water; thus, reverse osmosis becomes an overvalued and expensive option. Nanofiltration, electrodialysis and precipitation are options that under the proper membrane selection and specific conditions can provide suitable water quality for different mineral processing operations by removing divalent ions and a portion of monovalent ions at lower cost implications than reverse osmosis due to use of lower transmembrane pressures or selective use of energy.

The present study aims to address and review water treatment options that produce suitable water for flotation and other unit operations in mineral processing fixing a threshold limit of 50 ppm of divalent ions and 500 ppm of monovalent ions. The approach of the project was to use technologies such as nanofiltration, electrodialysis and precipitation to achieve water quality below the threshold. Additionally, understanding on the mechanisms by which each of the three methods studied (nanofiltration, electrodialysis, and precipitation) reject ions from the feed and investigating the economic aspect involved in each process.

13

In this study, the nanofiltration membranes used could reject more than 95% of divalent cations (Ca^{2+}, Mg^{2+}, and SO_4^{2-}) and more than 74% of monovalent ions (Na^+ and Cl^-) under the conditions of 12 bar of transmembrane pressure and 65% of the recovery. These rejection rates were found to be sufficient to produce fit-for-purpose water for mineral processing. In addition, the effect of pressure on the mass transfer mechanism of each membrane was determined. The results indicate that precipitation through the ultra-high aluminium method can reduce more than 97% of divalent ions such as calcium, magnesium, and sulphate and 68% chloride when a molar ratio Ca/anion of 1:1 and molar ratio of Al/anions of 3:1 was utilised. In addition, due to improvement in reagent selectivity, chloride removal could be improved by 22% by implementing a two stages process reducing reagent consumption. The main crystal phase identified by XRD in the precipitates from the second stage was hydrocalumite ($Ca_4Al_2(OH)_{12}(Cl)_2 \cdot 4H_2O$), bayerite ($Al(OH)_3$) and calcite ($CaCO_3$). In addition, operational conditions such as pH and temperature affect chloride removal positively. However, at temperatures over 40 ºC this effect is reversed due to the stability of calcium chloroaluminate compounds at high temperatures. From the electrodialysis experiments, was observed that increasing the flow velocity reduces the efficiency of the system by up to 8%. Additionally, higher flow rates increase the current density decreasing the cell performance. The optimum operating conditions at the flow rate recommended by the manufacturer of 45 L/h is an applied voltage of 1 V per membrane pair where the process can be easily controlled in large-scale operations. At these specific conditions (1V per membrane pair and 45 L/h) and 40 minutes of treatment the removal of ions achieved was more than 90%, 98% and 87% of monovalent ions (Na^+ and Cl^-), divalent ions (Ca^{2+}, Mg^{2+}, and SO_4^{2-}), and TDS respectively.

The study shows that nanofiltration and electrodialysis are efficient methods to achieve the quality of water required without exceeding the salinity threshold required for critical minerals processing by flotation. From the economic point of view, electrodialysis is the preferred option due to its low energy consumption and the relatively low replacement cost associated with a high membrane lifetime. These results would contribute towards further

consideration of the technologies studied in this study in process where certain quality of water is required, and reverse osmosis is an overestimated option.

1 CHAPTER ONE: INTRODUCTION

1.1 Background

The mineral processing sector consumes a considerable amount of water; for instance, processes that do not reuse water utilise between 1.9 to 3m^3 of water per ton of ore processed (Bulut and Yenial, 2016). Water is used in a wide range of mining activities, and due to the environmental preoccupation and the lack of water, the industry has become aware of its responsibilities. It is constantly evaluating the best way to use water. The search for improvements in conservation and reuse increases the recycling and the use of lower quality water, such as groundwater or seawater, that usually contains high concentrations of ions and salts. At the same time, processes tend to be in areas where the demand of different industrial sectors are competing with the use of domestic water, or in areas where the access to high quality water is scarce or expensive for the operation due to the transportation costs (Di Feo et al., 2021).

Several mine sites in Australia have introduced saline water in their mineral processing practice. Base metal sulphide flotation plants at Mt Keith, Leinster, and the Kambalda Nickel Concentrator in Western Australia use bore water with high ionic strength. Saline water is used at KCGM and Kanowna Belle for sulphide (gold ore) flotation. Saline or seawater is also used in many other flotation plants worldwide, including copper plants in Chile, gold-rich copper ore processing plants in Indonesia, and base metal sulphides flotation in South Africa. In some cases (e.g., Kanowna Belle gold mine), the salinity of the water used in flotation can reach up to 200,000 mg/L, which is several times higher than that of seawater (Wang and Peng, 2014).

As discussed previously, water is usually a significant concern in the mining industry in Australia and worldwide in general. It is becoming more relevant to find water treatment methods suitable for each operation financially viable considering the vast amount used in mineral processing operations. Currently, there are several treatment options involving physical, electro, and chemical processes that remove salts through a membrane or an ion exchange resin inducted by a specific current or precipitation of the ions as an insoluble salt.

Membrane separation methods such as reverse osmosis have been implemented in several processes because this method provides rates of removal of dissolved species as high as 98% (Wang et al., 2019). However, in many mineral processing water with ultra-high quality is not required, then, reverse osmosis becomes an overvalued option. Additionally, waters rich in sulphate (>700mg/L) and calcium (>100 mg/L) are not recommended in this process because of the high scaling potential of $CaSO_4$ and all the expenses associated with the frequent membrane replacement (Bowell and Parshley, 2000). Furthermore, reverse osmosis is an energy-intensive process, which accounts for around 44% of its operational cost. In countries like Australia where the energy cost has a fundamental role in the industry, it becomes an appreciable portion of the processing expenses (Bajpayee et al., 2011). On the other side, nanofiltration is an option that under the right membrane selection can provide suitable quality of water for mineral processing operations removing divalent ions and to some extent monovalent ions with less cost associated because this process uses lower transmembrane pressures as compared with reverse osmosis (Deepti et al., 2020).

Water treatment processes that eliminate the need of high pressures for desalination have been used through the years as an economical alternative. For instance, one of the most studied methods within the electro-driven category is electrodialysis, which is a technology that uses electric field to mobilize ions dissolved in solution through cation and anion exchange membranes (Patel et al., 2020). Kabay and co-workers (2002) used electrodialysis to remove divalent cations and monovalent cations with an applied current of 10V achieving more than 90% of ion removal. One of the main advantages of this technology in comparison with reverse osmosis is lower capital cost and higher energy efficiency as the grade of desalination can be adjusted according to the voltage applied making the separation more selective. However, reverse osmosis offers superior performance and less energy consumption when the feed salinity exceeds 10000 mg/L becoming the preferred technology for purification of seawater (Patel et al., 2020 and Generous et al., 2021).

17

Davidson and co-workers (1960) investigated the desalination of water with low salinity up to 5000 mg/L using a membrane-free technique of solvent extraction with amines. Boo et al. (2020), using the same technology studied an innovative technique called temperature swing solvent extraction (TSSE) which utilise low-polarity solvents as selective water extractor at low temperatures while ionic species are precipitated from ultra-high salinity solutions (292 g/L) with the advantages that the solvent could be recovered at relatively low temperatures (80ºC)

Precipitation is one of the oldest conventional methods which has been considered in many operations for its effective performance-cost ratio. For instance, Cruz et al. (2020), suggested a partial seawater desalination to remove calcium and magnesium ions to improve chalcopyrite floatability by the precipitation of carbonates promoted by the addition of sodium hydroxide in an atmosphere rich with carbon dioxide. Jeldres et al. (2017), in their research, used a mixture of lime and sodium hydroxide as pre-treatment of seawater to reduce the effect of calcium and magnesium ions in the flotation of copper-molybdenum sulphide ores. Different compounds have been studied in the process of salts precipitation, among which, oxalic acid, soda ash, aluminium compounds, and phenoxy acetic acids have been extensively studied with high precipitation efficiencies (Wang et al., 2019).

The use of desalinated water in some specific operations where a certain quality of water is required is fundamental to avoid detrimental conditions of recovery. To address this problem, having in mind the maximum concentration of ions where the flotation of minerals is affected, partial desalination treatments for reduction of problematic ionic species like calcium, magnesium, sodium, and chloride, is being considered as a promising solution instead of using fully desalinated water from a reverse osmosis treatment plant. In this study techniques such as precipitation, electrodialysis, and nanofiltration were considered to find the optimum process that provides reasonable balance between economics and plant performance.

1.2 Aim and objectives of the research.

The aim of this study was to conduct a series of experiments to assess different technologies such as nanofiltration, electrodialysis and precipitation to treat bore water with a high concentration of dissolved salts that usually have a detrimental effect on some mineral processing operations.

The objectives of this study are.

- Identify water treatment options that produce suitable water for flotation and other unit operations.
- Evaluate different chemical compounds as precipitants of dissolved salts in bore water of the Laverton region in Western Australia.
- Determine key parameters to produce water suitable for mineral processing operations from technologies such as nanofiltration and electrodialysis.
- Compare different technologies as alternatives to reverse osmosis in relation to operating cost, performance and ions removal.

1.3 Significance of the study

The need to purify water for mineral processing unit operations could cost mining companies millions of dollars annually. When it comes to removing large amounts of tiny ions like Na^+, Ca^{2+}, and Mg^{2+} using techniques like reverse osmosis, water treatment is extremely expensive. When thinking about expanding current operations, it becomes financially unviable due to the huge volume of processing water needed in processes like flotation. In many mineral processing operations across the world as well as in countries like Australia where freshwater resources are limited, the ability to use process water that has undergone minimum treatment would thus have considerable economic benefits.

1.4   Structure of the thesis

The body of this document consists of six chapters:

- The first chapter provides a short introduction to the study.
- The second chapter provides a literature review on the "state-of-the-art" of the studied domain. It also includes the quality of the water in Western Australia and a brief description of the effect of different qualities of water in some mineral processing operations. This is followed by a comprehensive review on each of the water treatments methods used in this work.
- The third chapter is dedicated to the description of the operating conditions of experiments carried out including a detailed description of the equipment used, reagents and the conditions of evaluation in each test.
- The fourth, fifth and sixth chapters are related to results and discussions of the findings of this work.

2 CHAPTER TWO: LITERATURE REVIEW

2.1 Resources and water availability

The Earth contains about 1,386 million cubic kilometres of water: The amount of water that our planet contains has not decreased or increased in the last 2 billion years (Kundzewicz, 2008). Water covers 71% of the surface of the earth's crust. About 96.5% of total water is concentrated in the oceans. Fresh water in glaciers, polar caps and underground deposits accounts for 3.46%; and 0.04% is distributed in lakes, soil moisture, atmosphere, reservoirs, rivers and living beings (Figure 1). Total rainfall on land is about 119,000 km3 per year (evaporated water that comes from the sea); of which 45,000 km3 are dumped back into the sea through rivers and the rest 74,000 km3 evaporate on land annually. Human consumption is nourished by this 0.04% of continental fresh water. And only 0.007% of the existing water on planet Earth is drinkable; an amount that is reduced every day due to the effect of pollution (Kundzewicz, 2008).

2.2 Water stress and water consumption worldwide

Currently 40% of the human population has problems of water scarcity, and it is estimated that by the year 2,025 this will affect 66% of the world population settled in countries of Africa and Western Asia. Of the 6,000 million people on the planet, more than 1,100 million of them lack direct access to drinking water sources, which is why they live in conditions of water stress. Human consumption of water in a developed territory of Europe is of the order of 150-200 litres per person per day; and 750-1,000 litres per person per day in the United States (USGS, 2019).
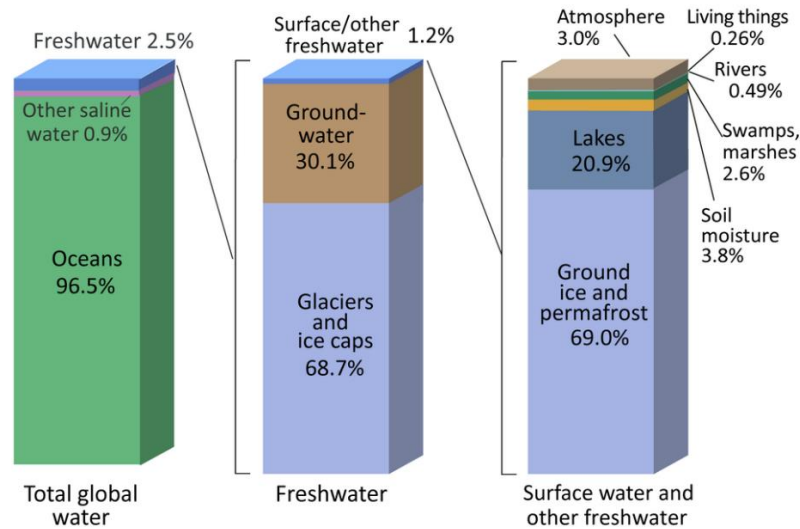
Figure 1 The distribution of water on, in and above the earth. (From: USGS, 2019)

In less developed regions, water consumption per person per day is less than 25 litres, due to its endemic scarcity in those regions. In 2025, about 2 billion people will live in regions of the planet where water scarcity will be absolute and water availability will be below 50 litres per inhabitant per day, the minimum amount of water that a person needs to lead a healthy and hygienic life. Human consumption of water is divided into domestic, industrial, and agricultural; and currently and in average terms, 65% goes to agriculture, 25% to industry and 10% to domestic use. By 2050, water consumption will have increased by 44% to meet industrial and domestic demands. Lack of clean water causes the death of 4,500 children per day, mostly in developing countries. And annually, 3.5 million people die due to diseases related to water quality. An estimated 98% of these deaths occur in developing countries (Kammeyer, 2017).

Although they will not face the alarming water stress that affects the Middle East, global superpowers such as the United States, China and India will have to face great problems due to the reduction of water, especially in some specific areas, such as the southwestern United States and the Chinese province of Ningxia. In South America, Chile is one of the countries in the most delicate situation and has gone from medium water stress in 2010 to being considered one of the places with extremely high stress in 2040, mainly due to

the rise in temperature and the changing behaviour of rainfall in that region. On the other hand, Spain and Greece are the nations that lead the ranking of European countries most affected by water stress, as well as their neighbouring countries in North Africa (Kammeyer, 2017 and UNESCO, 2016).

In Australia, ground water is one of the most appreciated water sources that supply almost 30% of the total water consumption to different sectors such as the agriculture industry, urban areas, and mining. However, the quality of groundwater around Australia changes dramatically depending on the area and rainfall levels. For example, around the southern coastal areas, due to the high levels of rainfall, the groundwater has low salinity and high quality. On the other hand, in the vast majority of the territory in the interior of the country the high temperatures and low levels of rainfall, lead to high water evaporation rates which generates percolating of high salinity water of up to 100g/L (Barnett et al., 2020)

Water is essential for life, communities, the environment, the economy and industrial activity. Given the scenario of water scarcity that we have been involved in in recent years, the competition for water continues to grow. The World Economic Forum recognizes a global water crisis and classifies it as one of the top three global risks. This situation can be reversed only if the necessary measures are taken for a more efficient management of water resources.

The supply of water is transcendental for the mining industry due to the number of processes that require water to function. Therefore, the impacts on the quality and quantity of water are one of the most controversial aspects of mining projects.

Not surprisingly, in this context, there is an unavoidable tension between the needs of the general population, who require water for survival and agriculture, and the needs of the mining industry. In this context of global water crisis, we see that Australia is no stranger. According to estimates by World Resources Institute in its water stress index (Reig and Schleifer, 2019), in relation to the countries with the highest risk of a water crisis, Australia ranks 50th, classified as medium-high risk. On the other hand, the increase in the population and the

growth of the most important industries in the country (agriculture and mining), imply a greater demand for water. For this reason, proper management of water resources in mining is essential for the sustainable development of the industry, and in line with the 2030 Sustainable Development Goals (SDG) of the United Nations Organization (UN) (UN, 2015), in particular in objective 6 of clean water and sanitation, and transversally with the other objectives, especially 3 (health and well-being) and 12 (sustainable production and consumption), and 14 (submarine life).

2.3   Quality of the water available for mining operations in Australia

The use of water in the mining industry in Australia represents only 4.4% of the water supply with an average consumption of 760 gigalitres of water per year (Australian Bureau of Statistics, 2016), However, as shown in Figure 2 many of the mining concessions and operations are located in areas where water scarcity and water salinity are limiting factors for regional development.

When analysing the water issue geographically, we see that Western Australia is one of the driest areas on the planet and where mining is concentrated, surface water resources are scarce and there is a growing demand for water by industrial users and, local communities. In this sense, it is important to highlight the effort made by mining companies to target other water sources such as seawater, in order to de-stress continental sources like freshwater for their operations (Prosser, Wolf and Littleboy, 2011).

There are multiple ion removal techniques that are utilized, depending on the amount of total dissolved solids present in the water. in desalination, the water is divided in two groups: brackish water and seawater. Usually, brackish water is characterised by concentrations of dissolved solids higher than potable water (1000 mg/L) and lower than sea water concentration (35000 mg/L). In some cases, water can be considered as hypersaline to refer to water with concentrations of total dissolved solids higher than the sea water. In table 1 the characterisation of the water used in different mine sites in Western Australia is shown and demonstrates the high proportion of mine site operating with TDS > 35000 mg/L which is the normal concentration of TDS in sea water (Tapley, 2017).

24

Table 1 Mining in Western Australia and hypersaline water

Site- Locality	pH	TDS mg/L	Cl mg/L	Ca mg/L	Mg mg/L	Na mg/L	Sulphate mg/L
Southern Cross	6.76	249,500	144,630	820	10,020	79,900	13,244
Norseman	7.3	280,000	130,000	780	9,100	82,000	18,000
Kalgoorlie- East	6.54	260,000	150,000	665	8,150	76,000	17,500
Kalgoorlie- East	6.4	124,000	143,400	584	7,940	78,100	-
Kalgoorlie- North East		88,000	69,000	101	7,210	36,300	-
Laverton- South	7.07	100,000	82,000	970	5,300	47,000	11,000
Laverton- South	7.4	230,000	130,000	840	5,000	78,000	15,000
Southern Cross	6.76	109,450	62,950	307	4,327	33,200	6,513
Kalgoorlie- South	5.9	104,600	58,700		4,300	34,800	6,100
Laverton- South		98,000	70,000	1,300	4,100	41,000	8,200
Wiluna- South East	7.6	42,528	65,518	739	4,073	35,610	12,563
Southern Cross	6.65	86,800	49,500	314	4,000	24,900	5,700
Menzies- West	7.72			3,000	4,000		800
Coolgardie	7.7	90,200	47,000	1,500	3,800	28,000	-
Southern Cross	6.9	83,200	48,000	254	3,800	24,600	5,400
Southern Cross	7.1	78,900	45,500	244	3,650	23,400	5,500
Southern Cross	6.6	73,100	41,000	239	3,550	20,900	4,950
Southern Cross	7.1	77,700	44,500	244	3,450	23,400	5,550
Kambalda	3.8	-	49,000	500	3,272		2,060
Kalgoorlie- North East	6.6	91,000	49,000	320	3,100	28,000	7,300
Southern Cross	4.5	70,000	37,000	300	3,000	19,000	4,900
Meekatharra- North West		39,300	23,000	510	2,600	14,100	
Coolgardie	-	66,300	36,750	635	2,570	20,300	1,900
Kalgoorlie- South East	5.85	57,950	11,800	475	2,490	25,000	4,365
Southern Cross	6.97	63,726	35,900	681	2,264	20,100	4,210
Coolgardie- West		47,000	30,000	210	2,100	17,000	
Southern Cross	7.2	37,000	19,000	610	1,900	7,100	2,400
Kalgoorlie- East	7.7	45,100	24,645		1,795	13,450	
Southern Cross	3.9	72,000	43,000	2,200	1,200	20,000	3,000
Southern Cross	5.6	51,000	28,000	1,300	1,200	15,000	1,500
Murchinson	8.3	24,000	-	150	850	7,000	2,900
Murchinson	8.5	6,200	2,900	98	240	1,900	730
Wiluna	7.7	4,525	1,600	143	215	945	985
Murchinson	7.8	4,500	1,800	285	138	1,300	
Meekatharra- North West		2,380	970	16	120	680	-
Wiluna- East	7.8	1,200	300	80	62	190	252
Wiluna- South West	7.69	740	170	102	40	59	120
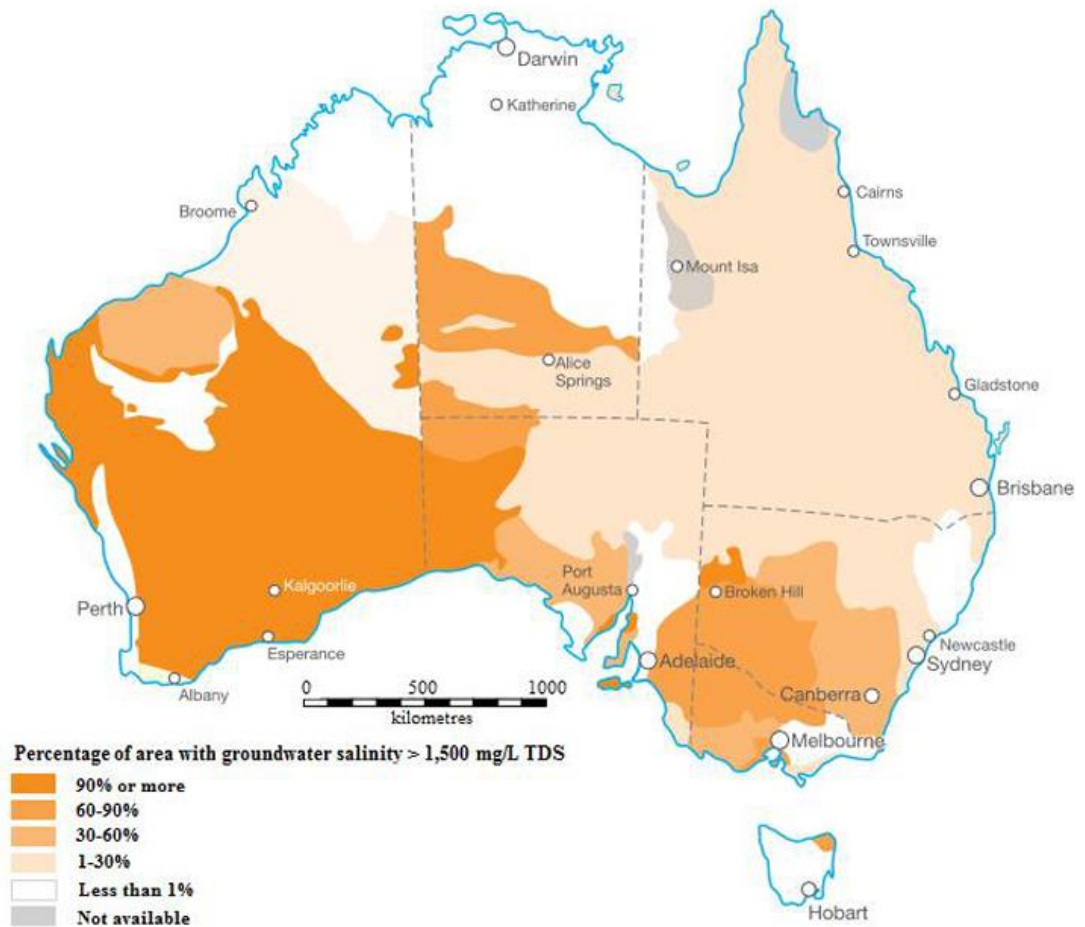
Figure 2 Water distribution in Australia with salinity >1500mg/L

2.4 Role of water in mineral processing operations

High concentrations of dissolved ions in groundwater, sea water or recycle water may alter the water structure, particle surface wettability and colloidal interactions between bubbles and particles, and therefore may have a positive or negative effect on mineral flotation.

Several of mine sites in Australia have introduced the use of saline water in their mineral processing practice. For example, base metal sulphide flotation plants at Mt Keith, Leinster and the Kambalda Nickel Concentrator in Western Australia use bore water with high ionic strength (Table 2). Saline water is used at Kalgoorlie Consolidate Gold mines and Kanowna Belle for sulphide (gold ore) flotation. Saline or sea water is also used in many other flotation plants worldwide including copper plants in Chile, gold-rich copper ore processing plants in Indonesia, and base metal sulphides flotation in South Africa. In some

26

cases (e.g., Kanowna Belle gold mine) the salinity of the water used in flotation can reach up to 200,000 ppm which is several times higher than that of sea water (Peng and Seaman, 2011 and Wang and Peng, 2014)

Table 2 Typical composition of bore water used at Mt Keith operation (mg/L). (From: Peng and Seaman, 2011)

Na^+	K^+	Ca^{2+}	Mg^{2+}	Cl^-	SO_4^{2-}
20,000	940	400	5100	32,000	23,000

Many Australian mine sites located around western Australia reduce the dependency on freshwater by increasing the recycling of water. For example, Mount Isa Mines has developed a project in which approximately 80% of the water used on site is recycled without suffering any negative effect on the performance of the operations and at the same time reducing the consumption of water across the mine operation by 50% of water (Grano et al., 1995).

However, one of the limiting characteristics of recycling water and the use of different sources of low water quality is the negative effect of dissolved ions in water on the performance of the mineral processing plants.

The effect of dissolved ions in water on flotation, seems to be related to the action of each ion to modify the structure of water molecules modifying the ability to adsorb collectors and frothers. Some of the ions that can produce negative effect on flotation are described as 'structure making', where these ions bond through hydrogen bonds to the water molecules avoiding the collector to reach the surface and be adsorbed (Ikumapayi et al., 2012 and Zhang et al., 2017).

Multiple studies have reported the effect of electrolytic species dissolved in water on the flotation processes (Wang and Peng, 2014). The quality of the water represents different impacts on the recovery of valuable minerals depending on the ore type and the physicochemical characteristics of the water. Generally, the flotation of copper sulphide minerals is positively impacted by the presence of high amounts of calcium and sulphate; For

example, in Chile multiple mine site use sea water to process copper sulphide minerals without the need of any water pre-treatment (Wang and Peng, 2014). However, in the case of lead-zinc sulphide minerals, such as galena the effect of high ions concentration seems to be dependent on the mineralogy of the ore, the chemical composition of the water and the process itself (Figure 3). There are mixed outcomes with some studies demonstrating enhancement in the recovery while other demonstrating suppression of recovery in flotation (Bulut and Yenial, 2016).
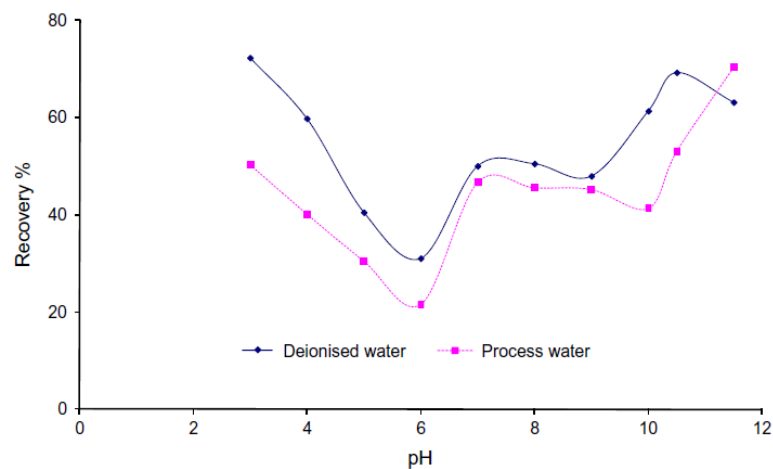
Figure 3 Effect of ions (process water) in galena flotation (From: Ikumapayi et al., 2012)

Flotation of phosphate minerals such as monazite, which is one of the primary sources for rare earth elements, is affected by divalent cations such as Ca^{2+} and Mg^{2+} charging the surface of the mineral positively and causing the increase in the consumption of reagents (Derhy et al., 2020). For example, Zhang et al. (2017) demonstrated that in the process of flotation of monazite with fatty acids as a collector, calcium ions present in the water from $CaOH^+$ which attach by hydrogen bonding at the surface of the monazite. The overall effect is decreasing the hydrophobicity of the monazite, hence reducing its recovery and grade as shown in Figure 4. Furthermore, salts and hardness in water are highly reactive, with fatty acids and form insoluble compounds resulting in loss of selectivity of the reagents, making froth flotation and tailing management challenging operations (Dos Santo et al., 2010 and Ozkan and Acar, 2004).

28
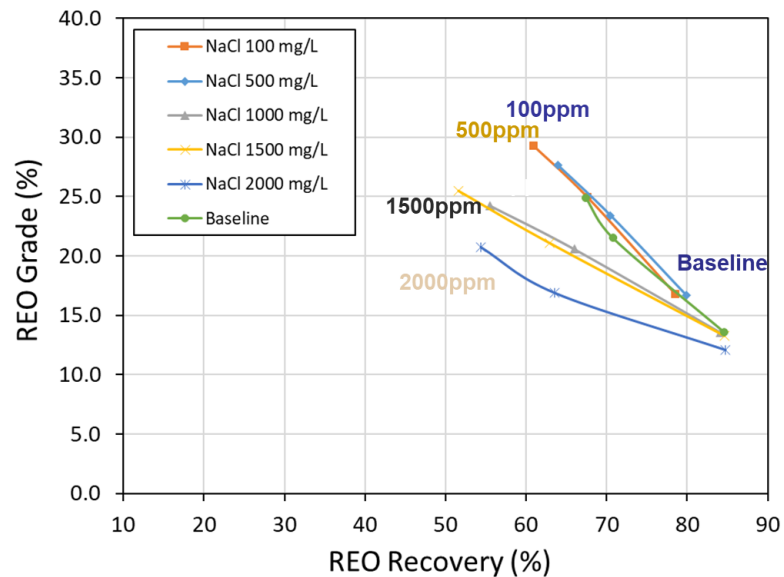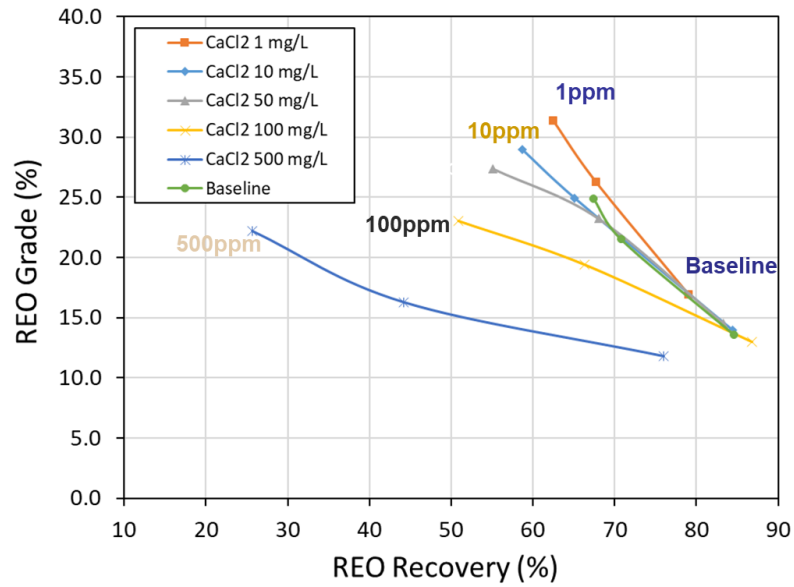
Figure 4 Effect of ions dissolved in water on monazite flotation (From: Tadesse et al., 2021)

Gold processing plants use different sources of water in their operations. However, in the Goldfields regions of Western Australia most of the mine sites use water with salinities of up to 200 g/L of total dissolved solids without significant impact on metal recovery (Wang and Peng, 2014). Improvement of quality of water can definitely be a potential opportunity to reduce some operating cost, reducing the consumption of key reagents for the gold extractions such as lime (used to increase the pH for the stabilization of

cyanide in solution). Consequently, a stable pH control will drive the process to subsequently consume less cyanide. A clear example of the operating cost reduction in leaching of gold was demonstrated by Tapley (2017) which indicates that using nanofiltration permeate in a gold leaching process it is possible to reduce lime and cyanide consumption by 80% and 20% respectively as shown in Figure 5.
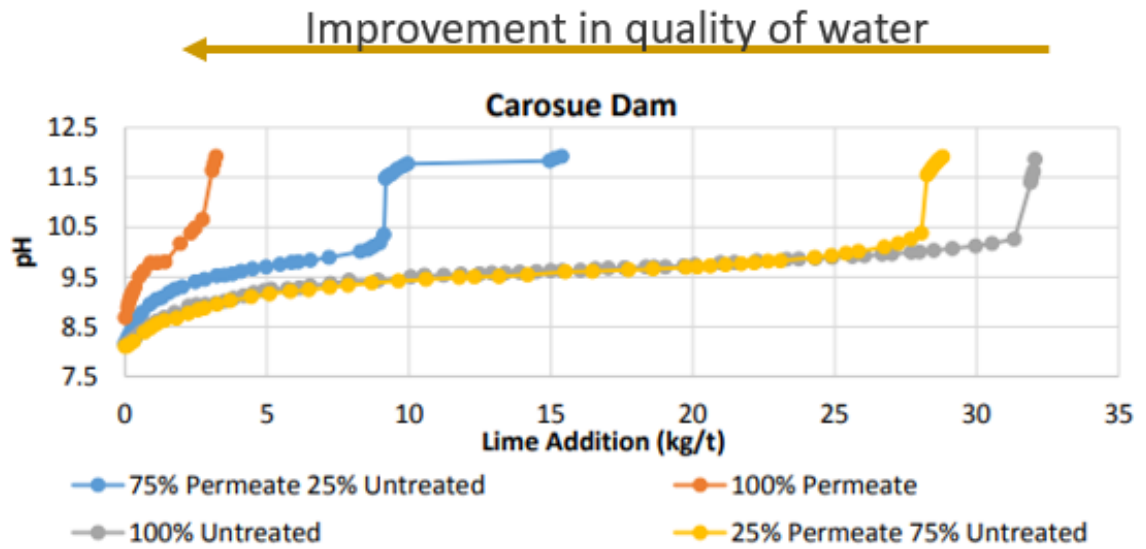
Figure 5 Impact of water quality on lime demand in gold cyanidation (From: Tapley, 2017)

Studies to determine the impacts of specific ions on froth flotation of sulphide ores have been conducted by many researchers (Manono and Corin 2022 and October et al., 2021). In an ongoing study at the Western Australia School of Mines, it has been identified that concentrations below 50 ppm for divalent ions and below 500 ppm of monovalent ions in water can be tolerated by the process without representing significant changes in recovery and grade (Jung et al., 2022). In accordance with these studies, it is of significant interest to investigate water treatment methods that enable the production of fit-for-purpose water for mineral processing including flotation of various ores.

2.5 Common water treatment methods.

2.5.1 Membranes processes

A membrane can be a permselective barrier or film between two fluid media, which allows the transfer of certain components from one medium to the other through it and prevents or restricts the passage of other components.

The membranes used to ensure adequate performance are of great diversity in both shapes and materials. In terms of the manufacturing material, membranes can be made of cellulose acetate (cellulosic), organic polymers (polysulfones, Teflon, propylenes, polyamides, polysulfides, polypropylenes), or composed of inorganic salts (ZrO_2, Al_2O_3, and TiO_2). (Cellulosic membranes tend to be more sensitive to temperature (50 °C maximum), chemical (pH between 3 and 8), and biological deterioration. On the other hand, although it is true that the polymeric ones better resist the above factors (pH 2-12, temperatures < 80 °C), they do not withstand compaction and chlorinated agents very well. Inorganic materials, show the most resistant to all the previous factors (pH 0-14, temperatures > 300 °C, pressures > 1 MPa) (Mahaut, 1992).

2.5.1.1 Organic Membranes

Organic membranes represent all those membranes whose active layer is made from an organic polymer or copolymer. Although there is an endless number of both natural and synthetic polymers and copolymers and mixtures, very few of them are suitable for manufacturing membranes. Most membranes are made from polymers except for those made from cellulose derivatives. The chemical and physical properties of these raw materials are of decisive significance for the properties of the finished membranes (chemical and thermal consistency, permeate flux and backing, interaction with feed etc (Ulbricht, 2006).

2.5.1.2 Inorganic membranes

This kind of membranes are made of wide variety of materials such as, glass, ceramic, and metals like zirconium aluminium and titanium. The main characteristic of inorganic membranes is that in comparison with organic

membranes, they present high thermal and high chemical stability on all the pH range which made them more flexible and adaptable to many solvents and any cleaning agents from strong acids to alkaline solutions. In addition, these membranes usually have longer lifetime than inorganic membranes, (Ding et al., 2017)

2.5.1.3 Cellulose acetate membranes

Cellulose acetate (CA) is obtained by acetylating cellulose from wood or cotton. Treating it with saponifying agents hydrolyses a small part of the acetate groups, thus improving its solubility and giving rise to modified cellulose acetate (Vatanpour et al., 2021). The first membranes used for desalination of water by reverse osmosis were made of cellulose acetate. This type of membrane has a high rejection of salts as well as high permeability and are even resistant to chlorine. However, it requires high working pressures and strict control of operating conditions (temperature and pH) to avoid hydrolysis and thus the risk of dissolution of the cellulose acetate membrane. Cellulose acetate was the first type of material used in reverse osmosis (RO), nanofiltration (NF) and ultrafiltration (UF). This material is low cost hydrophilic but susceptible to temperature, pH and the action of microorganisms.

2.5.1.4 Membrane formats and modules

The module is the centrepiece of the membrane installation which allows the membranes to withstand the different working pressures. On a commercial level, membranes configured with various geometries are available, namely: flat membranes, tubular membranes, spiral-shaped membranes, hollow fibre, or capillary membranes (Martin, 2016).

The plate modules are made up of a group of flat membranes, rectangular or circular in shape, and are supported by drainage meshes or porous plates (Figure 6). In this configuration, the membranes are separated with spacers with a thickness of the order of 2 mm (Berk, 2009)
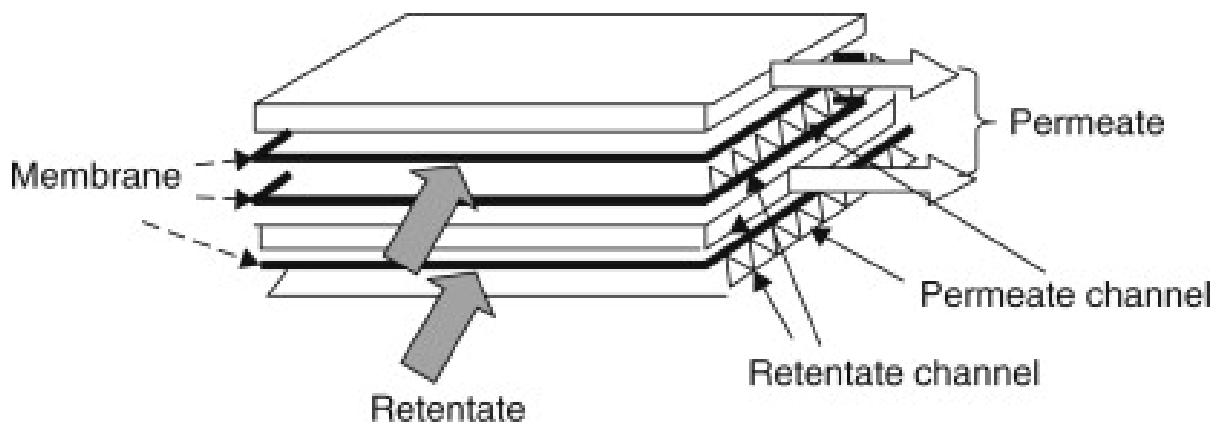
Figure 6 Plate flat membrane configuration (From: Berk, 2009)

The tubular modules are manufactured using a perforated or porous tube as a support, that host the tubular membranes (Figure 7).
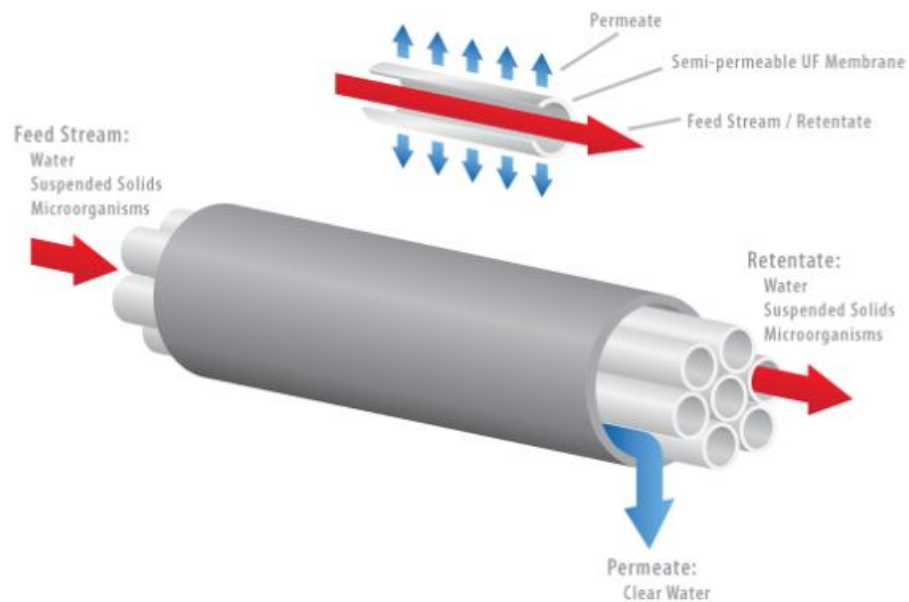
Figure 7 Tubular membrane configuration (From: Synder filtration)

Spiral modules are made up of flat membranes that are wound spirally around a central, plastic tube with holes. Figure 5 schematically illustrates the operation of a spiral module (Berk, 2009). The permeate flows through the central tube. The module is formed from a rectangular sheet of semi-permeable membrane that is folded in half, so that the active layer remains on the outside. A spacer is placed inside the two halves that allows permeate from the membrane to circulate and collect in the central tube. On the active layer of the membrane follows a mesh that has distribution channels, to distribute

33

the feed flow to be treated over the membrane. The seal between the feed flow and the permeate is maintained by bonding the permeate collecting fabric and the membrane with adhesive on the sides, in such a way that the adhesive perfectly penetrates the tissues. These sides of the permeate collecting fabric are also glued to the central tube. The entire package is wrapped around the central tube forming a cylinder, which is finally covered with a layer of fiberglass reinforced epoxy resin. (Berk 2009)
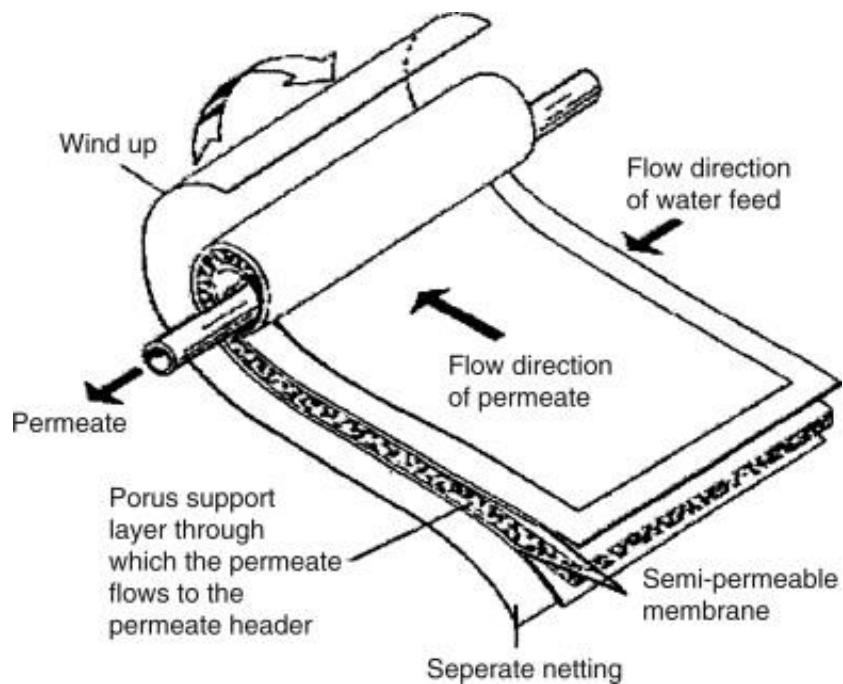
Figure 8 Spiral membrane configuration. (From: Berk, 2009)

Membrane process can be classified according to the driving force (Table 3). Typically, in industrial applications, the driving force is pressure across the membrane generating a pressure gradient that allows the separation of ions. The percentage of separation or retention of ions on the membrane surface depends on the pore size (Gennady et al., 2016). Therefore, based on the membrane pore size the pressure driving processes can be divided as follows:

Table 3 Driving force membrane processes (From: Gennady et al., 2016)

Driving force	Membrane process
Pressure difference	Microfiltration, Ultrafiltration, Nanofiltration, Reverse osmosis
Chemical potential difference	Pervaporation, Pertraction, Dialysis, Gas separation, Vapor permeation, Liquid Membranes
Electrical potential difference	Electrodialysis, Membrane electrophoresis, Membrane electrolysis
Temperature difference	Membrane distillation

2.6 Pressure difference membrane processes.

2.6.1 Microfiltration and ultrafiltration

Pressure difference membrane processes allow the mechanical separation of suspended or dissolved solids through a screen. The main difference between microfiltration and ultrafiltration processes is the pore size of the membrane, which determines which solutes can be removed in the filtration process. Substances larger than the pores of the membrane are fully retained, and even some substances smaller than the pores may also be partially or fully retained depending on the selectivity of the membrane.

In addition to the influence of pore size, the distribution of pores in the membrane structure is also important in both processes. Microfiltration is capable of separating small particles and ultrafiltration macromolecules. Specifically, microfiltration membranes have a pore size that allows the separation of particle sizes of different natures (suspended solids, fine particles, colloids, algae, and microorganisms such as bacteria) within the range: 0.1 µm – 10 µm, and microfiltration membranes ultrafiltration between 0.04 and 0.1 µm (Eykamp, 1995).

In addition, the productivity of both processes is high, although the permeability is higher in microfiltration membranes and the working pressures of this process are also the lowest, ultrafiltration is also characterized by quite low required pressure differences, since hardly any there are osmotic differences. Ultrafiltration membranes are generally porous membranes and are classified by molecular weight cut-off, which is equivalent to the molecular weight of the

smallest molecule that its pores can retain at 90%, and which ranges between 1,000 and 500,000, that is, molecules and macromolecules (Eykamp, 1995).

2.6.2 Reverse Osmosis

Reverse osmosis is currently the most widely used technique for desalination of water, since it allows the elimination of salts, as well as low molecular weight organic compounds, allowing the production of high-quality drinking water.

This membrane process retains virtually all smaller particle and salt molecules, including monovalent salts, while water molecules are free to pass through the membrane. The main characteristic of this process is that with reverse osmosis membranes the rejection of solutes does not occur through filtration, but rather the characteristic transport mechanism is dissolution-diffusion through the membrane, that is, the separation process is due to the different solubility and diffusivity in the membrane of the different components of the aqueous solution and therefore it is a physical-chemical process, since the interactions that exist between the water molecules, the membrane and the solutes are responsible for of separation. RO membranes are hydrophilic so that water molecules are easily attracted and by diffusion are transported through the polymeric structure of the membrane (Ismail, Khulbe and Matsuura, 2019).

Therefore, the components that constitute the permeate, that is, those that manage to cross the membrane, must have a certain affinity with the membrane material, since it is a decisive factor so that they can dissolve in its structure and subsequently diffuse through it. her. Hence, in reverse osmosis, the membrane material is much more important than in microfiltration and ultrafiltration processes. In addition, reverse osmosis membranes, being dense and non-porous, have lower permeability values, having to work at higher pressure values that allow overcoming the osmotic pressure to achieve a reasonable flux of fluid from the concentrated phase to the permeate (Ismail, Khulbe and Matsuura, 2019).

Table 4 Characteristics of pressure-driven membranes processes. (From: Gennady et al., 2016)

	MF	UF	NF	RO
Permeability(L/h. m².bar)	1000	10–1000	1.5–30	0.05–1.5
Pressure (bar)	0.1–2	0.1–5	3–20	5–1120
Pore size (nm)	100–10,000	2–100	0.5–2	< 0.5
Separation Mechanism	Sieving	Sieving	Sieving, charge effects	Solution diffusion
Applications	Removal of bacteria	Removal of bacteria, fungi, virses	Removal of multivalent ions	Desalination

2.6.3 Nanofiltration

Nanofiltration is an intermediate process between reverse osmosis and ultrafiltration due to the levels of separation it allows, and the pressure applied that it requires. Nanofiltration membranes have a microporous structure and can retain particles with a size of 0.1 nm-0.001 μm, which allows the majority of molecules to be separated from the water, although those of lower molecular weight are partially retained in the membrane. Therefore, this process allows the separation of organic substances (proteins, sugars), microorganisms and some multivalent salts (Chakrabarty, Giri, and Sarkar, 2022). In addition, in this process the separation of substances is carried out in a combined way both by the size of the pores, and by the dissolution-diffusion mechanisms that characterize ultrafiltration and reverse osmosis processes.

Nanofiltration is used for heavy metal removal from wastewater, for wastewater decontamination, for nitrate removal, for colour removal, and also can be used as pre-treatment before reverse osmosis. In general, to those applications in which conventional distillation or vacuum evaporation do not are viable alternatives, as is the case when you want to concentrate acids or corrosive substances. The chemical nature of the polymeric material membranes is made from affect the selectivity of nanofiltration membranes. While some polymers can be hydrophobic, the most recommended membranes to work with aqueous solutions are those with hydrophilic

characteristics since membranes with hydrophobic characteristics tend to get dirty more quickly.

The rejection rate is another parameter that allows quantifying the degree of selectivity of a membrane with respect to a certain solute, which never reaches 100%. A very low percentage of solute will pass with the permeate stream according to its partition coefficient (affinity of the solute for the membrane material) as well as the diffusion coefficient of the solute in the membrane. Also, the Donnan effect influences the selectivity of the membrane (Chakrabarty, Giri, and Sarkar, 2022).   In nanofiltration, part of the mass transfer mechanism is based on dissolution - diffusion, which is intrinsically related to the phenomenon of osmotic pressure.

2.6.4 Parameters of nanofiltration processes

2.6.4.1 Ion rejection on nanofiltration

It has been identified as a common pattern that the ion rejection by nanofiltration and reverse osmosis processes follows the Hofmeister series or lyotropic series which defined the process of silting out of salts by the hydrated radius of the ions. In this order of ideas ins with bigger hydrated radios tend to be rejected more than ions with lower hydrated radius (Wiesner et al.,1996).

Having in mind the lyotropic series the rejection of ions by pressure-driven process should follow the following order:

For cations:

$$Mg^{2+} > Ca^{2+} > Na^{+} > K^{+} \qquad\qquad\qquad [1]$$

And similarly for anions rejection:

$$SO_4^{2-} > Cl^{-} > NO_3^{-} \qquad\qquad\qquad [2]$$

To predict rejection series of ions in a multiple salt and ions systems the following empirical equation can be used:

$$\frac{\Delta P}{R} = \frac{Z_2}{Z_1}\,\Delta P + \frac{1}{Z_1} \qquad\qquad\qquad [3]$$

Where R is the rejection of the ion expected by the membrane at a determined pressure, z_1 and z_2 are the constants for each ion that define the series for each membrane (Wiesner et al., 1996).

2.6.4.2 Polarization by concentration in nanofiltration membranes

In membrane processes, when the solvent crosses the membrane, the concentration of solute in the concentrate increases, near the front face of the membrane, creating a concentration polarization phenomenon. In this way, the efficiency of the membrane depends not only on its properties but also on the operating conditions. The hydrodynamics of the system has a direct influence on the reduction of the transport resistance at the membrane interface. The system design plays a very important role in the flux distribution at the membrane interface, helping to reduce the effect that concentration polarization has on performance (Giacobbo et al., 2018).

By applying external pressure to the feed stream with a known concentration, on the face of the membrane, the solvent will pass through it. A part of the solute is rejected, which will accumulate on the surface, creating a concentration profile. This phenomenon is called concentration polarization. The solute distributed at the membrane/solution interface will be transported across the membrane by both convective and solution-diffusion mechanisms. On the permeate side, a second distribution process will occur, and a final solute concentration will appear in the permeate stream Cp (Dach, 2009).

In nanofiltration processes, the distribution of uncharged solutes at the boundary layer/membrane interface is due to the size exclusion or convective mechanism. This mechanism also appears in the microfiltration and ultrafiltration processes. Due to its size, a solute only has access to a part of the total surface area of a pore. This causes the exclusion of the solute from the membrane surface. The exclusion effect is given by the difference in molecular weight (MW) and the molecular weight cut off (MWCO) of the membrane, solutes with higher molecular weight than the molecular weight cut off of the membrane will not permeate easily through the membrane, hence the ions can be separate by the different on molecular weight. To determine

the molecular weight cut-off of the membranes, the below equation in which membrane selectivity and pore size are related can be used (Dach, 2009).

$$C_{CONV} = C_0 \left[1 - (1 - M/S_C)^{1/3} \right]^2 \qquad [4]$$

Where M is the molecular weight of the ion, Sc the Molecular weight cut off of the membrane and C_0 is the initial concentration of the ion in the feed.

Theoretical concentration polarization models analyse the increase in the concentration boundary layer of a solute due to rejection at the membrane surface. The analysis includes the solution of differential diffusion-convection equations under the appropriate boundary conditions and assuming some simplifications.

2.6.4.3 Charged solute transfer mechanisms.

In nanofiltration, the distribution of an uncharged solute at the boundary layer/membrane interface is considered to be almost exclusively determined by the mechanism of steric exclusion. Steric exclusion is not the typical mechanism of nanofiltration, contrary to what happens in ultrafiltration and microfiltration. Due to its size, a solute only has access to a fraction of the total surface area of a pore. This causes a geometric exclusion of the solute from the membrane. A separation between solutes can only be done when the solutes have different sizes.

For electrically charged solutes, there are two additional recognized distribution mechanisms:

 1. Donnan exclusion, which compared to other pressure-driven membrane processes, has a pronounced effect on NF separation. Due to the nature of membrane charge, solutes with the opposite charge to the membrane (counter-ions) are attracted, while those with similar charges (co-ions) are repelled. A distribution of co- and counter-ions will occur on the membrane surface due to the need to preserve the electroneutrality of the solution, causing additional separation. It can be predicted, then, that the membrane rejection will increase with increasing membrane charge and ionic valence (Suhalim et al., 2022).

2. Dielectric exclusion; due to the charge of the membrane and the dipole moment of the water, the water molecules show a polarization in the pore. This polarization results in a decrease in the dielectric constant within the pore, making the penetration of a charged solute into the membrane-less favourable. Generally, it does not play an important role in ultrafiltration and microfiltration, but it has great importance in electrodialysis (Suhalim et al., 2022).

The relative importance of the two mechanisms in NF is still a point of debate. Most of the NF literature uses Donnan exclusion as a distribution mechanism. The requirement of electroneutrality in ion-rejecting membrane concentrates and permeates can lead to a significant modification of the membrane's rejection characteristics against mixed solutes. For example, the presence of two competing anions in the concentrate can lead to less rejection of one of them as the concentration of the other increases.

2.6.4.4 Mass transport in nanofiltration processes.

Over the years the theory and models for mass transfer in membranes have progressed significantly, solute and solvent separation models can be separated into three categories: preferential adsorption, irreversible thermodynamics and solution diffusion.

2.6.4.5 Spigeler Kedem-Katchalsky (SKK) model to describe nanofiltration.

The model of Spiegler, Kedem and Katchalsky (SKK), presents the transport of the solvent trough membranes as a black box where principles of phenomenological mass transfer can be applied. This model approaches the transport phenomenon for a two-component system (solute and solvent) using the theory of irreversible thermodynamics with the following equations.

$$J_v = L_P(\Delta P - \sigma \Delta \Pi) \tag{5}$$

$$J_s = P_s \, \Delta C_s + (1 - \sigma)J_v \, \overline{C_s} \tag{6}$$

Where Jv and Js are the solvent and solute flux, LP is the hydraulic permeability, ΔP represents the pressure drop across the membrane, Ps is the solute permeability, ΔCs is the difference of concentration from the surface of the membrane in the bulk side and in the permeate, σ is the reflection

coefficient, and ΔΠ is, respectively the osmotic pressure through the membrane. In addition, the term (σ ΔΠ) can be defined as the critical pressure, which is the pressure when the transmembrane pressure is equal to osmotic pressure triggering the mobilisation of ions from the feed water to the concentrate (Kelewou et al., 2011). ($\bar{C}_s$) represents the solute concentration in the membrane which is represented as the average concentration on both side of the membrane. To represent accurately the solute concentration in the membrane Spiegler and Kedem applied equation 5 in a differential membrane layer and integrated it across a membrane resulting in the following expressions which are dependent on the experimental ion rejection (Robs) and the solvent flux Jv (Spieger and Kedem, 1996 and Hidalge et al., 2013).

$$R_{obs} = \frac{\sigma(1-F)}{1-\sigma F} \qquad\qquad\qquad [7]$$

And F:

$$F = e^{\frac{-J_v(1-\sigma)}{P_s}} \qquad\qquad\qquad [8]$$

The SKK model is a model that provides phenomenological information such as the ions permeability (Ps) and the reflection coefficient (σ) related to the transport of the solute. From the SKK expression, it can be noticed that if Jv tends to be infinite, then Robs = σ. Additionally, if the solutes are small enough to pass through the membrane pore, the σ is expected to be below 1 meaning that the convective solute transport takes place into the solute transport. Otherwise, the membranes will have dense structure with extremely low porosity where solute transport takes place only by diffusion as is the case on RO membranes.

It is well known that the SKK model was developed initially for uncharged membranes with dense structure such as RO membranes. Unlike RO membranes, NF membranes are characterized by slightly charged surface (Diwara et al., 2003). However, in this study we have neglected the membranes charge because those membranes have been classified by the manufacturer as tightest NF membranes with similar characteristics and behaviour as RO membranes.

In this study we have restricted the effect of concentration polarization using high flow rates and small volumes monitoring any changes in fluxes during each experiment that can indicate concentration polarization effect. In addition, the permeability of the membranes was restored by chemical cleaning after each experiment to reduce the concentration polarization effect at maximum.

The SKK model was applied in this study having in mind the following assumptions:

- The only forces affecting the mass transfer are pressure and concentration gradient.
- Regardless of the solute, charge, solvent, and membrane charge, the model predicts the solute and solvent mass transfer through the membrane.
- The concentration polarization is neglected due the high flow rates used and monitoring on fluxes changes during each experiment.

Having minimized and neglecting phenomenon of polarization and surface charge, σ and Ps parameters were calculate solving the equations 7 and 8 through the non-lineal method of the least-square which uses the minimum sum of the square deviations between R_{obs} and R calculated from the model for the different Jv given form the experimental data.

2.6.4.6 Hydrodynamical parameters involved in nanofiltration.

Models based on irreversible thermodynamics are classic in the description of membrane separation processes. Their level of description is phenomenological, and they use transport properties such as diffusivity for mass transfer and viscosity for momentum transfer (convective flow). They are not mechanistic models.

For pressure-driven systems like nanofiltration, the solute flux and solute rejection are described by the convective and diffusive phenomena. Convection is the result of the solute transport due to the pressure gradient across the membrane and diffusion is the result of the concentration gradient on both sides of the membrane.

The expression for the flow rate or volumetric flux of the total that crosses the membrane (water and solute),

$$J_v = L_p[\Delta P - \sigma \Delta \Pi] \qquad [9]$$

$$J_s = P_s \Delta C_s + (1 - \sigma)J_v C_{int} \qquad [10]$$

where Jv is the flux of the solvent, ΔP is the transmembrane pressure, ΔΠ is the osmotic pressure difference across the membrane, Lp is the coefficient solvent permeability and σ is the reflection coefficient (dimensionless). Ps is the solute permeability, $C_{int.}$ is the solute concentration in the membrane and $\Delta C_s = C_m - C_p$ being Cm and Cp the concentrations respectively at the surface of the membrane and in the permeate. Additionally, the term of reflection and osmotic pressure represent the critical pressure (Pc) which is the pressure at which the transmembrane pressure is equal to the osmotic pressure (Dach, 2009).

$$P_c = \sigma \Delta \pi \qquad [11]$$

While separation in the ultrafiltration process is described phenomenologically by size repulsion and reverse osmosis is driven by diffusive transport. Nanofiltration is a complex transitionary process between ultrafiltration and reverse osmosis in which the transfer of solute depends on a combination of size repulsion and gradient concentration. The model of Spiegler and Kedem-Katchalsky assumes that the membrane does not have a charge to express the global mass transfer of a solute in a pressurised nanofiltration membrane system from which the solute transport is quantified as the sum of both phenomena (convectional and diffusional) allowing to determining the dominant mass transfer mechanism in the process (Kelewou et al., 2011 and Diwara et al., 2003).

$$J_{diff} + J_v C_{conv} = C_p J_v \qquad [12]$$

$$C_p = \frac{J_{diff}}{J_v} + C_{conv} \qquad [13]$$

where J_{diff} is the solute flux due to diffusion (with $J_{diff.}=P_s \Delta C_s$), and C_{conv} is the solute concentration due to convection [with $C_{conv}= (1-\sigma)C_{int}$]. Hence, by plotting C_p versus the reverse of the permeate flux, it is possible to quantify the solute mass transfer occurring in NF by convection and diffusion. In addition, to compare both mechanisms the Peclet number, which is used in transport phenomena can be used to determine the dominant mechanism through the following equation.

$$P_e = \frac{J_v C_{conv}}{J_{diff}} \qquad [14]$$

where a Pe greater than 1 means that the dominant mass transfer is convective, and with Pe lower than 1 the mass transfer is dominated by diffusion.

2.7   Temperature difference processes

The driving force on this process to achieve the mass transfer across the membrane is a difference in partial pressure between the two ends of the membrane pores, that can be maintained by acting on the temperature difference across the membrane,

2.7.1   Membrane distillation

Membrane distillation is a thermal desalination process, in which the driving force is the vapor pressure gradient generated on both sides of a membrane due to the temperature gradient. Compared with membranes for reverse osmosis, with a pore diameter of 0.1 to 3.5 nm, membranes for distillation have a pore diameter of 0.1 to 0.4 microns. The separation with this type of membrane is based on its hydrophobic nature, passing only the water in the vapor phase. This allows volatile matter to be separated from non-volatile matter, potentially obtaining high-quality clarified water (Belessiotis, Kalogirou and Delyannis, 2016).

The choice of membrane is essential to the process's efficient operation. The most important membrane properties that affect the process are porosity, pore size, membrane thickness, thermal conductivity, and composition, which is linked to chemical assault resistance (Woo et al., 2019).

Membrane distillation is a technology that is becoming increasingly competitive in a wide variety of industrial sectors since it allows complex effluents to be treated. It is a technique that, together with vacuum evaporation, is one of the few technologies that allows saline effluents and brines to be treated without producing, if necessary, a reject current, since the separation is not limited by equilibrium. However, membrane distillation is not yet a technology with high energy efficiency due to heat losses due to membrane conductivity, so its application is restricted (Woo et al., 2019 and Belessiotis, Kalogirou and Delyannis, 2016).

2.7.2 Electrical potential difference membrane processes

The electrically driven process is characterised by the movement of ions due to an electrical potential difference, the most common processes that use electrical potential to move ion is electrodialysis.

2.8 Electrodialysis

The salts dissolved in the water are found as ions, that is, with a positive (cations) and negative (anions) electric charge. Based on the electrochemical properties of the ions in the water and on the properties that certain types of membranes present, electrodialysis has been developed for the separation of salts. This process is performed by electrically charged membranes that allow separating the ions from the water when an electrical current that originates that the cations (+) are moved to the cathode (-) and the anions move towards the anode (+). Cationic membranes allow the passage of cations and prevent the passage of anions, on the contrary, anionic membranes allow anions to pass through and reject cations. In a system where cationic and anionic membranes have alternatively arranged (Figure 9), a water that has lost dissolved ions decreased their salinity and a water that is receiving the ions increasing its concentration and therefore increasing its salinity. With electrodialysis, unlike reverse osmosis, what crosses the membranes are the ions and not the water (Montiel et al., 2014).

CONCENTRATE
DILUATE
A C A C A
ELECTROLYTE
ELECTROLYTE CONCENTRATE
DILUATE

A = Anionic Exchange Membrane
C = Cationic Exchange Membrane
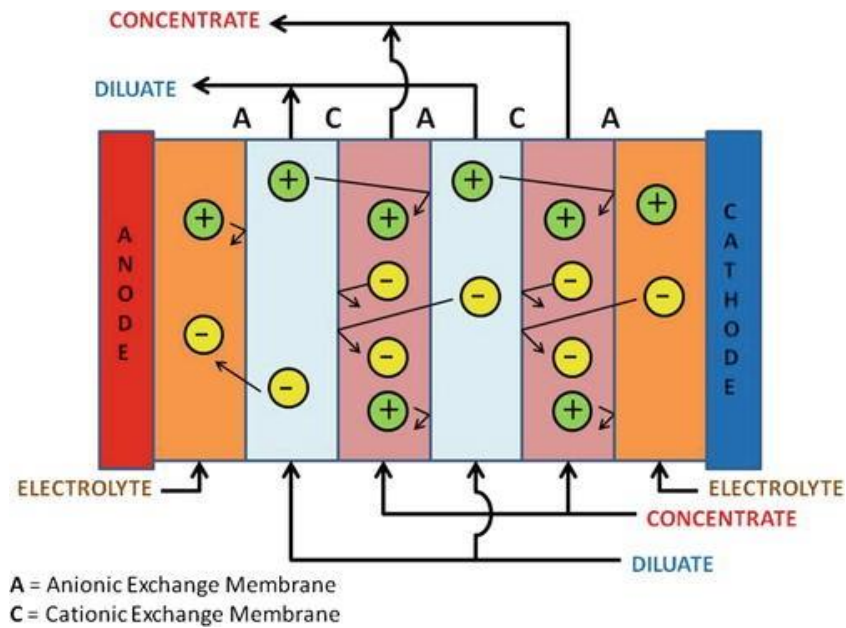
Figure 9 Generic structure of an electrodialysis cell (From: Montiel et al., 2014)

To achieve a certain reduction in ions, it is necessary to use a "cascade" of electrodialysis since with a single cell approximately 40% of reduction of ions is achieved (Montiel et al., 2014) .2014).

By applying a potential difference between the electrodes, the anions migrate through the anion exchange membranes from the diluted compartments to the concentrated ones, where they are trapped, since the ionic barrier constituted by a cation exchange membrane stands in their way. In the same way, the cations are concentrated in the concentrated compartments where the anionic membranes prevent their migration towards the cathode. Electrode reactions are only used to provide the electric field necessary for the anion and cation transport process to occur (Krol. Wessling and Strathmann, 1999).

Both electrodes are chemically inert metals. The cathode is generally made of stainless steel and the anode of tantalum or titanium coated with platinum or niobium. Thus, the electrodes are not oxidized or reduced. The more easily oxidizable species are oxidized at the anode and the more easily reducible species are reduced at the cathode. With inert electrodes the result at the cathode is the discharge of water (Krol. Wessling and Strathmann, 1999):

$$2H_2O + 2e^- \rightarrow 2OH^- + H_{2_{(g)}}, \quad E^0 = 0.828\,V \qquad [15]$$
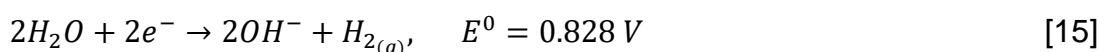
And the oxidation reaction in the anode is:

$$H_2O \rightarrow 2e^- + 0.5\, O_{2_{(g)}} + 2H^{\mp}, \quad E^0 = -1.23\, V \qquad [16]$$
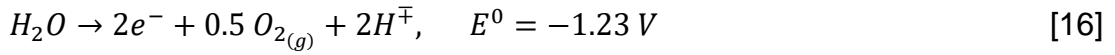
Hence the net reaction is:

$$H_2O \rightarrow H_{2_{(g)}} + 0.5\, O_{2_{(g)}} +, \quad E^0 = -2.188\, V \qquad [17]$$
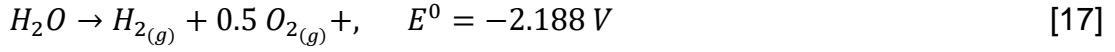
The most important parameters in the design of the electrodialysis process are, the membrane area and the necessary electrical energy. The membrane area is estimated from the current density, rather than from the permeability and resistance to mass transfer, applying Faraday's law:

$$A = \frac{zFQ\Delta C}{i\xi} \qquad [18]$$

where A is the total area of the cell (m²), z is the charge of the ions to be transported through the membrane, F is the Faraday constant (96.487 C/mol), Q is the volumetric flow rate of the dilute (m³/s), ΔC is the difference in concentration of the ion between feed and dilute (mol/m³), i is the current density (A/m²), generally 80% of imax , and ξ is the efficiency of current (< 1) (Yoshino, 2017).

The flow of electric current is usually given from the equation:

$$I = \frac{zFQ\Delta C}{n\xi} \qquad [19]$$

where n is the number of cell pairs (anion-cation membrane pairs)

Membrane ions selectivity (S^A_B), is a way to establish a comparison of ions transport velocity through the membrane and it is calculated according to the following equation.

$$S^A_B = \frac{CF_A - CF_B}{(1 - CF_A) + (1 - CF_B)} \qquad [20]$$

Where CF_A and CF_B are the concentration factor of the ion A and B which is represented as $CF_A = \frac{C_A(t)}{C_{A,0}}$ where is compared the concentration of the ion at determined time with its initial concentration. Positive values of membrane selectivity means that the ion in comparison A is transported slower that the

48

ion B and negative membrane selectivity means that the ion in comparison B is transported slower through the membrane.

2.8.1 Limiting current density on electrodialysis processes

The current density in electrodialysis can be increased until the ion transfer current exceeds the number of ions available to be transferred, this point is called the limiting current density. It is well acknowledged that when an electrodialysis stack is run at a higher LCD, the process exhibits higher electrical resistance or poorer current utilization because the ions to be separated at this current level do not have sufficient charge transport capacity and which is compensated by protons and hydroxyls produced by the hydrolysis of water. Additionally, it may lead to issues like salt precipitation or water dissociation. The limiting current typically depends on the membrane and solution characteristics, the design of the electrodialysis stack, and several operational factors including the flow rate of the diluted solution. Therefore, to avoid issues and properly run the electrodialyzer, the LCD must be determined. One method is by plotting the electrical resistance across the membrane stack.

2.8.2 Modelling of electrodialysis ions removal based on Nernst-Planck

Many models have been developed for the purpose of predicting and improving electrodialysis operations. Typical components of these models include process factors like cell structure, distinctive membrane properties, and operating variables like voltage and current. In this study the model and the process were validated through the use of 5 g/L NaCl synthetic solution so the effect of other ions in process can be neglected.

The following assumptions were taken into consideration in order to understand the behaviour of the electrodialysis stack used for this specific bore water treatment.

I.   Because the model was based on the Nernst Planck model, convection and ion interaction were not considered while calculating transport. Also, the effect of fouling and scaling on the membranes' surface were also neglected.

II. Since the ion concentration varied throughout the experiments, it was assumed that the solutions' viscosities would not vary.

III. Membranes were considered ideal at all times, where the cationic membrane is permeable only for cations and the anionic membrane is permeable only to anions.

IV. The concentrate and diluate tanks and the electrodialysis cell are considered a perfect mixed reactor.

In electrodialysis, different mass transport phenomena occur inside the stack when current is applied. To begin with, the process of ion migration flow (M), where the ion exchange membranes carry the charged species in the solution to the cathode or anode.

$$M = \frac{\eta \, I \, N}{F} \tag{21}$$

Where η is the efficiency of the process, N is the total number of membrane pairs in the stack, I is the current applied and F is the Faraday constant.

Another mass transport phenomenon is diffusion flux (D), which is related to the ion's migration due to the gradient concentration between the concentrate and the diluate which becomes bigger through time.

$$D = \frac{D_{cl\ am}\, S}{\sigma_{am}} (C_{c\ am} - C_{d\ am})N + \frac{D_{Na\ cm}\, S}{\sigma_{cm}} (C_{c\ cm} - C_{d\ cm})N \tag{22}$$

Where σ is the cationic and anionic membrane thickness, S is the surface are of the membrane, $C_{c\ am}$, $C_{d\ am}$, $C_{c\ cm}$ and $C_{d\ cm}$ are the NaCl concentration on the membrane surface.

$$C_{d\ am} = C_{d\ 0} - \frac{(1 - t_{Cl^-})\, \eta \, I}{F \, K_m \, S} \tag{23}$$

$$C_{c\ am} = C_{c\ 0} + \frac{(1 - t_{Cl^-})\, \eta \, I}{F \, K_m \, S} \tag{24}$$

$$C_{d\ cm} = C_{d\ 0} - \frac{(1 - t_{Na^+})\, \eta \, I}{F \, K_m \, S} \tag{25}$$

$$C_{c\,cm} = C_{c\,0} + \frac{(1 - t_{Na^+})\,\eta\,I}{F\,K_m\,S} \qquad\qquad [26]$$

Where t_{Na^+} and t_{Cl^-} are the transport number of sodium and chloride and K_m is the mass transport coefficient.

Additional to the mass transport equations described above, to calculate the changes of NaCl concentration in the diluate and concentrate the mass balance equations in the compartments and the tanks were required (equation 27, 28, 29, and 30).

$$N\,V_{cell}\,\frac{d\,C_{c\,0}}{dt} = (C_{c\,i} - C_{c\,0})\,Q_c + M - D \qquad\qquad [27]$$

$$N\,V_{cell}\,\frac{d\,C_{d\,0}}{dt} = (C_{d\,i} - C_{d\,0})\,Q_c - M + D \qquad\qquad [28]$$

$$V_{tank}\,\frac{d\,C_{c\,i}}{dt} = (C_{c\,0} - C_{c\,i})\,Q_c \qquad\qquad [29]$$

$$V_{tank}\,\frac{d\,C_{d\,i}}{dt} = (C_{d\,0} - C_{d\,i})\,Q_d \qquad\qquad [30]$$

Where C_d and C_c are the concentration in the diluate and the concentrate compartment and the sub script "i" and "0" means the inlet and the outlet concentration. As it can be seen the mass balances represent the change in concentration taking in to account the migration and diffusion phenomenon. Since the mass balance equations are polynomial the function fsolve in Matlab was used to solve the system and determine the change of concentration in the diluate and the concentrate with time.

2.8.3 Electrodialysis Module Configuration

The electrolyser used in ED is composed of modules with vertically oriented selective membranes, separated by flow spacers, gaskets, a pair of electrodes, the turbulence promoters, and the necessary tubing to assemble and form the battery.

2.8.3.1 Ion exchange membranes in electrodialysis

An ion exchange membrane is made up of cross-linked macromolecular chains, forming an insoluble three-dimensional network, on which the ionized functional groups that give it its specificity are fixed.

If the ionization of these groups gives a network of negative charges, the membrane is called a cation exchange membrane (CEM), if these charges are positive the membrane is called an anion exchange membrane (AEM).

The dissociation of an electrolyte within a AEM will give cations called co-ions since they have the same sign of charge as the fixed sites, and anions called counter-ions. In the case of a CEM, the cations will be the counter-ions and the anions the co-ions (Galama, 2015).

The most frequent exchanger groups in ion-exchange membranes are sulfonic, phosphoric, carboxylic for CEM and alkylammonium, vinyl pyridinium, alkyl phosphonium and alkyl sulfonium for AEM. Depending on the nature of the fixed group, the membrane is acidic or basic, weak or strong (Galama, 2015).

The ion exchange membranes used in ED can be classified in terms of their mechanical and electrical properties, their perm selectivity, and their chemical stability:

I.   Structural properties: these include parameters such as the type of membrane (anionic or cationic), its texture (homogeneous or heterogeneous), the chemical nature of the organic matrix, the presence or absence of a frame arming the membrane.

II. Mechanical properties: mainly include thickness, resistance to breakage and traction, and dimensional stability.

III. Physical-chemical properties: among them are:

- Exchange capacity: represents the number of fixed ionic groups per unit mass of dry (dehydrated) membrane.
- Water content and swelling contact with solutions causes the membrane structure to allow the solvent to penetrate inside, solvating the ions and

fixed ionic groups. The degree of swelling varies according to the nature of the equilibrium electrolyte as well as the membrane.

- Perm selectivity: a membrane is said to be permselective if it allows the passage of counter-ions from one compartment to another, preventing the passage of co-ions. The perm selectivity of a membrane for a given ion is characterized by the transport number, defined as the fraction of current carried by this ion. A perfectly permselective membrane has a transport number of counter-ions equal to unity, while that of co-ions is zero. But in aqueous solution the transport numbers of both types of ions are different from these values. The sum of the transport numbers is in all cases equal to unity.

- Electrical resistance: the use of ion exchange membranes requires that the electrical resistance of the membrane be as low as possible to avoid excessive consumption of electrical energy, which would constitute an economic impediment. However, it is generally considerably less than the resistance of the dilute solutions surrounding the membrane since the ionic concentration in the membrane is very high.

- Chemical stability: the economy of ion exchange membranes in different applications is determined by their chemical stability under conditions of process. The deterioration of the membranes after exposure for certain periods of time to solutions containing acids, bases or oxidizing agents is estimated by comparison with unexposed samples and determination of changes in their mechanical and electrical properties (Tanaka, 2015).

2.8.3.2 Dividers of cell pairs

The separators or spacers separate the membranes and provide a path in the cell for the flow of water. Parallel flow and tortuous flow path are the two most commonly used designs. Flow switch spacers are a modification of those for tortuous paths.

The cells are arranged with alternate stacking of concentrate and dilute to form a stage. In each stage, the feedwater is exposed only to the electronic force for the cell path distance called the hydrating stage. By using spacers more than one hydraulic stage can be placed between a batch of electrodes (Tanaka, 2015).

2.8.3.3 Electrodes in electrodialysis stack

One pair of electrodes is needed for each electrical stage. Electrodes are typically made of niobium or titanium with a platinum coating. Graphite is also sometimes used. At each electrode a chemical reaction takes place (Tanaka, 2015 and Galama, 2015).

2.8.4 Operation parameters that affect electrodialysis performance

2.8.4.1 Dilute, concentrate and electrode feed concentration.

If the effluent to be demineralized contains both non-ionized and ionized solutes, the given relationship between these determines that the electrical conductivity reaches a maximum value as the total concentration increases, after which the concentration decreases due to the effects of viscosity.

The solution in the concentrate compartment should be as concentrated as possible without impairing the efficiency of the membrane due to back diffusion. Regarding the feed solution to the electrode, the circulation of a solution consisting of 0.1 to 0.2 mol/L of Na_2SO_4 acidified to pH 2 or 3 is suggested (Membrain, 2019).

2.8.4.2 Feed flow into the cell

In relatively dilute solutions, the higher the flow rate, the higher the allowable current density. The area is inversely proportional to the current density, so the higher the flow rate, the smaller the total area required.

It is important to maintain strong turbulence over the entire surface of the membrane to avoid forming stagnant zones. A local layer of polarization would cause a localized alteration that could lead to membrane shear rupture (Membrain, 2019).

2.8.4.3 Effect of Temperature on ions removal

The increase in temperature leads to an increase in the mobility of the ionic species and a decrease in the electrical resistance of the system and in the viscosities of the solutions. The process will be limited by the chemical resistance of the membrane at high temperatures and of the materials that make up the electrodialysis cell.

2.8.4.4 Effect of Current density on ions removal

Current density is defined as the current per unit of available electrode area. The applied current density directly influences the flux of the species through the ion exchange membrane. The speed of the process is directly proportional to this variable. In the case of dilute solutions, the current-transmitting capacity of the ions in the solution will be lower (Montiel et al., 2014).

2.8.5 Limitations of the electrodialysis processes

The transfer of ions in the membranes gives rise to phenomena that limit the process:

I.   Primary polarization: also called concentration polarization. It occurs when seeking to increase the flow of ions transferred through the membrane. It is avoided by limiting the applied current density and increasing the rate of recirculation of the solutions in the vicinity of the solution-membrane interface.

II. Secondary polarization: it is the functional alteration of the membrane due to the formation of deposits on its surface or the penetration of substances that poison its interior. It is minimized by performing polarity reversals.

III. Water transport: its consequence is the limitation of the concentration of the solution.

IV. Proton leakage: occurs in anion exchange membranes due to their lack of perm selectivity.

The implementation of many ED systems allows savings in the recovery of raw materials and the reduction of the use of chemical products in traditional treatment, together with the reduction of sludge generated (Tanaka, 2015).

2.9 Precipitation

Chemical precipitation in water treatment involves the addition of chemical products in order to alter the physical state of dissolved and suspended solids and to facilitate their removal by sedimentation. In some cases, the alteration is small, and elimination is achieved by being trapped within a voluminous precipitate consisting mainly of the coagulant itself. Another direct

consequence of chemical addition is the net increase in dissolved constituents of the wastewater. Chemical processes, along with some of the physical unit operations, have been developed to provide complete secondary treatment of untreated raw water and wastewater, including removal of critical ions such as calcium, magnesium, chlorides, and sulphates. In the case of dissolved solids Ions combine with reactants to form insoluble or poorly soluble salts, which are then separated from the water by some other auxiliary operation, such as sedimentation or filtering.

2.9.1 Precipitation of oxalates

Many of precipitation processes are operated under alkaline conditions. However not all the processes work at high pH. Oxalic acid is an alternative for the treatment of process water through the complexation of ions such as calcium and magnesium to form oxalates.

$$M^{+2} + C_2O_4^{-2} + H_2O \rightarrow MC_2O_4.H_2O \qquad [31]$$

$$M^+ + C_2O_4^{-2} + H_2O \rightarrow M_2C_2O_4.H_2O \qquad [32]$$

Where M^{+2} is a divalent cation and M^+ is a monovalent cation

The precipitation of oxalate represented by the above equation happens under different conditions for each ion. For instance, calcium oxalate is the more favourable complex trough precipitate as it could precipitated in a wide range of pH and it start to be formed from very low concentrations of calcium (20 mg/L). In the case of magnesium and sodium oxalate the concentration of magnesium and pH play and important role (Figure 10). The lowest concentration of magnesium required in solution should be around 200 mg/L with a medium pH greater than 4.7 and lower than 10, over this pH the magnesium will precipitated as magnesium hydroxide. On the other hand, the precipitation of sodium oxalated has the particularity that its concentration in solution must be at least 105 g/L (Tran et al., 2013).
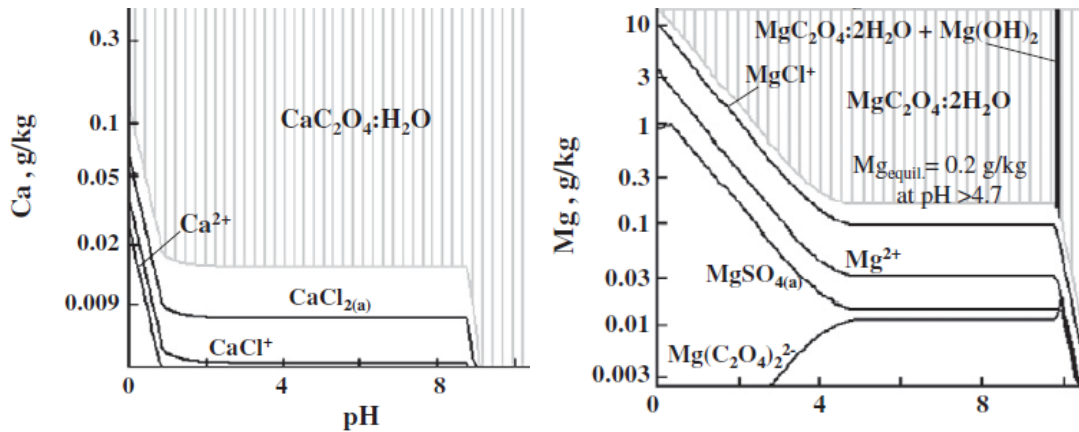
Figure 10 Ca, Mg Oxalate precipitation (From: Tran et al., 2013)

2.9.2 Precipitation (lime softening)

It is the most used reagent, mainly due to its economic advantages, this reagent eliminates the temporary hardness of water by reacting with calcium and magnesium bicarbonates to produce calcium carbonate and magnesium hydroxide respectively, which, being very insoluble, separate easily from the water.

$$Ca(HCO_3)_2 + Ca(OH)_2 = 2CaCO_3^- + 2H_2O \qquad [33]$$

$$Mg(HCO_3)_2 + 2Ca(OH)_2 = Mg(OH)_2^- + 2CaCO_3^- + 2H_2O \qquad [34]$$
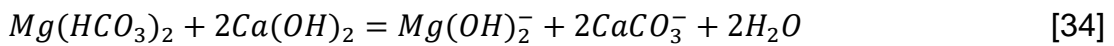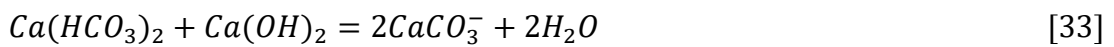
These reactions are carried out to a more effective degree at a high pH, having to operate above 9.5 to obtain good yields. The reaction time in this case, as in most, depends to a considerable degree on the temperature of the reacting substances; That is why this process, which would take approximately 6 hours cold, was carried out in 1 hour operating at high temperatures. This reduction in reaction time results in a decrease in equipment size and initial capital investment since smaller reaction and settling tanks can produce the same amount of treated water per hour (Minnesota Rural Water Association, 1994).

In this process the effectiveness of magnesium removal will depend on the amount of hydroxyl alkalinity excess in the system. For that reason, to improve magnesium reduction, sodium aluminate can be used as this compound is an excellent provider of hydroxyl without increasing the calcium concentration (Eq. 35).

$$Na_2Al_2O_4 + 4H_2O = 2Al(OH)_3^- + 2NaOH \qquad [35]$$

57
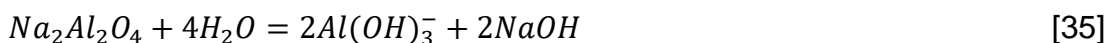
2.9.3 Ultra-high lime with aluminium (UHLA)

This method is a modification of the lime softening that is overcome the limitation of the lime softening of ions removal. UHLA, uses aluminium and calcium in excess to form aluminates compounds removing critical ions that usually are related to escalating problems such as Ca^{2+}, Mg^{2+}, CO_3^{2-}, PO_4^{3-}, Cl^-, SO_4^{2-} and SiO_2.

The process consists of two stages. In the first stage, the excess calcium reacts with the silica, phosphate, magnesium, and carbonate to form precipitates. In the second stage, the aluminium and the excess of calcium react with chloride and sulphate to form precipitates of calcium sulfoaluminate ($Ca_6Al_2(SO_4)_3(OH)_{12}$) and calcium chloroaluminate ($Ca_6Al_2Cl_2(OH)_{12}$) (Almasri, 2013 and Abdel-Wahab, 2003).

The precipitates formed in this process belong to a group of solids called layered double hydroxides (LDHs) and usually are known as anionic clays. These chemical compounds are conformed by two different types of metallic cation anionic species and water molecules. The general composition of these anionic clays can be represented as follows:

$$M_x^{2+}\ M_y^{3+}\ (OH)_{2x+3y-nz}(A^{n-})_z\ mH_2O \qquad\qquad [36]$$

Where M^{2+} = divalent cations (Ca^{2+}, Mg^{2+}, Zn^{2+}, Co^{2+}, Ni^{2+}, Cu^{2+}, Mn^{2+}), M^{3+} = trivalent cations (Al^{3+}, Cr^{3+}, Fe^{3+}, Co^{3+}, Mn^{3+}), A^{n-} = interlayer anions with charge (n-) (almost freely selected, organic and inorganic anions), and x, y, and z = The stoichiometric ratios of M^{2+}, M^{3+}, and A^{n-} (Olanrewaju et al., 2000, Rives, 2001, and Ulibarri and Hermosin, 2001)

Chloride compounds formed in this method have positively charged main layers of composition $[Ca_2Al(OH)_6]^+$ and negatively charged interlayers of composition $[Cl^-, 2H_2O]$ which make up calcium chloroaluminate. Ten hydrogen atoms, six of which are in hydroxyl groups and four of which are in water molecules, surround the chloride anions. Because the interlayer anions in an AFm phase are only weakly held together by electrostatic forces, inter-ionic exchange between two or more solids of AFm phases via the aqueous phase with which they are in contact is conceivable. This exchange reaches

equilibrium, resulting in solid solutions with different compositions. For instance, the interlayer Cl in calcium chloroaluminate can be replaced by OH from the aqueous phase to generate hydroxyaluminate ($Ca_4Al_2(OH)_{14}$) in solutions containing OH^- and Cl^-. When the chloride is only partially replaced, a solid solution made of a combination of chloroaluminate ($Ca_4Al_2 Cl_2(OH)_{12}$) and hydroxyaluminate ($Ca_4Al_2(OH)_{14}$) is created (Almasri, 2013).

Some of the conditions to drive the reaction toward the precipitation of calcium chloro and sulfo aluminates are the pH in the range of 11 to 12.5 to avoid des stability and dissolution of the sulphate and aluminium ions. Another important factor is the temperature, temperatures over 50 ºC favoured the formation of calcium aluminate monosulfate over the sulfoaluminate, however at high ratios of 3:1 (aluminium: Chloride/sulphate) aluminate precipitates can be formed in a wide range of temperatures (30-90 ºC) (Almasri, 2013).

2.10 Summary of literature review

The literature review presented in this chapter has shown that there is a need to demonstrate that other methods different than reverse osmosis can be applied in mineral processing processes. the major findings of this literature review on the technologies to be used in this study may be summarised as follows:

- Nanofiltration membranes have a microporous structure and can retain particles with a size of 0.1 nm-0.001 μm, which allows most impurities to be separated from the water, although those of lower molecular weight are partially retained in the membrane. In this process, the separation of substances is carried out both by the size of the pores and by the dissolution-diffusion mechanisms that are characteristic of processes such as ultrafiltration and RO. Therefore, nanofiltration allows the separation of organic substances (proteins, sugars), microorganisms and some multivalent salts. Different studies with brackish water have demonstrated that nanofiltration can remove up to 98% of calcium and magnesium salts and up to 66% of sodium chloride.
- In the electrodialysis process, cation and anion exchange membranes alternately sit between the cathode and the anode. Anions travel towards

the anode and cations towards the cathode when a voltage difference between the two electrodes is applied. The anion-exchange membranes retain the cations after they have passed through the cation-exchange membranes, which contain sulphone groups on their surface. On the other hand, the cation-exchange membranes retain the anions, which move via the anion-exchange membranes, which have quaternary ammonium as ion-exchange fixed groups. As a result of this flow of ions, concentration rises in the concentrate compartment of the cell while falling in the diluate compartment.

- Precipitation is one of the oldest conventional methods, but it has been considered in many operations for its effective performance-cost ratio and depending on the critical ions for each specific process selective precipitation can be achieved and in some cases recovery of precipitates as valuable minerals.

3   CHAPTER THREE: MATERIALS AND METHODS

3.1   Introduction

As was already indicated previously, the goal of this work is to study different water treatment methods to produce water for mineral processing operations. This is accomplished by treating bore water from Western Australia through methods such as nanofiltration, electrodialysis and precipitation. This chapter discusses the reagents, equipment, conditions, and methodologies utilised in each experiment.

3.2   Reagents

The synthetic saline water and the correspondent solutions were prepared with ultrapure water and the main reagents used in this section of the research were: calcium chloride (99.9% Chem supply), magnesium chloride (99% thermos Fisher Scientific), sodium chloride (99.9% Chem supply), sodium sulphate (99%) and sodium bicarbonate (99% Fisher Scientific),

The reagents used in the precipitation test were oxalic acid (99.9% Chem supply), calcium hydroxide (>99%, Sigma Aldrich), sodium aluminate (99%), and nitric acid and sodium hydroxide at analytical grade to adjust pH.

Reagents used for chemical cleaning of the membranes ($NaOH$ and HNO_3), the Na_2SO_4 used as the electrolyte in the electrode compartments of the electrodialysis stack and the $NaCl$ used for synthetic solutions were analytical grade and they were supplied by Chem-Supply, Australia.

3.3   Water characterization

3.3.1   Cations

These analyses have been performed using the inductively coupled plasma optical emission spectroscopy (ICP OES) technique following the USEPA 6010 standard procedure.

This analysis is based on the vaporization, dissociation, ionization and excitation of the different chemical elements of a sample inside a plasma. During the deexcitation process of the neutral atoms and ions inside the plasma, electromagnetic radiation emissions are produced in the UV-visible

zone. These radiations, characteristic of each element, are separated according to their wavelength and finally, their intensity is measured. This technique, therefore, provides the concentrations of the chemical elements present in each sample. It was used for the determination of Ca, Na and Mg in the samples obtained experimentally.

3.3.2 Anions

The sulphate concentration was measured following the standardised procedure APHA 4500 SO_4^{2-} E in which the sulphate is precipitated in an acetic acid medium with barium chloride producing crystals of barium sulphate which are measured by a photometer and compared with a standard curve.

For the analysis of chloride was used the standard method APHA 4500 Cl G in which N, N-diethyl-p-phenylenediamine reacts with free chlorine producing a red colour indicator which then was compared with a standard curve by spectrophotometer.

The raw water for this study was provided by a mining operation in the Goldfields region of Western Australia, and the characterization of the water is shown in Table 5. Bore water quality in the Goldfields region may range from extremely low (1 g/L of TDS) to extremely high (up to 250 g/L of salinity). The bore water used in this study contains relatively low Total Dissolved Solids (TDS) with the main ions of interest being Mg^{2+}, Ca^{2+}, Na^+, Cl^- and SO_4^{2-}. Additionally, synthetic water was prepared for some of the precipitation and electrodialysis experiments. their composition is listed in Table 5.

Table 5 Characterisation of water samples used.

Parameter	Unit	Bore water	Synthetic water	Synthetic sea water
pH	-	7.5	7.8	8.0
Conductivity	µS/cm	8280	24000	49400
TDS	mg/L	4150	11970	24700
TSS	mg/L	<10	<10	<10
Alkalinity (total)	mg/L	265	70	180
Alkalinity (OH)*	mg/L	0	0	0
Alkalinity (CO_3)*	mg/L	0	0	0
Alkalinity (HCO_3)*	mg/L	265	70	180
Calcium	mg/L	140	150	310
Magnesium	mg/L	167	290	600
Sodium	mg/L	1547	4700	10600
Chloride	mg/L	2340	5170	11420
Sulphate	mg/L	735	1300	2560

3.4 Nanofiltration

The filtration experiments were conducted in a pilot unit supplied by Ecotechnol Australia (figure 11). This pilot unit was designed to test different ultrafiltration and nanofiltration membranes under other conditions such as pressure and permeate recovery. The Ecotechnol rig is mainly composed of one feed tank with a volume of 0.1 m^3, a high-pressure booster pump which was used for the filtration and for the cleaning of the membrane, and one pressure vessel housing on a standard 40" X4" membrane module with retractile end and feed caps allowing the change of membrane, a manual regulation valve on the concentrate line to adjust the pressure of operation and the permeate and concentrate lines which can be fitted as recirculation loop with the feed tank and an external scale to measure the weight of the desirable recovery of permeate.
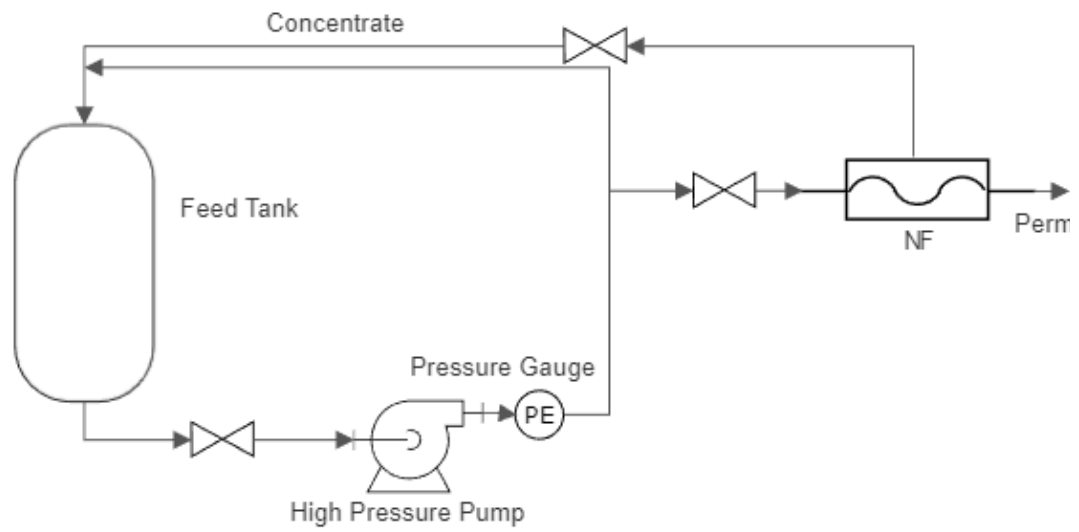
Figure 11 Ultrafiltration / Nanofiltration rig used in this study (Ecotechnol).

Two organic nanofiltrations (NF) membranes fabricated by different companies (Dow Filmtec and Ecotechnol) were studied. The nanofiltration membranes used are thin-film composite membranes. NF90-4040 and 4040 A are

64

characterised as tight nanofiltration membranes with relatively high sodium chloride rejection (>85%). In addition, one ultrafiltration (UF) membrane was used as pre-treatment to remove suspended solids to avoid undesirable fouling of the NF membranes studied. Table 6 shows the commercial names of the membranes and their corresponding suppliers as the primary polymer used for their fabrication.

Table 6 Commercial name and manufacturer of the NF and UF membranes

Commercial name	Application	Manufacturer	Polymer
UF Ecotechnol	Ultrafiltration	MDS- Ecotechnol	Polyamide
NF90-4040	Nanofiltration	DOW Filmtec	Polyamide
4040 A Ecotechnol	Nanofiltration	MDS- Ecotechnol	Polyamide

Before each experiment, the membranes were washed with caustic solution (0.2% w/w) to restore the membrane's permeability. Each membrane was pressurised using deionised water at 4 bars for 30 min until the conductivity of the permeate was steady and similar to the initial deionised water.

As the raw water used in the experiments was obtained from one of the bores at Mt Weld mine, an ultrafiltration stage was required as pre-treatment to avoid nanofiltration membrane fouling. The nanofiltration experiments were carried out with three different nanofiltration membranes and an initial mass of 22 kg of ultra-filtrated bore water from the Mt Weld mine site. The concentrate was recirculated to the feed tank, and the permeate was collected and sampled at three different recoveries (15, 45 and 65%). The feed pressure was adjusted for each test and was varied in the range of 8 to 20 bar. Additionally, the permeate flux and the ion's rejection were determined by measuring the permeate flow and the concentration of ions in the permeate.

3.5 Precipitation

The precipitation experiments were executed by adding the respective precipitant (oxalic acid, lime, sodium aluminate) to the synthetic water and the bore water.

3.5.1 Oxalic Acid

3.5.1.1 Effect of oxalic acid dose on ions removal

For the precipitation with oxalic acid, a volume of 0.6 L of both sources of water bore water (BW) and synthetic water (SW) was used in each experiment. This set of experiments were conducted with synthetic and bore water as the concentration of magnesium in the bore water is low to evidence the selective precipitation of magnesium. A jar tester apparatus with a gradual stirring rate was used as a batch mixed reactor equipped with 1 L beakers. The precipitation experiments were carried out at ambient temperature (20-24ºC) and a mixing rate of 200 rpm. To evaluate the effect of oxalic acid a set of experiments was conducted at different oxalic acid molar ratios (1, 1.2, 1.5 and 2 for each mol of Ca and Mg) with a fixed mixing time of 120 min.

3.5.1.2 Kinetics of calcium precipitation

Kinetics and equilibrium experiments were developed to establish the minimum time required to achieve the equilibrium of ions removal. This set of experiments was conducted at a stoichiometric ratio of 2 to (Oxalic acid: Magnesium + Calcium) ensuring that there is an excess of reagent to complete the reaction of all the ions in solution. During the kinetics and equilibrium experiments samples were taken at different times (30, 60, 120, and 240 min) which were filtrated by vacuum filtration through a Whatman 0.8 μm membrane filter of polyvinylidene fluoride for further ion analysis.

3.5.1.3 Effect of pH on calcium and magnesium precipitation

The experiments performed to evaluate the effect of the pH on the ion precipitation were conducted under similar conditions as established in the kinetics and equilibrium experiments. However, these experiments were carried out in two different stages in which 0.5 L of solution were mixed with oxalic acid at molar ratio of 2:1 for 120 min followed for 30 min of settling. After

the settling time the supernatant was filtered through a Whatman 0.8 µm membrane. A volume of 0.3 L of the filtrate was collected, and its pH was adjusted to the desired pH (1, 3, 5, 7, 11) with sodium hydroxide 1 M. The solutions with the pH adjusted were stirred for 120 min and 30 minutes of settling to finally be filtrated by vacuum filtration through a Whatman 0.8 µm membrane filter of polyvinylidene fluoride for ion analysis.

3.5.2 Ultra-High Lime Aluminium

3.5.2.1 Effect of reagents dose on ions removal.

In the case of the UHLA precipitation test, a volume of 0.3 L of bore water was used and the experiments were conducted in 0.5 L sealed plastic bottles to avoid CO_2 contamination and alteration of the precipitation process. The bottles were shaken at 200 rpm in a room-controlled temperature (25 ºC) shaking incubator Labwit ZWY-211B for 24 hours with different ratios of calcium/anions (1:1, 1,5:1 and 2:1) and different aluminium/anions ratios (1, 2 and 3). Also, a series of experiments of two stages (Figure 12), structured by the first stage with half of the lime dosage and a second stage with half of the lime dosage plus the different doses of aluminium at the different Al/anions ratio were performed to optimise the chloride and sulphate removal avoid the competition between ions with high affinity for the formation of calcium and aluminium complexes.
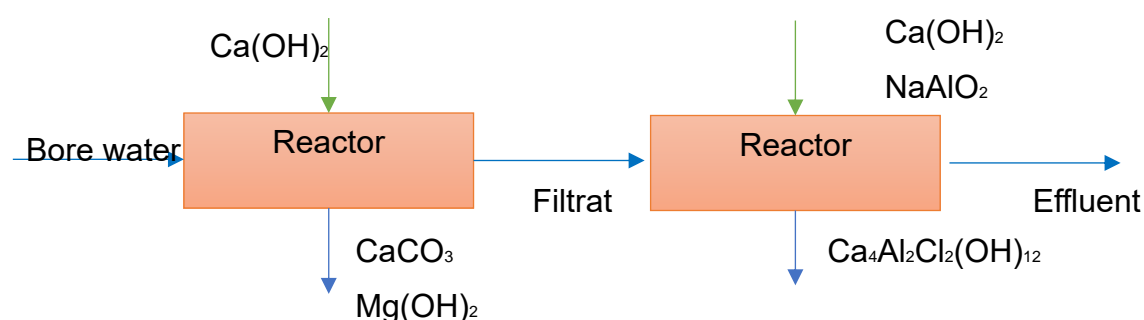
Figure 12 Two stages UHLA precipitation

3.5.2.2 Kinetics of ions removal

In addition, A series of kinetic experiments were performed to determine the reaction equilibrium. In this set of experiments, 0.9 L of bore water reacted with

calcium hydroxide and sodium aluminate at molar ratios of Ca/Anions of 2:1 and ratio of Al/anions of 1.5:1. The solution was kept under constant agitation at 200 rpm and 25 ºC ± one ºC in a shaking incubator and aliquots of the solution of 200 ml were taken at different times (2, 4, 8, and 24 hours) to determine the equilibrium time.

3.5.2.3 Effect of pH on chloride and sulphate removal

A set of experiments were performed to evaluate effect of the pH on chloride and sulphate precipitation. The experiments were carried out at 200 rpm in a room-controlled temperature (25 ºC) shaking incubator during 24 hours at different pH (4, 7, 9, 11 and 13) adjusted with nitric acid 1 M. The Ca/anions ratio and Al/anions ratio used in these experiments were of 1.5:1 and 1:1 respectively. After the 24 hours of mixing the reactors were left to settling time of 30 minutes and filtered through 0.8 µm membranes for further analysis.

3.5.2.4 Effect of temperature on chloride and sulphate removal

In order to evaluate the effect of temperature on the chloride and sulphate removal a series of experiments were conducted by mixing 0,3 L of solution and Ca/anions ratio of 1.5:1 and Al/anions ratio of 1:1at mixing conditions of 200 rpm and different temperatures (25, 35, 45, and 55 ºC) for 24 hours. After the 24 hours of mixing the reactors were left to settling time of 30 minutes and filtered through 0.8 µm membranes for further analysis.

Samples from the precipitation experiments were taken and filtrated by vacuum filtration through a Whatman 0.8 µm membrane filter of polyvinylidene fluoride. The solids were washed with deionized water and dried at ambient temperature for further analysis by x-ray diffraction (XRD). The filtrates were collected and analysed by inductively coupled plasma optical emission spectroscopy (ICP OES) technique following the USEPA 6010 standard procedure to determine cations concentration and by photometric methods APHA 4500 SO_4^{2-} E and APHA 4500 Cl G for sulphate and chloride determination respectively.

3.6 Electrodialysis

Electrodialysis module EDR-Z/2X10-0.8_19 (Membrain) was utilised in this section (Table 7). This module was fitted with ten pairs of Ralex® membranes of 1344 cm^2 total effective surface, arranged by pair of cation and anion exchange membrane. 1L of bore water was fed to the module through the concentrate and dilute compartment by two peristaltic pumps (Master flex L/S) at different flow rates and recirculated in the stack until the concentration of ions desired was achieved. The effect of different applied voltage was investigated adjusting the applied voltage through a rectifier. Na_2SO_4 solution was recirculated at a flow rate of 25L/h through the electrode compartment to avoid electrode reaction during experiments. Samples were taken at different times to analyse concentration of ions, conductivity, and total dissolved solids.

Table 7 ED module set up and characteristics.

Component		Characteristics
ED Stack EDR-Z/2 X10-0.8_19		Two electrodes with the capability of reversal
		Dimensions:
		Width 90mm
		Length 128 mm
		height 250 mm
	One hydraulic stage	10 membrane pairs
Electrodes (anode, Cathode)		Ti+Pt
Ion Exchange membranes	Anion exchange membranes	Ralex ® AM(H)-PES
		Active area: 64 cm2
	Cation exchange	Ralex ® CM(H)-PES
	membranes	Active area: 64 cm2
Spacer	Thickness	0.8mm
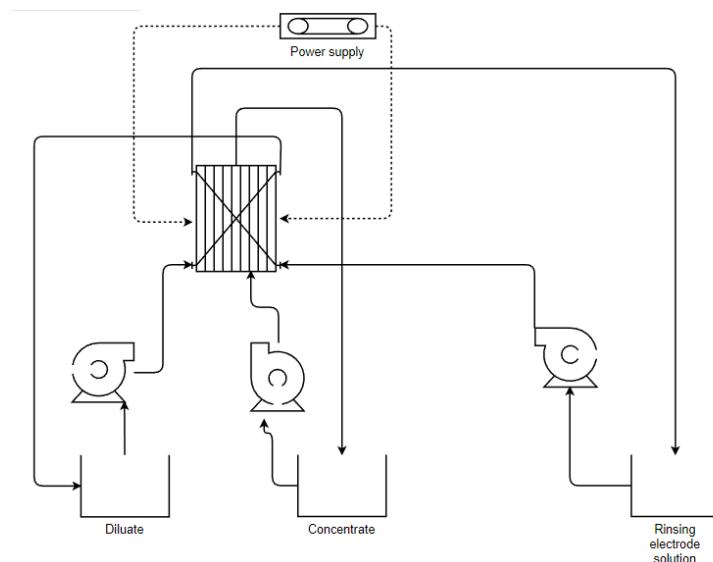
The membranes fit in the electrodialysis stack were manufactured by Mega, Czech Republic. The Ralex ® AM(H)-PES (anionic) which contains quaternary ammonium as ion exchange group and the Ralex® CM(H)-PES (cationic) which contains sulphon as ion exchange group (Figure 13). The electrodialysis stack hold 11 cation exchange membranes and 10 anion exchange membranes trough a total of 10 membrane pairs and each membrane has an effective surface are of 64 cm^2 with a total installed surface of 1344 cm^2 along the stack.
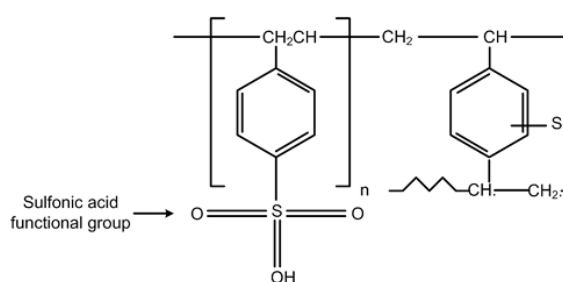
Cation exchange membrane   Anion exchange membrane
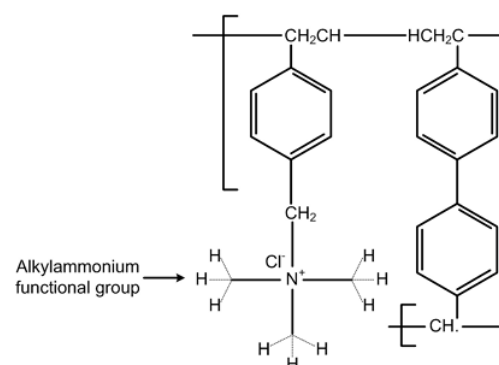
Figure 13 ion exchange functional group for cationc and anionc menmbrane

Different parameters considered critical for the performance of an electrodialysis system were evaluated. To maintain similar conditions and avoid the concentration polarization, before each experiment the ED stack was chemically cleaned by a sequence of recirculation of 2% NaOH for 30 minutes

followed by flushing with deionised water, then circulation of 2% HNO_3 for 30 minutes followed by flushing with deionised water.

Table 8 Parameters evaluated ED.

Parameters	Levels evaluated
Applied voltage	0.4, 0.6, 1 and 2 V/membrane pair
Flow rate	2.3, 3.3 and 4.2 cm/s
Ion concentration	Bore water and synthetic water with higher ions concentration

4 CHAPTER FOUR: NANOFILTRATION RESULTS AND DISCUSSION

4.1 Abstract

Limited freshwater availability, increasing competition for water among multiple users, cost of purification, corporate sustainability goals, etc., are the main factors driving many industries to focus on water quality and usage. Increasing water reuse and accessing alternative sources of freshwater are potential strategies to improve water efficiency. This chapter investigates the performance of nanofiltration membranes in producing suitable water quality for the separation of minerals based on the ionic strength tolerance threshold at which impurities begin to impact the separation process. In this study, the membranes used could reject more than 95% of divalent cations (such as Ca^{2+} and Mg^{2+}) and more than 74% of monovalent ions (e.g., Na^+ and Cl^-) under the conditions of 12 bar of transmembrane pressure and 65% of the recovery. These rejection rates were found to be sufficient to produce fit-for-purpose water for mineral processing. In addition, the effect of pressure on the mass transfer mechanism of each membrane was determined.

4.2 Introduction

This chapter shows the results based on the experiments performed with two different nanofiltration membranes at different operational conditions. The conditions evaluated in the results of this section were the recovery of permeate, transmembrane pressure and type of membrane. Also, phenomenological parameters related to the mass transfer and characteristics of the membranes were investigated. Furthermore, considering the ion rejection and the pressure economic analysis was performed.

4.3 Nanofiltration performance and ion rejection

The performance of the two membranes (i.e., 4040A and NF90 4040) towards the rejection of calcium, magnesium, sodium, sulphate, and chloride ions was evaluated under various conditions. The pattern of ion rejection is similar for the two membranes; as the transmembrane pressure increases, the ion rejection increase, which agrees with results reported by other researchers (Ahmad, et al., 2004). From figure 14, it can be noticed that while the recovery increases, the membrane performance decreases. This is because the

concentration returns to the feed stream, increasing the concentration of ions to be rejected, growing the ion driving force and changing membrane surface characteristics affecting the rejection of ions. Table 9 shows the concentration of the ions achieved at different conditions of operation. Removal of problematic ions in mineral processing operations such as calcium, magnesium and sulphate are removed at concentrations where their concentration has a negligible effect on the processes (<50 mg/L) whit low pressures as 4 bar. For processes such as flotation of monazite where the concentration of monovalent ions such as sodium and chloride are also important, it is required to go for operational pressures over 16 bar to achieve concentrations (<500 mg/L) where the process is not affected.

a)

b)

c)

d)

e)
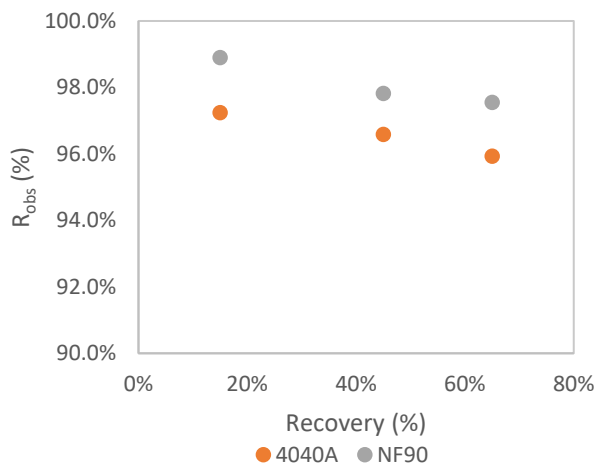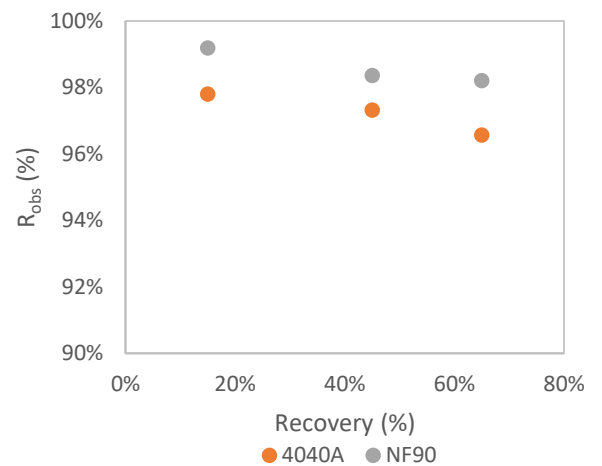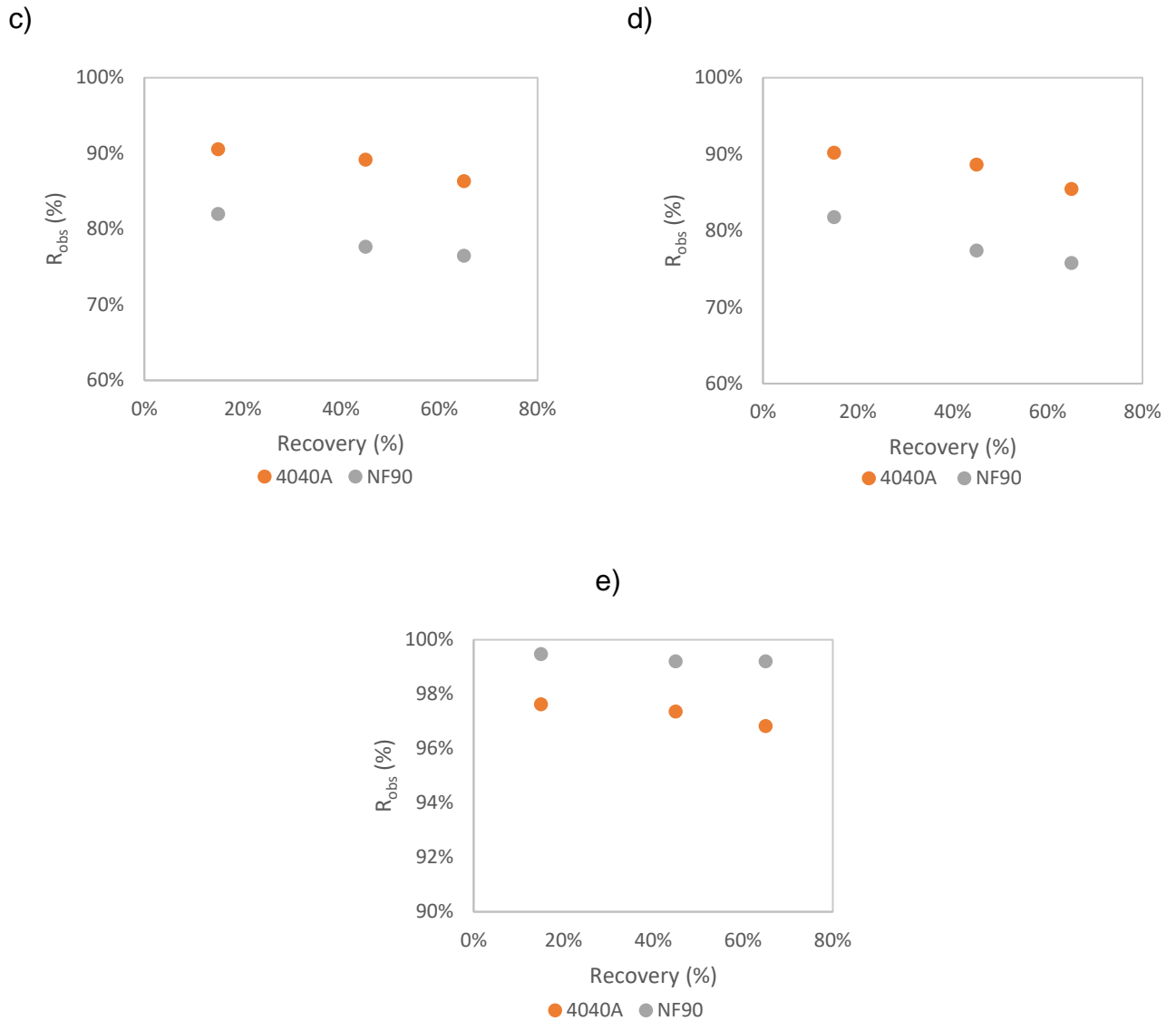
Figure 14 Effect of water recovery on ion rejection at 12 bars. a: Ca^{2+}, b: Mg^{2+}, c: Na^+, d: Cl^- and e: SO_4^{2-}

Figures 14 and 15 show the trend of ions rejection by the membranes, which revealed that 4040A and NF90 4040 performed better overall. The rejection mechanisms with these membranes seem to be strictly driven by the transmembrane pressure, where rejection increase with the applied pressure achieving the maximum rejection over 12 bar of pressure. On the other hand, the NF90 4040 seems to have a high rejection of divalent ions when 8 bar of pressure was applied.

Table 9 Ion concentration in the permeate as a function of pressure and recovery.

Pressure (bar)	Recovery	Ca^{2+} (mg/L)		Mg^{2+} (mg/L)		Na^+ (mg/L)		SO_4^{2-} (mg/L)		Cl^- (mg/L)	
		NF90 (±0.06)	4040A (±0.39)	NF90 (±1.03)	4040A (±0.83)	NF90 (±19.45)	4040A (±15.67)	NF90 (±1.00)	4040A (±1.41)	NF90 (±30.41)	4040A (±67.18)
8	15%	1.55	16.45	1.51	8.72	325.03	274.57	4.00	58.00	473.00	416.00
	45%	3.17	16.09	2.92	11.18	366.61	365.45	6.00	59.00	532.00	545.00
	65%	3.35	27.96	3.12	20.21	398.95	605.75	6.00	96.00	595.00	886.00
12	15%	1.54	3.88	1.35	3.68	278.22	146.15	4.00	18.00	403.00	216.00
	45%	3.07	4.80	2.74	4.49	345.56	167.46	6.00	20.00	499.00	251.00
	65%	3.44	5.72	3.00	5.75	364.08	211.43	6.00	24.00	535.00	321.00
16	15%	1.74	4.14	1.22	4.04	203.71	147.68	3.00	18.00	300.00	214.00
	45%	2.11	4.45	2.11	4.83	258.16	170.50	4.00	21.00	384.00	257.00
	65%	2.54	5.83	2.50	5.98	304.52	212.84	5.00	25.00	456.00	308.00
20	15%	1.26	3.79	1.35	4.35	195.10	150.24	4.00	20.00	288.00	231.00
	45%	3.22	4.74	2.68	5.30	257.73	180.50	5.00	23.00	377.00	270.00
	65%	2.78	5.90	2.93	6.60	309.76	222.19	6.00	28.00	458.00	335.00

a)

b)

c}

d)

76
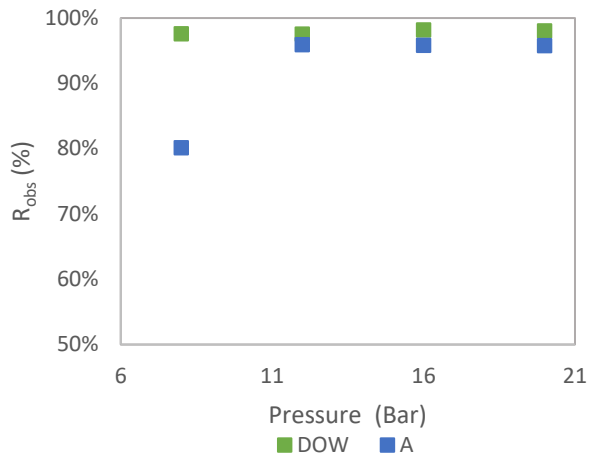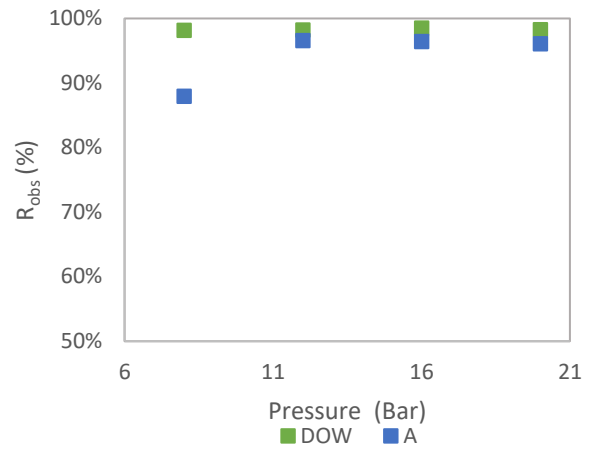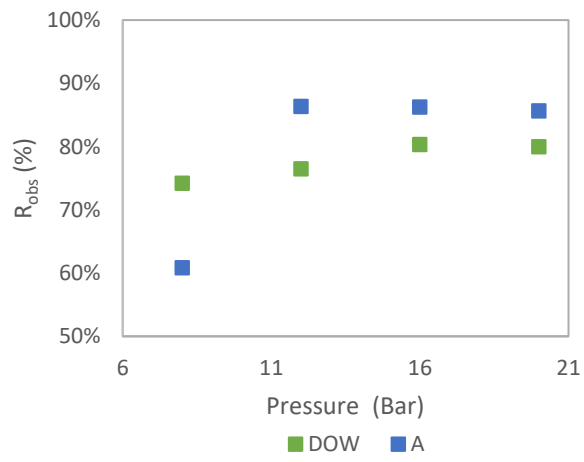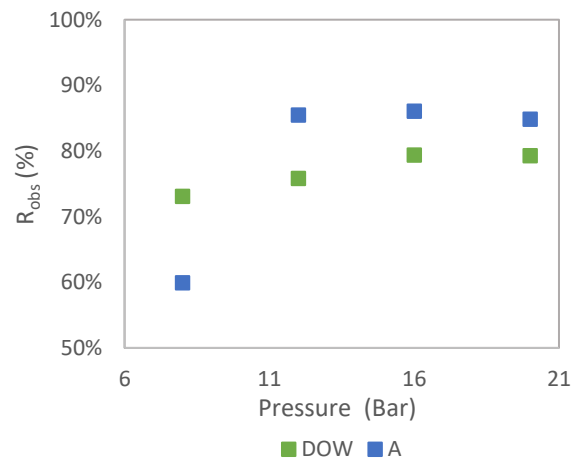
e)
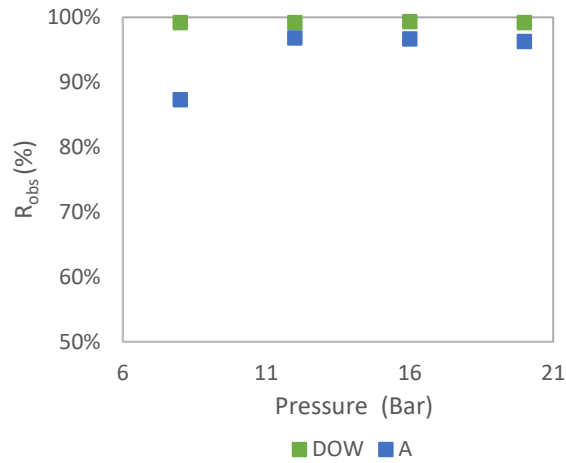
Figure 15 Ion rejection at different pressure at 65% recovery DOW (NF90 4040), A (4040A). a: Ca^{2+}, b: Mg^{2+}, c: Na^+, d: Cl^- and e: SO_4^{2-}

It can be further seen from Figure 15 that the 4040A and the NF90 4040 membranes reject more than 95% of the divalent cations (Ca^{2+} and Mg^{2+}) and more than 74% of Na^+ at a pressure higher than 12 bar and all recovery range evaluated. In the case of the anions, membranes 4040A and NF90 4040 could reject over 87% of sulphate and over 73% of chloride.

77

4.4 Estimation of reflection coefficient and ion permeability through the Spiegler-Kedem-Katchalsky model

Table 10 Reflection coefficient and ion permeability predicted using the SKK model.

Recovery		σ			Ps (m/h)		
		N90 4040	4040A		N90 4040	4040A	
15%	Ca^{2+}	0.989	0.973		6.4×10^{-5}	1.3×10^{-4}	
	Na^+	0.903	0.925		3.8×10^{-3}	1.7×10^{-3}	
	Mg^{2+}	0.993	0.983		9.0×10^{-5}	4.9×10^{-4}	
	SO_4^{2-}	0.898	0.923		3.8×10^{-3}	$1.9E \times 10^{-3}$	
	Cl^-	0.995	0.976		4.1×10^{-5}	9.4×10^{-5}	
45%	Ca^{2+}	0.981	0.968		2.4×10^{-4}	1.5×10^{-4}	
	Na^+	0.848	0.934		3.7×10^{-3}	2.8×10^{-3}	
	Mg^{2+}	0.984	0.982		2.0×10^{-5}	6.7×10^{-4}	
	SO_4^{2-}	0.841	0.931		3.7×10^{-3}	2.9×10^{-3}	
	Cl^-	0.992	0.995		2.0×10^{-5}	9.0×10^{-4}	
65%	Ca^{2+}	0.981	0.962		2.4×10^{-4}	1.7×10^{-4}	
	Na^+	0.839	0.881		4.2×10^{-3}	2.3×10^{-3}	
	Mg^{2+}	0.983	0.965		5.0×10^{-5}	1.6×10^{-4}	
	SO_4^{2-}	0.803	0.876		3.6×10^{-3}	2.4×10^{-3}	
	Cl^-	0.992	0.967		2.0×10^{-5}	1.6×10^{-4}	

Table 10 shows the P_s and the σ for the different ions for the membranes evaluated. The reflection coefficient of the NF90 for calcium ions was the

highest of the two membranes as the divalent ion rejection of this membrane was superior to the other membrane. On the other hand, the σ value for monovalent ions was greater for the 4040A which was the membrane that better performed on monovalent ions rejection. From figure 16, it is acceptable to conclude that the SKK model can be used to explain the retention obtained experimentally as the experimental data fits well with the theoretical data from the model.
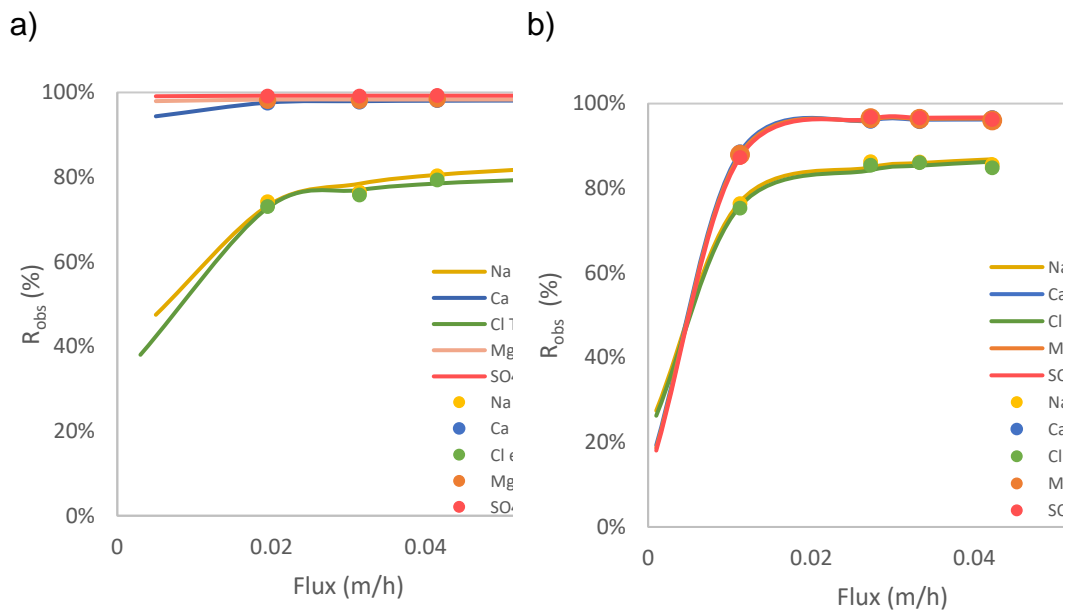
Figure 16 SKK NF modelling. a. NF90, b. 4040A

4.5 Membrane properties

4.5.1 Hydraulic permeability of the membranes

As it has been reported in previous studies with similar membranes, It was found that the flux through the membranes is proportional to the transmembrane pressure (figure 17) (Yammine et al., 2019 and Aktas et al., 2017), obeying the homogenous solution diffusion through the polymeric membrane model. That describes the proportionality of the water mass transfer flux and the pressure differential across the membrane. The permeate flux with the membranes NF90 4040 starts at an applied pressure of 0.884 while with the membrane 4040A start at 2.45 bar. On the other hand, membrane 4040A could present a surface with the tightest pores and is more dependent on osmotic pressure, requiring more force to mobilise the feed

79

through the membrane. Additionally, because of the differences in pore size between the membranes, the permeability of the membranes differs from one to another; as the pore size decrease, the ions in the solution make the surface of the membrane more compact, reducing the permeability of the membranes.
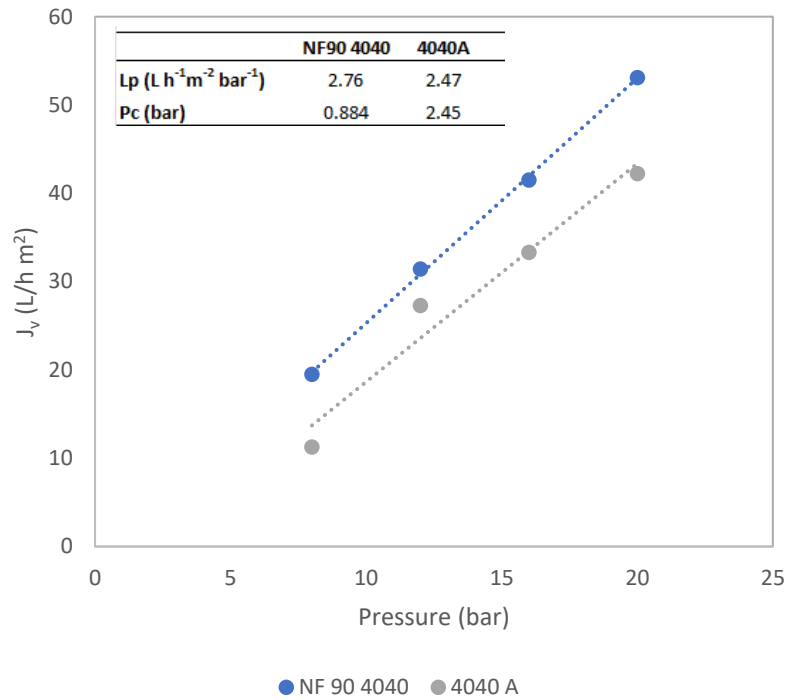
Figure 17 Bore water flux as a function of pressure.

4.5.2 Calculated molecular weight cut-off (MWCO) values.

The MWCO on this occasion was established by the C_{conv} of each membrane determined for the main salt in the feed, sodium chloride. Table 11 shows the MWCO values calculated for the two membranes. The MWCO can be related to mass transport as bigger molecules will diffuse more slowly than smaller molecules; in this order of ideas, when the MWCO is small, the diffusion and the chemical interactions will increase for monovalent ions (Kelewou et al., 2011 and Van de Bruggen et al., 1999). It means that membrane 4040A is the one with the more diffusive transfer.

Table 11 MWCO calculated from NaCl data for each membrane.

Membrane	MWCO calculated (Da)	MWCO theoretical (Da)
NF90 4040	167	100-200 (Hidalgo et al., 2013, Luo et al., 2010, Jadhav et al., 2016, Krieg et al., 2005 and Tanne et al., 2019)
4040A	131	No Reference available

.

4.5.3 Estimation of membrane pore radius

Table 12 Average pore radius from SHP model.

Membrane	Recovery	Ca^{2+}	Na^+	Mg^{2+}	SO_4^{2-}	Cl^-	Average P_r	Theoretical P_r (nm)
	15%	0.34	0.25	0.38	0.25	0.16		
NF90 4040	45%	0.35	0.27	0.39	0.25	0.18	0.29	0.31 (Ramdani et al., 2021)
	65%	0.35	0.27	0.39	0.25	0.19		
	15%	0.36	0.24	0.39	0.27	0.16		
4040A	45%	0.37	0.24	0.39	0.25	0.16	0.29	No reference Available
	65%	0.37	0.26	0.42	0.27	0.17		

An average pore radius was determined using the data of the reflection coefficient determined by the SKK model for each ion at each recovery. Table 12 shows, that the NF90 and 4040A have similar pore radius. The findings demonstrate that a pore size dispersion rather than a fixed pore size was more a distribution pore size with not geometrically define pores for these membranes. It was expected to have a similar pattern to the one obtained with the MWCO, 4040A smallest pore radius than the other membrane. However, the ionic interactions, the complex separation mechanism of NF membranes and ions present in the bore water that might not be accounted in the analysis are obstacles for the accuracy of any model implemented.

4.6 Mass transport through each membrane - hydrodynamical approach

By plotting the concentration of ions in the permeate (C_p) and the flux trough each membrane (J_v), it is possible to determine the solute flux due to diffusion by the slope (j_{diff}) and the solute transport due to convection by the intercept (C_{conv}).
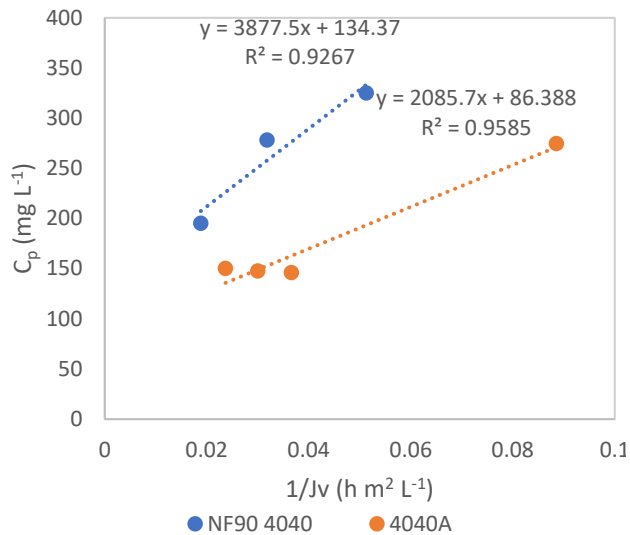
Membrane	C_{conv} (mg L^{-1})	j_{diff} (mg m^2 h^{-1})
NF90 4040	134.37	3877.50
4040A	86.39	2085.70

Figure 18 Permeate NaCl concentration as a function of the inverse of flux at 15% of the recovery.

In nanofiltration, the transport of ions is not well defined. It seems to be a complex mechanism that combines the sieving effect of the ultra and microfiltration and the diffusion transport by membrane ionic strength that is characterised in reverse osmosis processes. Figure 18 displays an hydrodynamical approach however it is limited due the assumption of non-charged membranes.

Table 13 Peclet (Pe) number of each membrane for Na at different pressures.

Membrane	8 bar	12 bar	16 bar	20 bar
NF90 4040	0.68	1.09	1.44	1.84
4040A	0.47	1.13	1.38	1.75

Table 13 shows the Pe values for each membrane at different operating pressures. The mass transport through the membranes is affected by the changes in pressure. At low pressures, the diffusional mass transfer is

82

dominant for the NF90 4040 and 4040 A (Pe<1). This effect is due that convective mass transfer being governed by physical parameters such as pressure (Lhassani et al., 2001). Additionally, diffusive mass transfer is stronger than convective mass transfer, which means that the solvation energies and the effect of ion concentration are more notorious at low operation pressures, as discussed previously (Dach, 2009).

4.7 The effect of a second nanofiltration stage on water recovery

Recovery of high percentages of water is one of the main limitations of water treatment processes. Figure 19 shows the implementation of two stages of nanofiltration using the membrane 4040A membrane. This experiment was evaluated at 12 bar of pressure and by recovering the concentrate from the first stage which is mixed in the same proportion with bore water. This mix is fed into a second nanofiltration stage and filtration was conducted from these experiments, it was determined that the final ion removal at 90% recovery of the permeate was 91% for Ca^{2+} and Mg^{2+}, 70% for Na^+, 63% for Cl^- and 93% for SO_4^{2-}. For mineral processing operations where the presence of divalent ions (Ca^{2+}, Mg^{2+} and SO_4^{2-}) is critical such as the flotation of phosphate minerals, the operation of a two-stage system could be a promising option to maximize water resources utilization. The removal of monovalent ions through the two-stage system may not be adequate for operations such as the monazite flotation where the concentration of monovalent ions (Na^+ and Cl^-) over 500 ppm could slightly affect the recovery and grade of the concentrate. These results indicate that nanofiltration systems could be tailor-made according to the necessities of each operation as different minerals are susceptible to a different ion in solution.
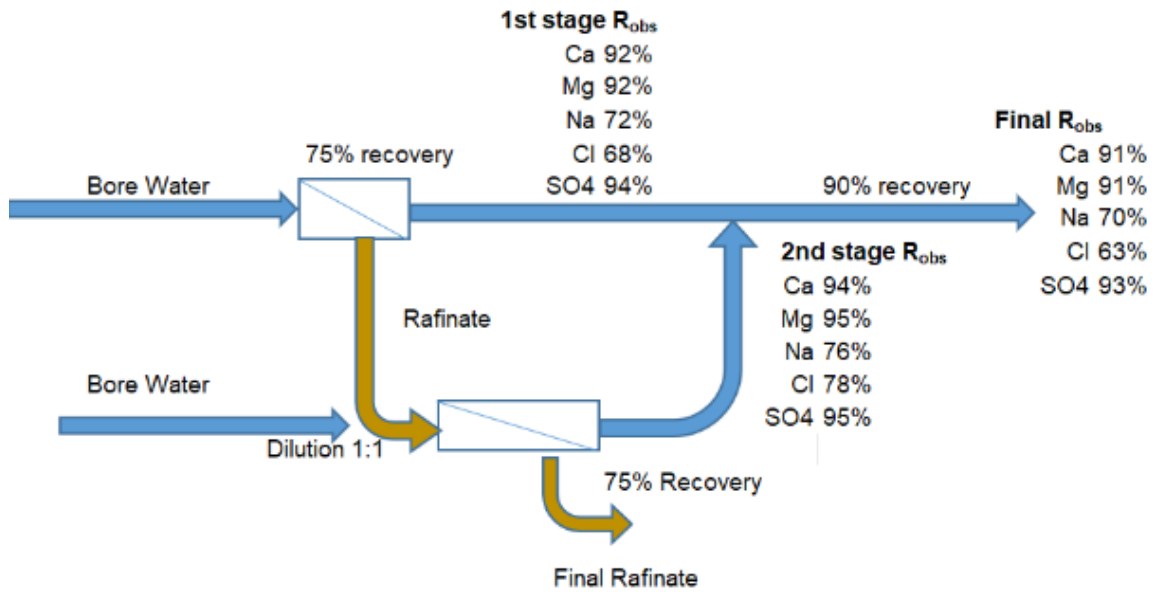
Figure 19 Two-stage nanofiltration process at the recovery of 90% of permeate.

4.8 Energy cost estimation for single stage and two-stage processes

In pressure-driven processes, energy cost is the main component in the operating cost of these systems representing. The high consumption of energy in processes such as nanofiltration and reverse osmosis are principally associated with the high-pressure pumps used which could represents up to 60% of total water treatment cost (Grano et al., 1995). The specific energy requirements for a pressure-driven process can be quantified by the correlation of the pressure and the recovery of permeate, and generally, the energy requirement increases linearly with increasing the pressure of the system (Dach, 2009 and Kiitchen and Wang 2022). The specific energy consumption (SEC) of membraned-based water treatment can be given by:

$$SEC = \frac{\Delta P}{\eta\, r}\frac{100}{36} \qquad [37]$$

Equation 1 Specific energy consumption nanofiltration

Where ΔP is the transmembrane pressure in bar, η is the global pumping efficiency (generally 85%) and r is the water recovery of the system.

Table 14 Estimated specific energy consumption and cost as a function of pressure.

Pressure (bar)	Single stage		Two-stage	
	SEC (kWh/m^3)	$/ton	SEC (kWh/m^3)	$/ton
12	0.523	0.192	0.697	0.257
16	0.697	0.257	0.930	0.343
20	0.871	0.321	1.162	0.429
25	1.089	0.401	1.452	0.536

Table 14 shows the comparison of specific energy consumption at different transmembrane pressures. In this comparison, an assumption of standard water consumption in mineral processing operations of 3 m^3 per ton of ore processed, and electricity prices of 0.123 $/kWh for industry reported by the Australian energy council in 2022 were considered (Bulut and Yenial, 2016 and Kitchen and Wang, 2022). In this study, it was found that a single stage with 4040A membrane at 12 bar of transmembrane pressure resulted in conditions to produce water with sufficient quality for mineral separation processes representing an energy cost of 0.192$/ton. Comparing a single stage with the two-stage process can be notice that the increment on energy cost is 33% on the other hand the water recovery increases up to 90%. Comparing the result in table 14 with high pressure systems such as reverse osmosis that usually require around 20 bar to treat brackish water with similar quality as the one tested in this study is expected an estimated energy cost increase of up to a 67% rising the energy consumption from 0.871 to 0.523 kWh/m^3 and producing water with ultrahigh purity that in mineral processing operations sometimes is not required (Grano et al., 1995 and Guimares and Peres 1999). Even though, comparing the two-stage nanofiltration process will represent a 25% less energy consumption than process with high transmembrane pressure.
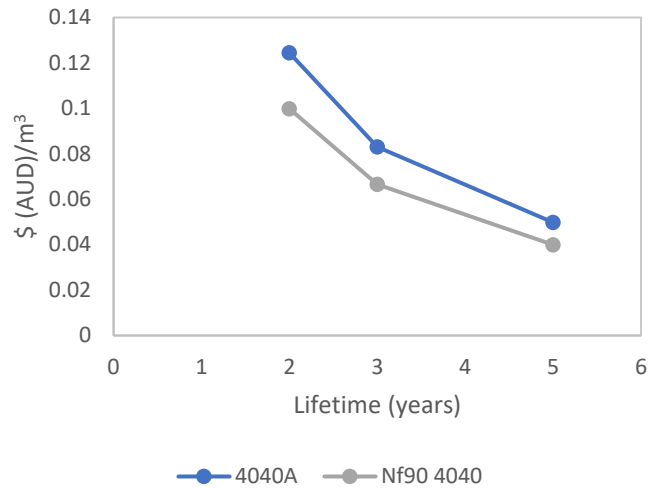
Figure 20 Membrane replacement cost at different lifetimes (at 16 bar of transmembrane pressure and 65 % recovery)

Membrane replacement cost is another key operating cost. This variable is associated with the permeability, production rate of each membrane and its lifetime. This parameter can be expressed through the following expression (Winston and Sirkar, 1992):

$$RC = 2.74 \ F_R \ M_C \ M_P^{-1} M_l^{-1} \hspace{3cm} [38]$$

Where RC is the unit replacement cost represented in AUD per every m^3 of water produced at different time of membrane lifetime, M_C is the cost of the membrane (AUD/ft^2) which was obtained from a local membrane provider, F_R is the water recovery, Mp is the membrane productivity and M$_l$ is the membrane.

Figure 20 shows how membrane with different permeabilities can have different the cost of replacement of a unit for each m^3 of water produced. Therefore, a membrane with low MWCO will represent an increase in cost due to the low membrane production rate. In that order ideas, the cost of replacement of membranes that performed with low ion rejection but high permeate flow rate will be lower than membranes that have similar characteristics to a reverse osmosis membrane such as the 4040A or the NF90 4040. A factor to consider in the membrane replacement cost, Is the lifetime of the membrane. As the ion rejection increase, the lifetime of the membrane is reduced due to multiple factors, such as fouling and concentration polarization

86

resulting in increase of pressure to achieve the same results (Govardan et all., 2020 and Liu et al., 2020). Hence, comparing nanofiltration membranes with reverse osmosis membranes, since in nanofiltration the ion rejection is lower than in RO, it is expected to have a higher lifetime operating with nanofiltration membranes resulting in reasonable membrane replacement costs producing water with the quality required. It is important to mention that cost optimization in pressure-driven processes will depend mainly on the operation pressure of the system and the right selection of membrane to achieve the water quality required.

4.9 Conclusions

The nanofiltration membranes NF90 4040 and 4040A were considered in a pilot scale rig to study their performance in producing water with concentrations under the threshold of 50 mg/L of calcium and magnesium and 500 mg/L of sodium. The influence of pressure was evaluated, and it was found that the ion rejection is proportional to the transmembrane pressure. Additionally, it was determined that pressure is an important factor in the transfer mass mechanism. In this case, the rejection of ions by nanofiltration through the 4040A and the NF90 membranes at low pressures was driven by diffusional mass transfer, however, over 12 bars of transmembrane pressure the process is driven by convection or sieving effect through the pores. From the hydraulic point of view, it was demonstrated that the high permeate leads to a low ion rejection, concluding that the highest permeate flux between leads to low rejection. Also, it was found that both membranes (NF90 4040, 4040A) reject more than 95% of calcium and magnesium and more than 74% of sodium at pressures over 12 bar and recovery of 65%.

The MWCO determined in this study of 4040A (Ecotechnol) was lower than the other membrane used. MWCO and theoretical pore size of NF90 4040 estimated in this study agrees with the range reported in other studies that used this membrane in similar conditions. The SKK model was fitted to predict the ion removal of the two nanofiltration membranes used. The solute permeability and reflection coefficient constants were obtained, reflecting a satisfactory representation of the nanofiltration process of the bore water used

in this study. Furthermore, it was demonstrated that the permeability of divalent ions is lower than that of monovalent ions.

# 5   CHAPTER FIVE: ELECTRODIALYSIS RESULTS AND DISCUSSION

5.1   Abstract

In this chapter, bore water from the Goldfields area in Western Australia was treated by electrodialysis (ED) evaluating its performance to produce fit-for-purpose water for mineral processes. Various operating conditions such voltage and flow velocity for ED systems were studied, achieving removals of more than 90% and 98% for monovalent ions (Na^+ and Cl^-) and divalent ions (Ca^{2+}, Mg^{2+} and SO_4^{2-}), respectively, at 87% TDS. It was observed that increasing the flow velocity reduces the efficiency of the ED system by up to 8%. Additionally, higher flow rates increase the current density decreasing the cell performance. The optimum operating conditions for ED were determined as an applied voltage of 1 V per membrane pair, flow rate of 45 L/h and 40 minutes treatment time. The results show that ED is a efficient method to achieve the quality of water required without exceeding the ion concentration threshold for mineral processing. From an economic point of view, ED is the better option in comparison to the former method used (NF) due to its low energy consumption and the relatively low replacement cost associated with a high membrane lifetime.

5.2   Introduction

This chapter shows the results of the electrodialysis experiments. In this part of the study was determined the limiting current density to set up maximum conditions of operation to evaluate parameters such as flow velocity, voltage, and concentration of ions in the feed. Also, a modelling of the system was performed to identify the main ions transfer mechanism in the electrodialysis stack used. In addition, optimal conditions for dimensioning were determined and utilised to perform an economic analysis of the system.

5.3   Effect of flow velocity on limiting current density
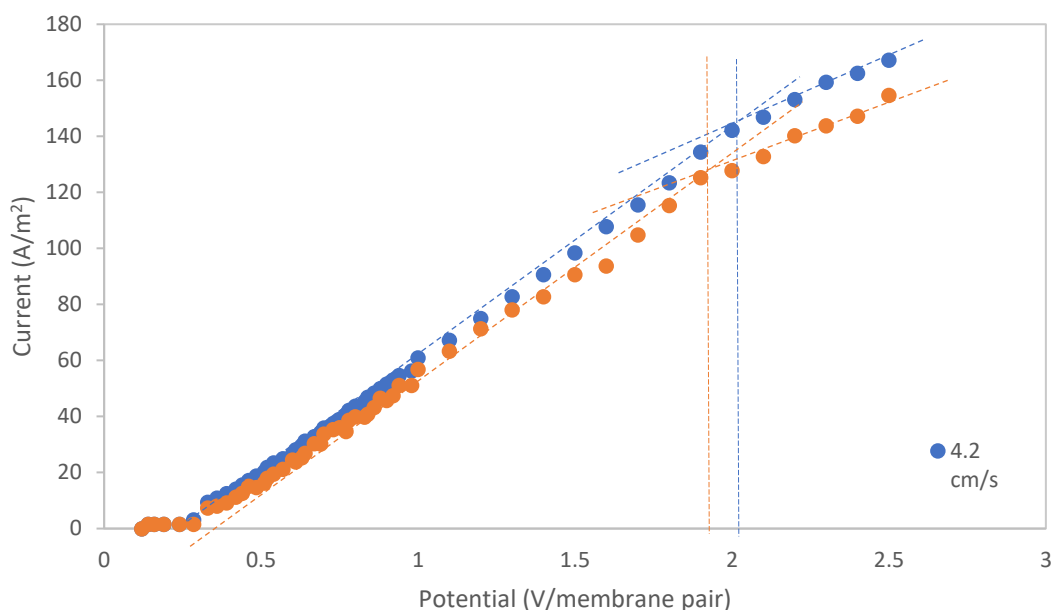
Figure 21 Limiting current density - Bore water at different flow velocities.

Figure 21 shows the curve to determine the limiting current density. in general, it can be seen that the plateau region is not clear to identify, However, it can be identified a changed in slope beyond approximately 1.8 V and 2.1 V representing the LCD at around 120 A/m^2 and 145 A/m^2 for the two flow velocities tested, 2.3 and 4.2 cm/s respectively. Possible events that contribute to not visualize properly the change from the ohms law to the characteristic plateau of the LCD can include the strength of the electric field, which obscures the current limit's value, is one potential contributing factor and the cell's structure and the turbulence promoters inside that tend to lessen the visibility of the plateau. The experimental data for the bore water at two different flow velocities shows that the LCD increases as the flow velocity gets higher. This is because high flow rates cause more turbulence, reducing the thickness of the diffusion layer allowing electroactive species to move through cells more quickly, reaching the membrane surface faster than at low flow velocities. Additionally, because current is proportional to the speed of ion movement, the latter increases at higher flow velocities (Devora-Isiordia et al., 2021).

90

5.4 Effect of ions concentration on Limiting Current Density
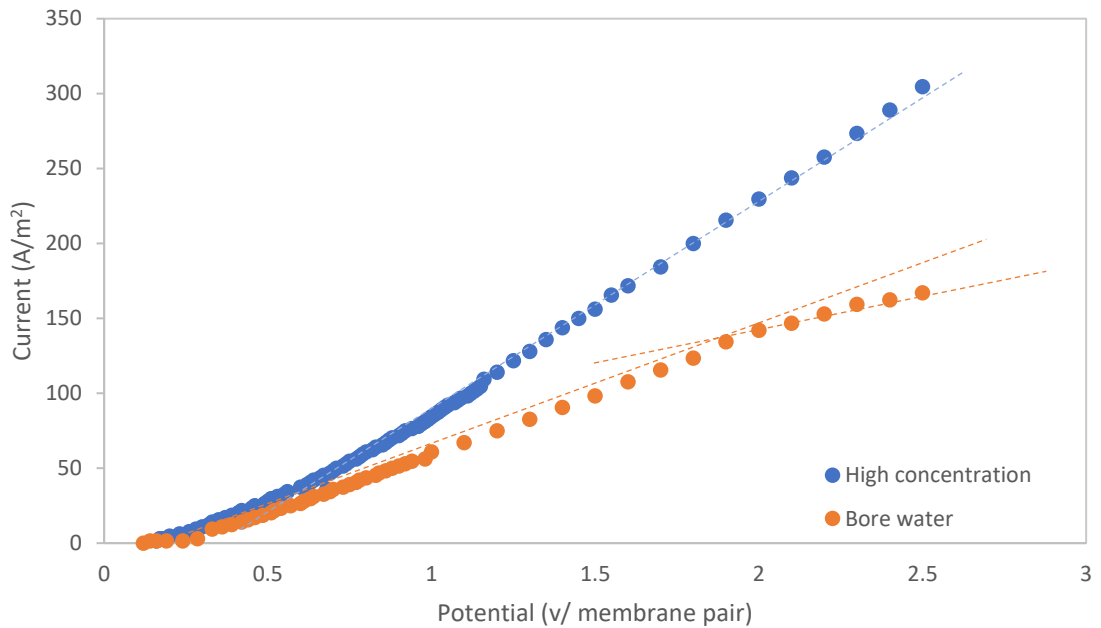
**Figure 22** Limiting current density at different ion concentrations.

As mentioned in previous chapter, the limiting current density is an important parameter on electrodialysis operation. This parameter defines the maximum electric current that can be used in a specific system. The figure 22 shows the voltage-current plots for the bore water and for synthetic water with three times the ion concentration of the bore water. Generally speaking, can be noticed that the slope increases with the increment of ions concentration in the feed solution. Also, it is important to mention that the slope moderately increase over 0.5 V/membrane pair applied, and this is due to the increase of ion mobility triggered by the Joule heat production with the increase of current (Bo et al., 2019). The bore water curve shows a slightly change on slope indicating that the limiting current density was reached at voltage applied of ~2.1 V/ membrane pair. which means that over this current the concentration of the electrolyte in the dilute tends to zero in the diffusion layer on the membrane surface.

5.5 Effect of applied voltage on Ions removal
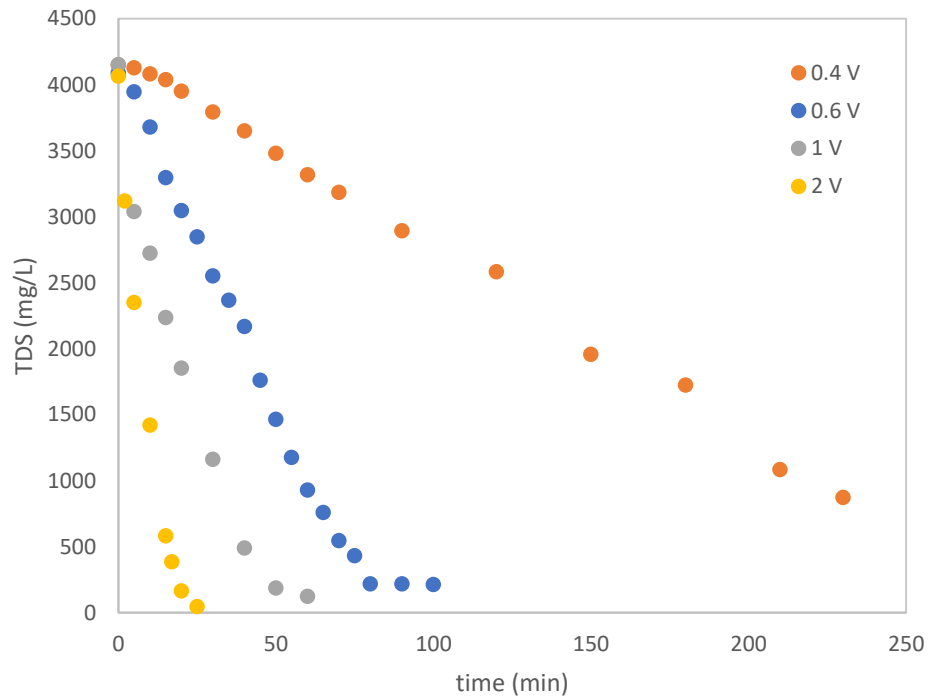
Figure 23 TDS removal in the diluate stream at different voltages

The performance of the ED module tested was evaluated through the concentration of ions and the change in concentration of total dissolved solids. The removal of total dissolved ions from the bore water is shown in figure 23. In general, the total dissolved solids are removed faster at higher voltage applied to the ED stack as the current flow is higher mobilising, more ions from the dilute to the concentrate. It can be seen that at higher potential applied, the concentration required is reached faster. It has been defined that a concentration of total dissolved solids below 1000 mg/L will provide the cations and anions concentration required for the mineral processing operations such as the monazite flotation.

a)

b)

c)

d)
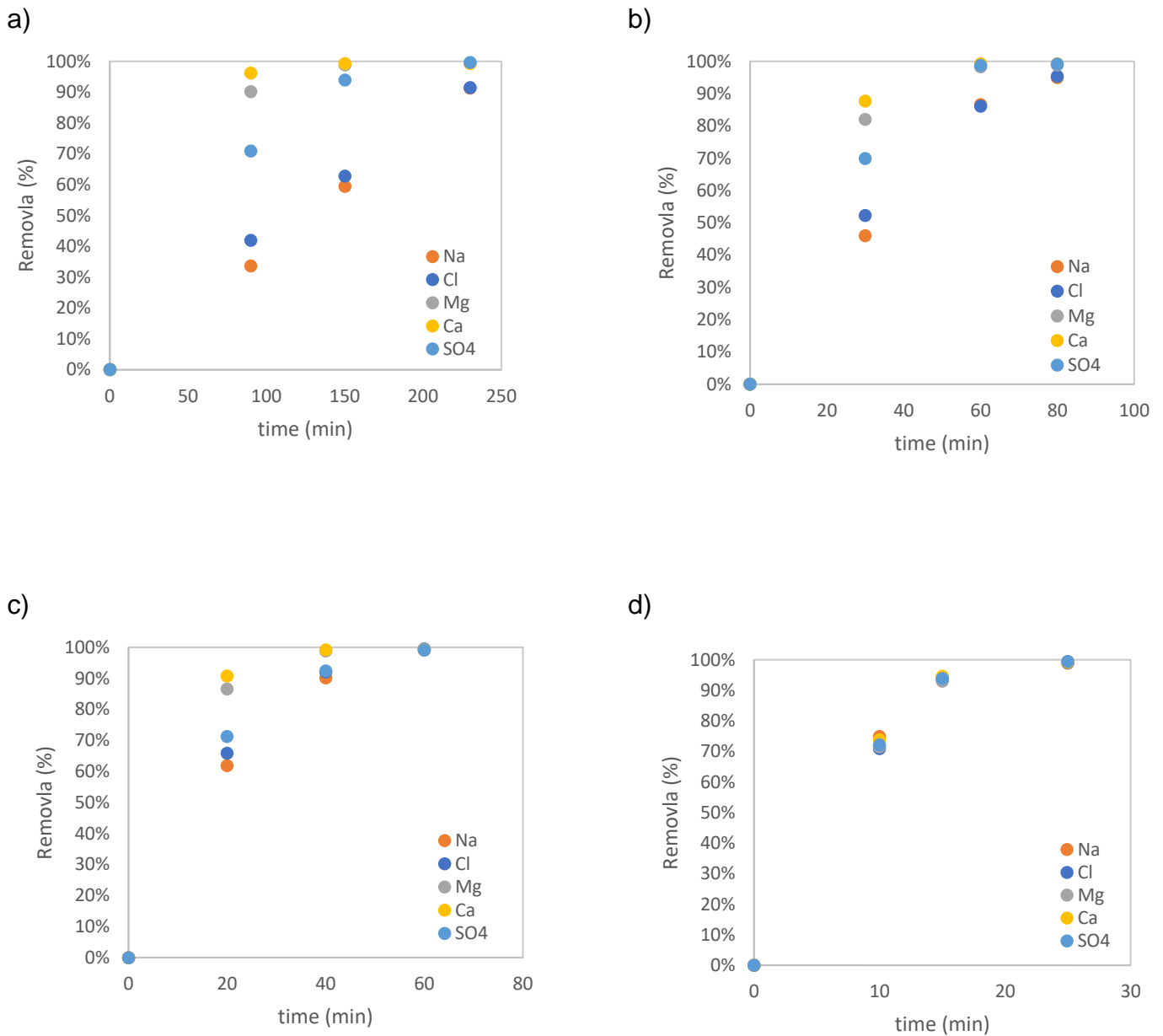
Figure 24 Effect of voltage on ions removal. a) 0.4, b) 0.6, c) 1, and d) 2 V/ membrane pair

The ion exchange membranes make the way easy for the selective permeation of ions with opposite charges facilitating the transport of co-ions. Figure 24 is shown the depletion of cations and anions from the dilute stream (Bore water). the applied voltage influence how the different ions are depleted from the diluate. As the voltage is increased, the removal of ions is faster as the current flow is increased. At low voltages, such as 0.4 V/membrane pair, divalent and monovalent ions are depleted differently. The depletion rate at 4 V/ membrane

93

pair depends on the charge of each ion. It can be seen that divalent ions such as calcium, magnesium and sulphate are depleted at a slower velocity than monovalent ions. This is due to the fact that monovalent ions are less hydrated, making them more susceptible to pull out faster from the diluate. In addition, the bulkier the ion, such as monovalent ions, the more it is removed by the membrane, this agrees with the results displayed by Table 15 which shows the ion selectivity of the membranes towards the cations and the anions at 3 different voltages applied. For the cations it can be seen that calcium is transported slower than sodium and magnesium and for the anions, chloride ions are transported faster than the divalent ions of sulphate. It can be seen that the membrane selectivity changes at different voltages applied. This is due that monovalent ions are less hydrated, making them more susceptible to be pull out faster from the diluate. In addition, the buliker the ion, such as monovalent ion the more it is removed by the membrane (Walha et al., 2007 and Patel et al., 2020)

5.6 Modelling of synthetic NaCl (4.5 g/L) solution by Nernst-Planck model
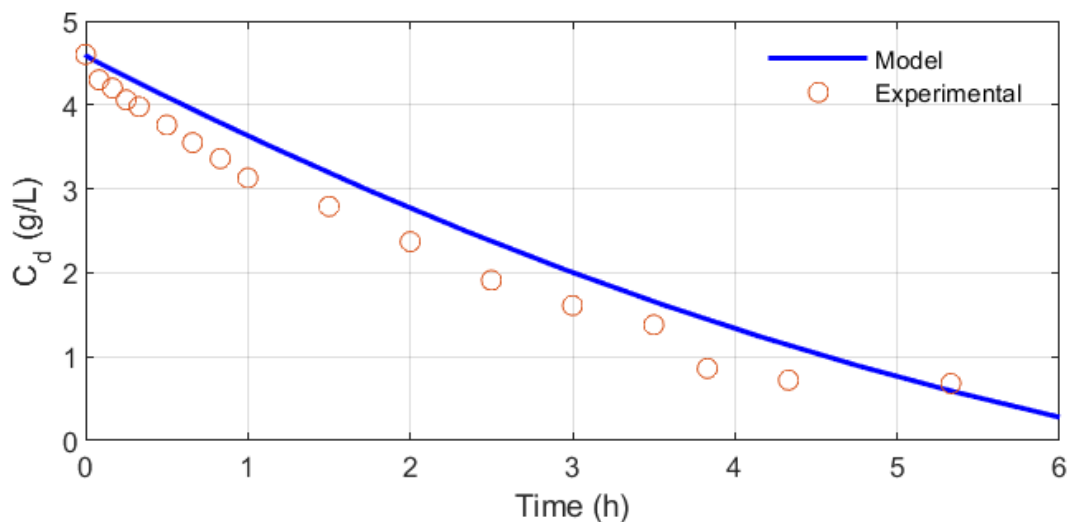
Figure 25 Modelling of 4.5 g/L NaCl solution.

Figure 25 show experimental and theoretical data for the concentration of NaCl in the diluate through the time at a current density of 14 A/m^2. Despite the fact that the model was created on a fairly idealised foundation and had a number

94

of restrictions and suppositions, comparing the experimental results with the predicted results there was an average relative error of 12%, It has been reported on literature relative error between 2% and 10% on this model and it has been associated mainly to the assumption of maximum efficiency of the process and parameters assumed from theory and not measured experimentally. Also, problems of scaling of the membranes may have had an impact on the deviations of the model evidenced (Casas, 2011). Also, from the model was identified that migration (M=5.18x10^{-4} m^2/h) forces are stronger than diffusion (2.61x10^{-9} m^2/h) mass transfer, however, in figure 26 can be seen that the diffusion coefficient increase as the gradient of concentration is bigger between the concentrate and the dilute.
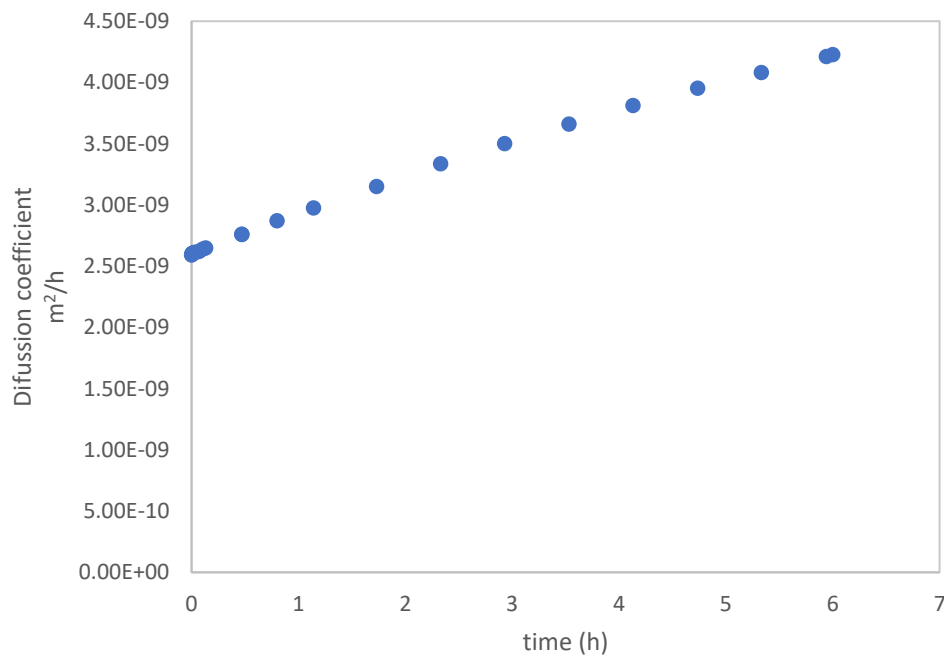
Figure 26 Diffusion coefficient through time

5.7 Membrane selectivity

Table 15 Membrane selectivity

	0.4 V/pair	1 V/pair	2 V/pair
S_{Mg}^{Ca}	-0.00494	-0.00199	-0.000849
S_{Na}^{Ca}	-0.06307	-0.04801	-0.00200
S_{SO4}^{Cl}	0.068325	0.00223	0.002299

5.8   Effect of flow rate on TDS removal

The effect of the feed velocity on the desalination was evaluated (figure 27). Regardless of the feed velocity, the pattern of TDS decreases when the velocity is increased. This trend is explained by the shortened residence time of contact between the streams and the membranes. This is explained by the free movement of monovalent ions at low velocities allowing the monovalent ions to find exchange sites available on the membrane, which are usually occupied first by divalent ions, which impose stronger electrostatic forces (Karimi, Ghaseemi and Zamani, 2018).
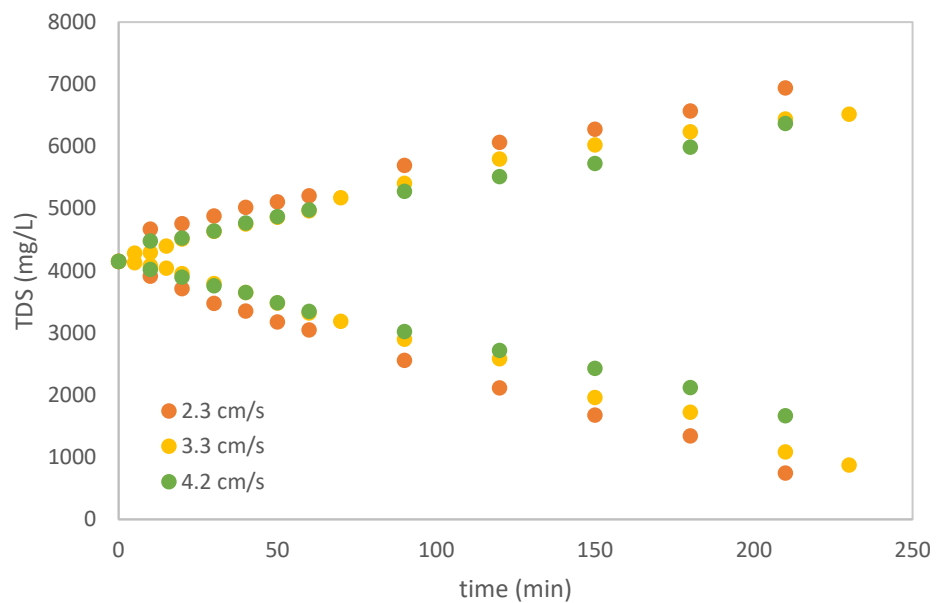
Figure 27 Effect of linear velocity

5.9   Specific treatment capacity (STC)

Table 16 shows the treatment capacity for the bore water and the synthetic water. the results indicate that the treatment capacity highly depends on the ion concentration and the number of ions to be removed. The STC calculated for the two different samples demonstrates that the capacity is reduced when the ions concentration in the feed water increases. It has been demonstrated that systems with SPC higher than 30 L/h m^2 are difficult to operate and require high control and optimisation due to high current densities (PCCell). Having in mind the current characteristics of the bore water, it is not recommended to remove of ions with applied voltage over 1 V/ membrane pair.

Table 16 Effect of voltage on Specific treatment capacity

Applied voltage. (V/ membrane pair)	Water	STC (L/h m^2)
0.4	Bore water	2.13
0.6	Bore water	7.44
1	Bore water	14.88
	Synthetic water	5.58
2	Bore water (4.2 g/L)	37.20
	Synthetic water (12 g/L)	16.53

5.10 Effect of ion concentration

a)   b)
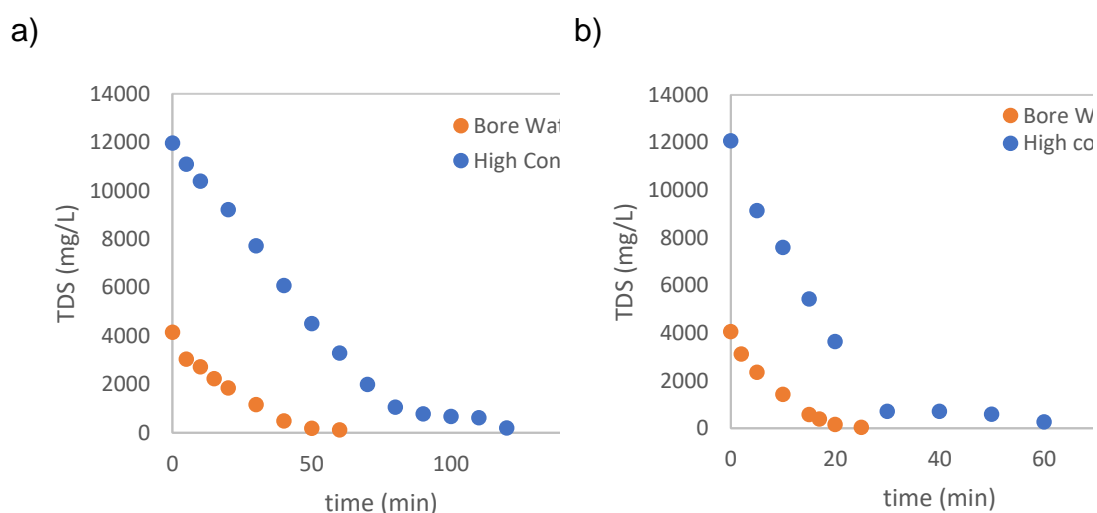
Figure 28 Effect of feed ion concentration on process time

One of the characteristics of the groundwater in Western Australia is the variability of the ion concentration. Synthetic water with three times the concentration of ions in the bore water was tested. the results in the figure 28 shows that it will require 2.6 and 2.3 times more time (1 V and 2 V per cell pai respectively) to reach a concentration of around 1000 mg/L.

5.11 Energy cost estimation

In membrane processes, energy cost is the main component in the operating cost of these systems. The high consumption of energy in processes such as

97

nanofiltration and electrodialysis are principally associated with the energy associated with the ions mass transfer associated with high voltage which could represent up to 60% of total water treatment cost (Grano et al.,1995).

The desalination energy for a specific flow rate is determine by:

$$SEC_{ED} = \frac{U \int_0^t I \, dt}{Q_{d*} * t}$$ [39]

Where U is the applied voltage, I is the current and t is the time to achieve a concentration of TDS below 1000 mg/L (Sosa et al., 2021).

Figure 29 shows the energy consumption, SEC, of ED for two different ion concentration feed waters. Figure 29 shows the energy consumption, SEC, of ED for two different ion concentration feed waters. Bore water and synthetic water with higher concentrations of ions were tested at fixed productivity of 14.8 L m^{-2} h^{-}. As was expected, the SEC increases exponentially with the depletion of ions from the diluate stream and increases with the feed ions concentration.
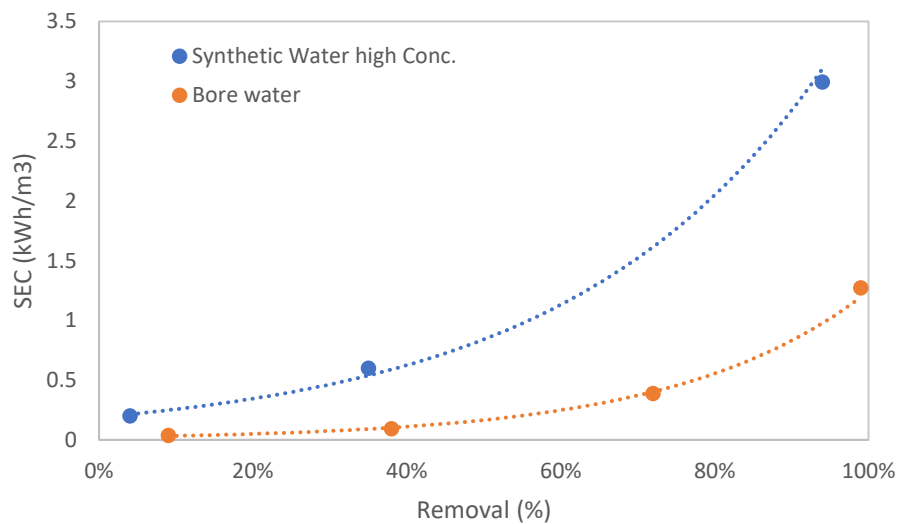

Figure 29 Effect of feed ion concentration on energy consumption

98

Table 17 Estimated specific energy consumption and cost for 75% TDS removal in ED.

Electrodialysis	
SEC (kWh/m³)	$/ton
0.45	0.167

Table 17 shows the specific energy consumption to achieve 75% of TDS removal which is the removal required to reach the ion concentration below the threshold in the diluate. For this estimation an assumption of standard water consumption in mineral processing operations of 3 m^3 per ton of ore processed, and electricity prices of 0.123 $/kWh for industry reported by the Australian energy council in 2022 were considered (Bulut and Yenial, 2016 and Kitchen and Wang, 2022).
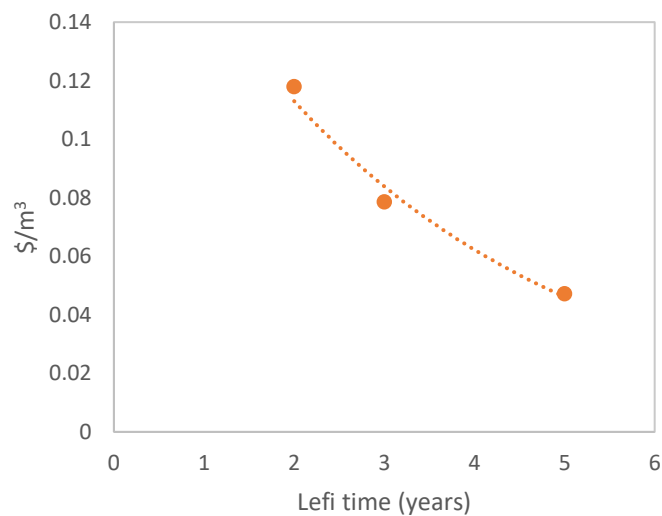
Figure 30 Membrane replacement cost at different lifetimes

Membrane replacement cost is another key operating cost. This variable is associated with, production rate of each membrane and its lifetime. This parameter can be expressed through the following expression (Winston and Sirkar, 1992):

$$RC = 2.74 \, F_R \, M_C \, M_P^{-1} M_l^{-1} \qquad [40]$$

99

Where RC is the unit replacement cost represented in AUD per every m^3 of water produced at different time of membrane lifetime, M_C is the cost of the membrane (AUD/ft^2) which was obtained from a literature (Nayara et al., 2016), F_R is the water recovery, Mp is the membrane productivity and M_l is the membrane.

The main advantage of ED systems is that these, usually provide long membrane lifetime and depending on the critical ions for each mineral processing operation, the membranes can be perm-selective to monovalent ions prolonging the lifetime reducing the polarisation by other ions that are not critical (Amshave et al., 2020). It is important to mention that cost optimisation in membrane processes will depend mainly of driven force of the system and the right selection of membrane to achieve the water quality required.

5.12 Conclusions

Electrodialysis results indicate that parameters such as ion concentration, linear velocity and voltage are key to considering electrodialysis as an alternative. The limiting current density in the ED system was affected by the concentration and the flow velocity in the cell, and it should be having into account by every change in the feed. Since the ion transport force is increased, a higher applied voltage will make the process of ion removal faster. Also, from the results can be concluded that the ion removal is inversely proportional to the feed flow velocity, and it is associated with the reduction of contact time between the different streams and the membranes. The best performance achieved was at the applied voltage of 1 V/membrane pair, given that at this voltage the treatment capacity was higher within the real processes. At these specific conditions (1V per membrane pair and 45 L/h) and 40 minutes of treatment the removal achieved was more than 90%, 98% and 87% of monovalent ions (Na^+ and Cl^-), divalent ions (Ca^{2+} Mg^{2+} and SO_4^{2-}), and TDS respectively. The model of Nernst-Planck demonstrates that the dominant force that mobilize ions in the system is migration, however, diffusion of ions increases as the gradient of concentration increases between the concentrate and the diluate.

From the point of view of energy consumption, ED is 13% more efficient than nanofiltration. However, in terms of membrane replacement cost seems to be not much difference between both technologies.

6 CHAPTER SIX: PRECIPITATION RESULTS AND DISCUSSION

6.1 Abstract

This chapter aims to study precipitation as an option to produce suitable water from groundwater enriched with dissolved solids. It discusses the performance of precipitation with two different methods the first method is the ultra-high lime aluminium (UHLA) which uses lime and sodium aluminate to remove critical ions such as calcium, magnesium, sulphate and chloride and the second method of precipitation with oxalic acid. The results indicate that precipitation can reduce more than 97% of divalent ions such as calcium, magnesium, and sulphate and 68% chloride. In addition, due to improvement in reagent selectivity, chloride removal could be improved by a further 22% by implementing a two stages process. The main crystal phase identified by XRD in the precipitates were hydrocalumite ($Ca_4Al_2(OH)_{12}(Cl)_2 \cdot 4H_2O$), bayerite ($Al(OH)_3$) and calcite ($CaCO_3$). In addition, operational conditions such as pH and temperature affect chloride removal positively. However, at temperatures over 40 ºC this effect is reversed due to the stability of calciumchloroaluminate compounds at high temperatures.
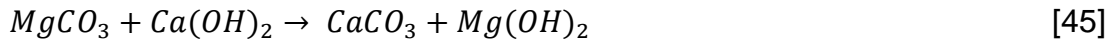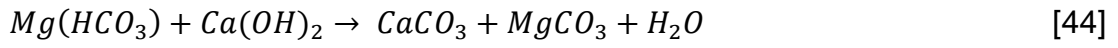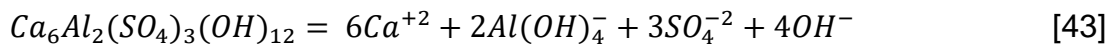
6.2 Introduction

This chapter discuss the results based on the experiments performed with two different precipitants (oxalic acid and lime combined with sodium aluminate) at different operational conditions. The operational conditions evaluated in the results of this section were the time of reaction, the dose of precipitants, pH and temperature. Also, XRD was performed in the precipitates to confirm and discuss the reactions involved in the system. Furthermore, different configurations of reagents dose were evaluated to establish optimal conditions of the systems.

6.3 Ultra-High Lime Aluminium (UHLA) precipitation.

6.3.1 Equilibrium time of ions removal.

An experiment was conducted to study the reaction's kinetics and the removal of ions during precipitation by UHLA. The main reactions expected in the system are as follows (Almasri, 2013 and Abdel-Wahab, 2003).

102

$$4Ca^{2+} + 2Al(OH)_4^- + 2Cl^- + 4OH^- = Ca_4Al_2Cl_2(OH)_{12} \qquad [41]$$

$$Ca^{2+} + SO_4^{2-} = CaSO_4 \qquad [42]$$

$$Ca_6Al_2(SO_4)_3(OH)_{12} = 6Ca^{+2} + 2Al(OH)_4^- + 3SO_4^{-2} + 4OH^- \qquad [43]$$

$$Mg(HCO_3) + Ca(OH)_2 \rightarrow CaCO_3 + MgCO_3 + H_2O \qquad [44]$$

$$MgCO_3 + Ca(OH)_2 \rightarrow CaCO_3 + Mg(OH)_2 \qquad [45]$$
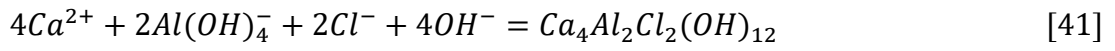
a)
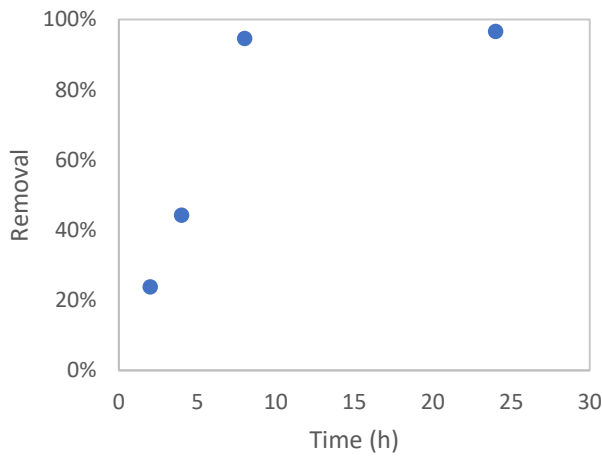
b)
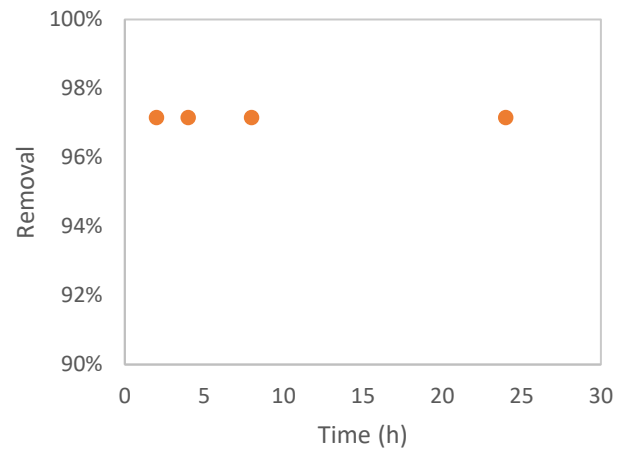
c)

d)

Figure 31 kinetics of ions removal (Ca^{2+}/Cl^-, SO_4^{2-} ratio 2:1 and Al^{3+}/Cl^-, SO_4^{2-} ratio 1.5:1) a: Ca^{2+}, b: Mg^{2+}, c: Cl^- and d: SO_4^{2-}

103

Having in mind the main chemical reactions expected in the system, a kinetic study has been made using calcium hydroxide and sodium aluminate/chloride and sulphate ratio of 2:1 and 1.5:1 respectively. Figure 31 shows the removal of calcium, magnesium, chloride, and sulphate over time. These results suggest that the equilibrium is reached after four hours, and the concentration of the ions was steady in almost all cases. Since the aluminium source for the experiments completed was sodium aluminate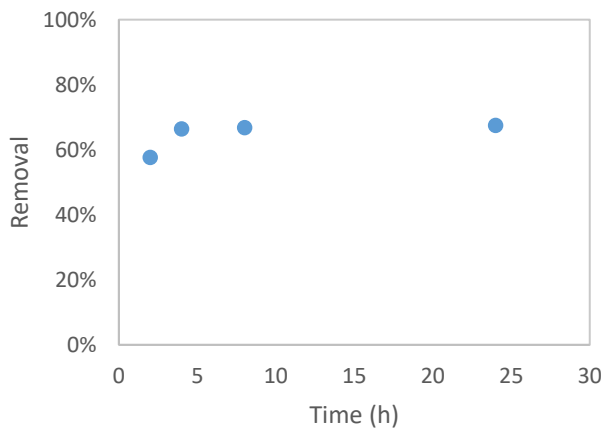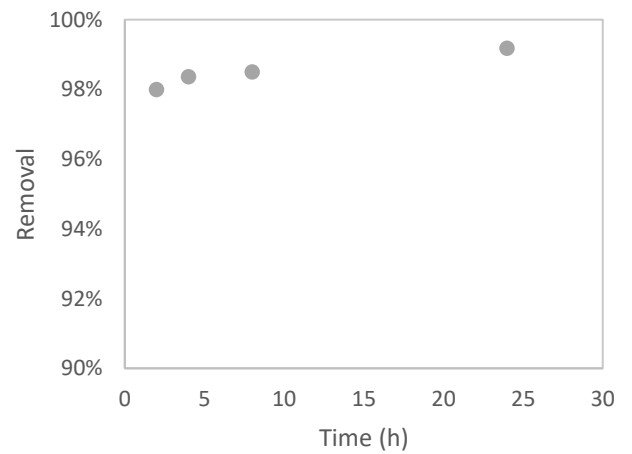, it was expected to have an increase in the concentration of sodium at the same rate as the precipitation. These results imply that kinetics for the precipitation of Ca^{2+}, Mg^{2+}, Cl^-, and SO_4^{2-} are faster, and that the residence time should not be any problem applying this precipitation method in mineral processing operations where sodium has a negligent effect on the process. Additionally, it also demonstrated that UHLA could be used for calcium, magnesium, chloride, and sulphate removal with an equilibrium after four or eight hours depending on the target ions concentration required.

6.3.2 Effect of lime and sodium aluminate concentration

Figure 32 displays the effect of lime and sodium aluminate on removing chloride and sulphate. Magnesium removal reaches its maximum point of 97% from the lowest concentration of lime and sodium aluminate. This was expected as the non-carbonate hardness species compounded by SO_4^{2-} and Cl^- are used to form aluminium precipitates. This allows the excess lime added forces the precipitation of magnesium as magnesium hydroxide, obeying the reactions described previously (Equation 25)

The calcium removal is influenced by the amount of lime added and the aluminium available to react with it. As it can be expected when high doses of lime are used more aluminium is required to achieve low concentrations of calcium. In addition, the calcium hydroxide used was calculated on the basis of the initial concentration of anions (Cl^- and SO_4^{2-}), so at low concentrations of aluminium, the calcium added in excess to the system gets dissolved, increasing the dissolved calcium.
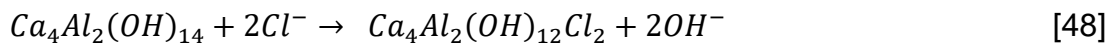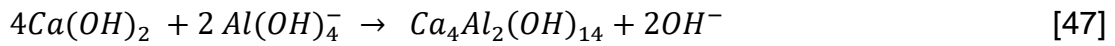
a)

b)
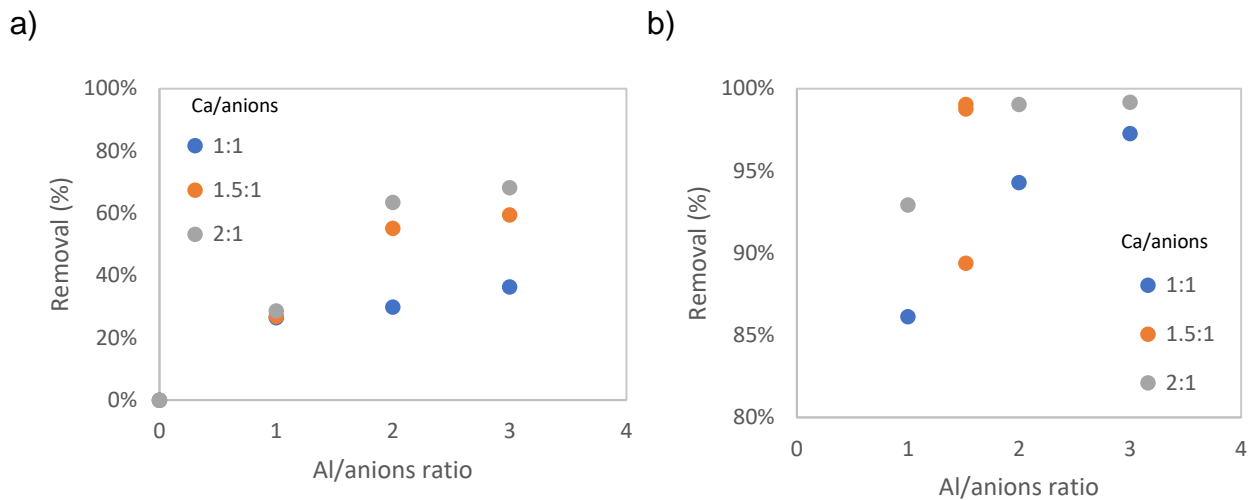
Figure 32 Effect of lime and aluminium dose on ions removal a): Chloride, b): Sulphate

The precipitation of chloride is highly dependent on the concentration of lime and aluminium added. Lime ratios over 1.5:1 resulted in higher removals of chloride. However, increasing the lime ratio from 1.5:1 to 2:1 resulted in a slight increase in chloride removal. As Almasri (2003) through his studies suggested that sulphate removal is independent of the concentration of chloride following the reactions (equation 20). Also, Abdel-Wahab and Batchelor (2006) indicate that because of the low solubility of calcium, aluminium and sulphate compounds and the high affinity between those ions, species such as calcium sulphate and calcium carbonate are the dominant species to be formed instead of calcium chloroaluminate when both ions are present (Cl$^-$ and SO$_4^{2-}$), in the precipitation process, resulting in lowest chloride removal. The former theory agrees with the result obtained in figure 32, as 99% of the sulphate was removed whilst the maximum chloride removal was 68%. One of the aspects that can affect the performance of chloride precipitation is the presence of bicarbonate ions that, due to their high affinity with calcium and aluminium, can compete with chloride ions for the precipitated formation. The mechanism of chloride removal in a multi-ions system could be complex. However, the most reasonable path for its removal is through the formation of tetracalcium hydroxyaluminate (Ca$_4$Al$_2$(OH)$_{14}$) followed by the replacement of ion hydroxyl

by free chloride. in solution (Eqs. 46, 47 and 48) (Me et al., 2015 and Yi et al., 2020).

$$AlO_2^- + 2H_2O \rightarrow Al(OH)_4^- \qquad [46]$$

$$4Ca(OH)_2 + 2\,Al(OH)_4^- \rightarrow Ca_4Al_2(OH)_{14} + 2OH^- \qquad [47]$$

$$Ca_4Al_2(OH)_{14} + 2Cl^- \rightarrow Ca_4Al_2(OH)_{12}Cl_2 + 2OH^- \qquad [48]$$

6.3.3   Ion removal optimisation

Two stages of experiments were conducted to optimise the precipitation of anions (chloride and sulphate), expecting a reduction of bicarbonate ions in the first stage that negatively impacts the efficiency of anions precipitation. These experiments were performed under the same conditions as in the single-stage precipitation; however, in these experiments, half of the dosage of lime was fed in the first stage and the other half in the second stage with different concentrations of sodium aluminate.

Chloride   Sulphate

a)
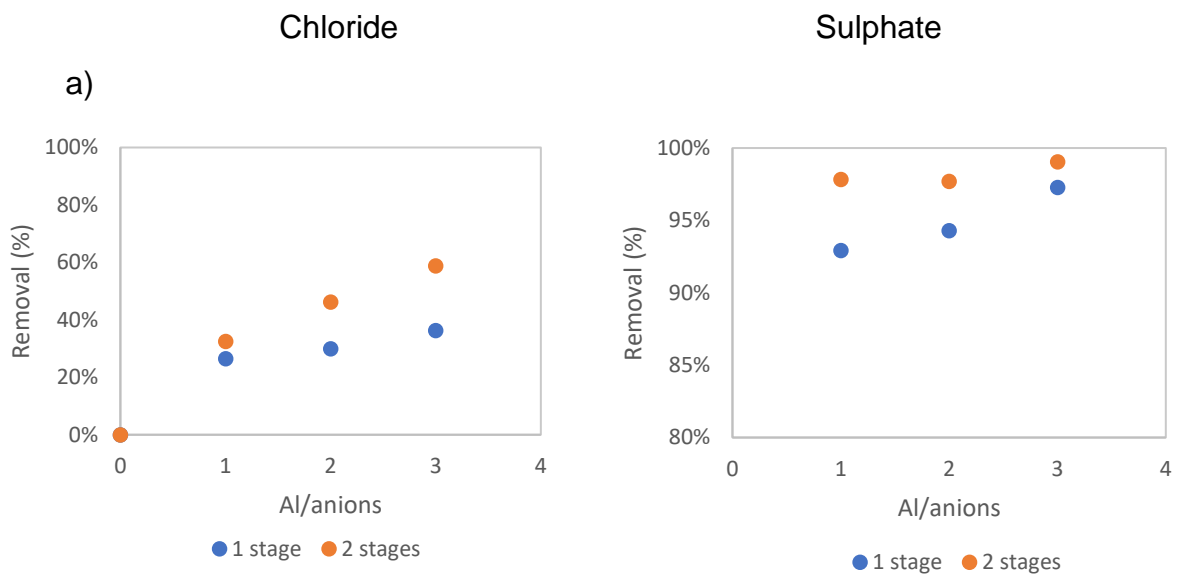
b)
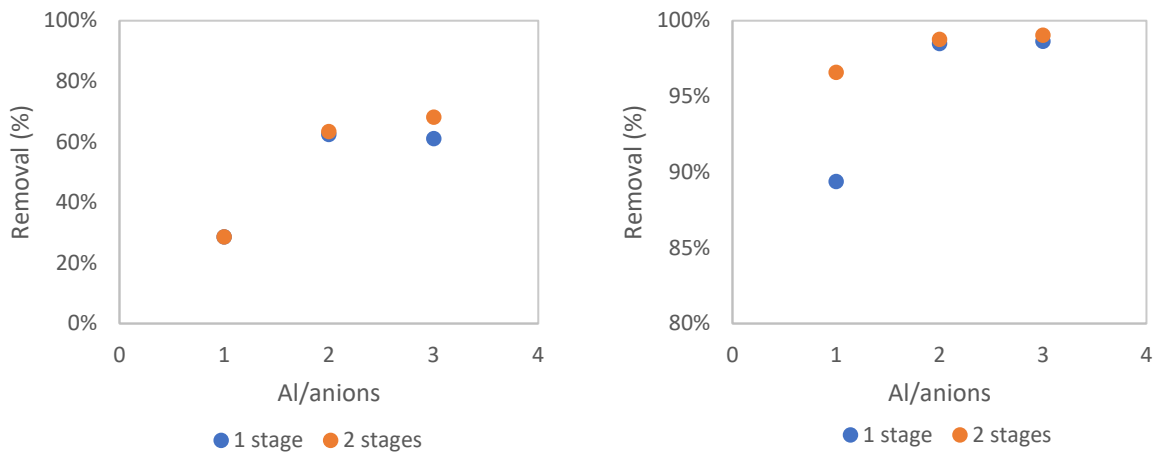
c)
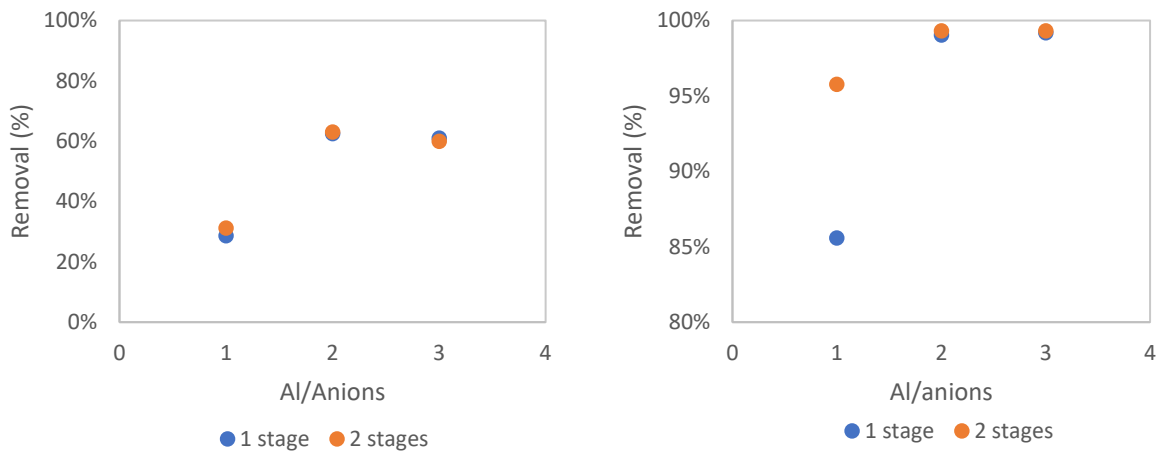
Figure 33 Comparison of anions removal of the two one two-stage precipitation: ratio Ca/anions; a) 1:1, b) 1.5:1 and c) 2:1

The precipitation process with two stages has a negligible impact on the calcium and magnesium precipitation reaching low concentrations below 10 ppm in the filtrate. Those divalent cations are mainly used in the first stage on the precipitation of sulphate as calcium sulphate due to the solubility; therefore, more than 95%percent of calcium and magnesium removal was achieved in both processes one and two stages. In addition, the excess of calcium concentration in the first stage reacts with the carbonate ions producing calcium carbonate. A secondary effect of the calcium carbonate precipitation and calcium sulphate is the improvement of chloride removal efficiency as the calcium and aluminium added in the second stage react mainly with chloride

107

ions. In figure 33, the sulphate and chloride removal performance by the two-stage process improves the precipitation, reducing the concentration by up to 5% and 22% of these anions, respectively, compared with the one-stage process.

XRD was used in order to determine the presence of crystalline phases of the precipitates. Figure 34 show the XRD pattern of the solids obtained at 1.5:1 lime ratio and 3:1 $NaAlO_2$ ratio from which could be identified that the dominant phases in the precipitate were hydrocalumite ($Ca_4Al_2(OH)_{12}(Cl)_2 \cdot 4H_2O$), bayerite ($Al(OH)_3$) and calcite ($CaCO_3$). The presence of these minerals confirm that the first stage reduces the presence of sulphate precipitating it as calcium sulphate allowing that the aluminium on the second stage have more selectivity towards ions chloride.
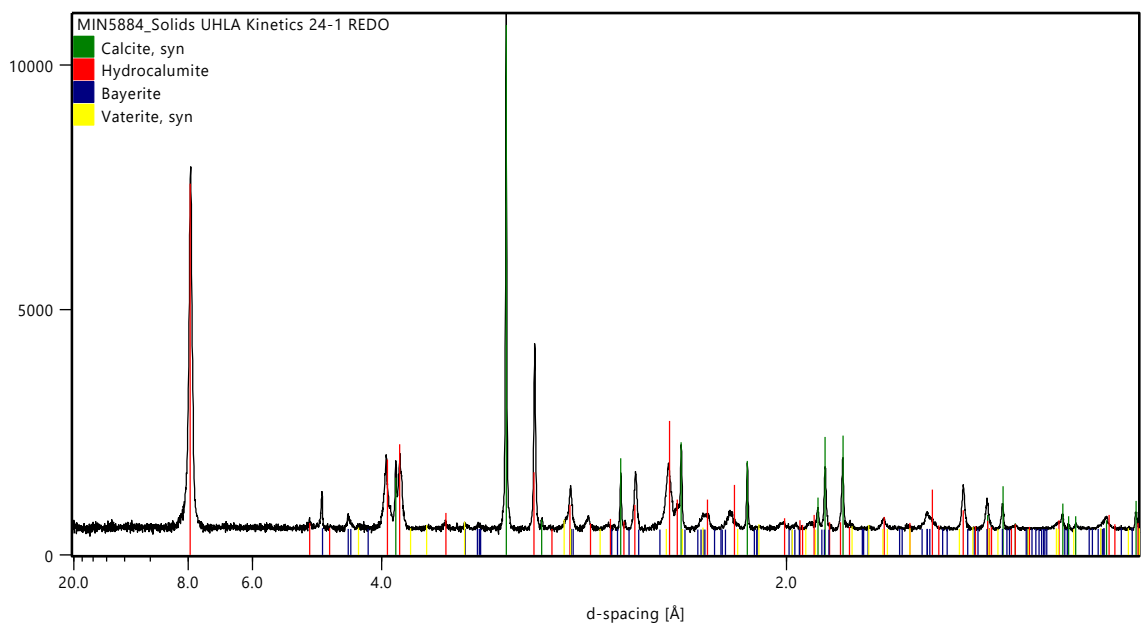
Figure 34 X-ray diffraction results for final

6.3.4 The effect of Temperature on ion removal

Figure 35 shows the effect of different temperatures (25, 35, 45, 55 ºC) on the final concentration of chloride and sulphate. From the graph, it can be noticed that temperature has a negligible effect on the final sulphate concentration. Also, it was identified that the final chloride concentration decreases between the temperatures of 25 ºC and 45 ºC, improving the percentage of chloride removal by 13.8% from 60.1%at 25 ºC to 73.9% at 45 ºC. On the other side, at

108

a temperature of 55 ºC, the final concentration of chloride increases again the efficiency of chloride removal is decreased by 17.1% compared with the chloride removal achieved at 25 ºC. This decrease in chloride removal could be related to the calcium chloroaluminate temperature of stability which is 40ºC. At temperatures above 40 ºC, the calcium chloroaluminate is unstable, decompounding the calcium chloroaluminate precipitate favouring the formation of more stable solids such as calcium aluminate such as $Ca_3Al_2(OH)_{12}$. It means that for industrial applications of this process, if the temperature of the effluent to treat is high will be required to cool down the stream to achieve high chloride removal (Xiaofang et al., 2021, Ping et al., 2018 and Abdel-Wahab, A. 2003).
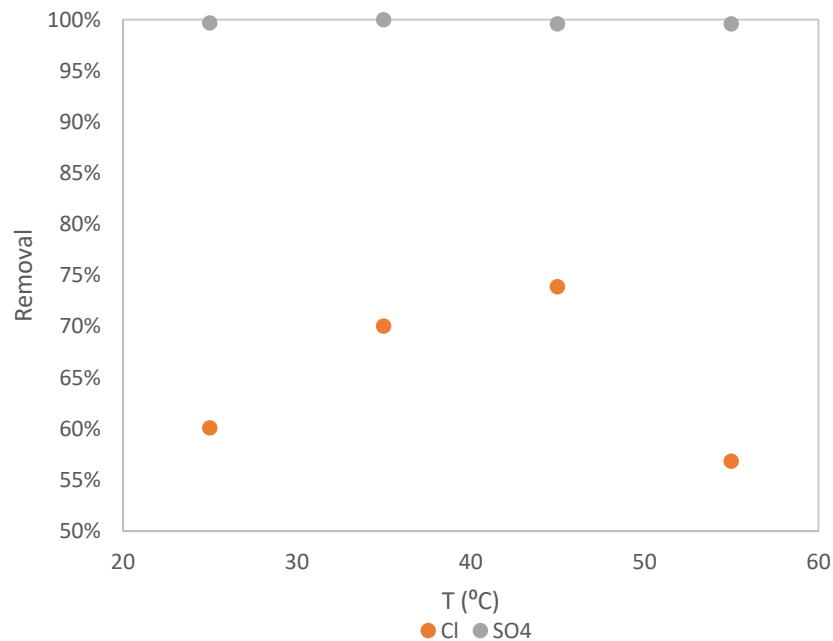
Figure 35 Temperature effect on ion removal 1 stage process, Ca/anions ratio of 1.5:1 and Al/anions ratio of 1:1.

6.3.5 The effect of pH on chloride and sulphate removal
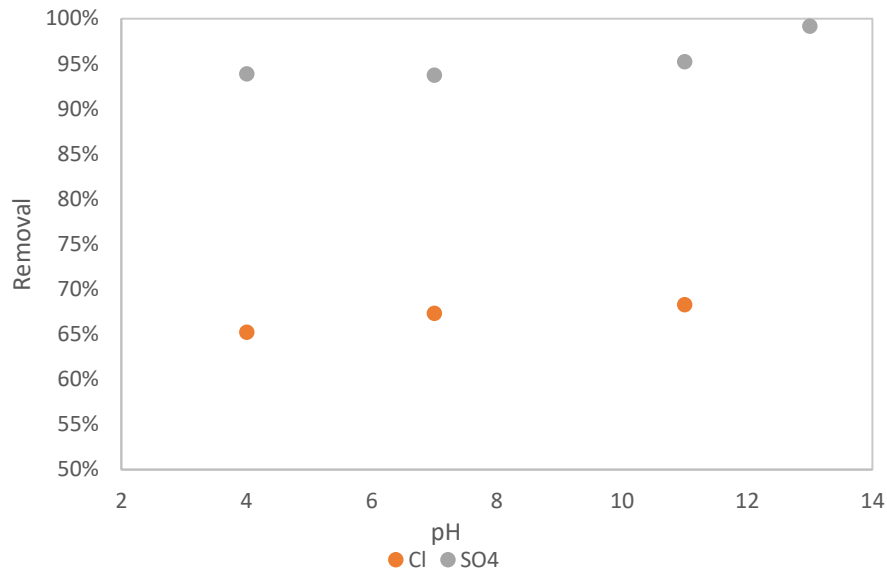
Figure 36 pH effect on ion removal 1 stage process, Ca/anions ratio of 1.5:1 and Al/anions ratio of 1:1 at 25 ºC

Figure 36 shows the effect of pH on the final chloride and sulphate concentrations. It can be noticed that chloride and sulphate concentrations in the effluent increase with decreasing pH. In the case of chloride, the overall removal was increased by 3% from pH 4 to pH 11, reducing the final concentration by 71 mg/L. The effect of the pH on the final chloride concentration can be related to the fact that the formation and stability of solids of calcium chloroaluminate and calcium hydroxylamine are favoured at high pH above 12. The sulphate removal is improved, increasing the pH and reaching a maximum removal of 99%. Wing and George (1978), in their study, argued that acids inhibit the growth of sulphate crystals with high negative charges, which are more likely to increase the separation of the ions by electrophoresis, avoiding crystal growth.

6.3.6 Economic analysis of UHLA process

Figure 37 illustrates the change in the cost of chemical consumption for the system of two stages and 1:1 Ca/anions ratio. The precipitation of calcium, magnesium, sodium, chloride, and sulphate ions is mainly driven by chemical consumption (Xiaofang, 2021). The best performance was achieved at Ca/anions ratio of 1:1 and Al/anions ratio of 3:1 in a two stages process. the chemical used CaOH and $NaAlO_2$ can be purchased at a commercial price in Australia of 0.055 AUD/kg and 1.305 AUD/kg, respectively. The average dose of the reagents used in this scenario includes 0.0052 kg/L of CaOH on each stage for a total of 0.104 kg/L and 0.015 kg/L of $NaAlO_2$, resulting in a total cost of 0.02017 AUD/L. Recent studies using similar processes, have published data of total operational cost related with chemical consumption between 0.008 AUD/L and 0.03 AUD/L agreeing that the Friedel's salt precipitation is enhanced at two stages processes (Yi et al., 2020 and Xiaofang et al., 2021).
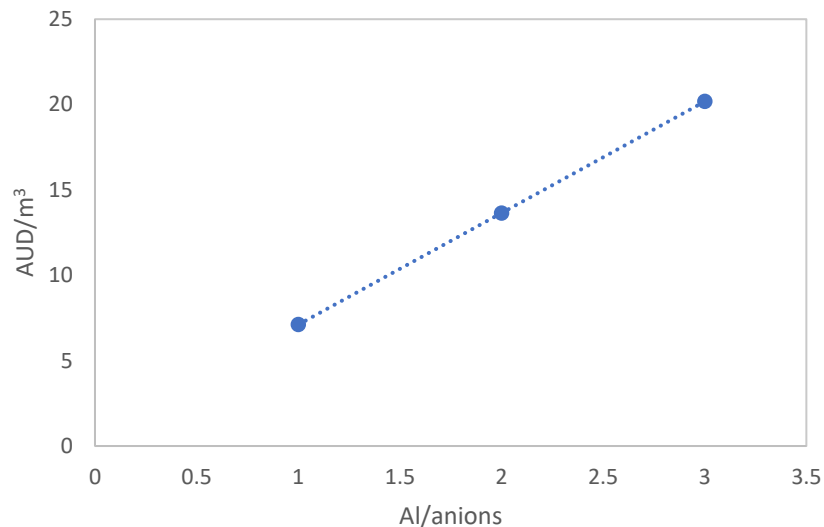
Figure 37 Effect of Al/anions ratio on chemical precipitation cost in two stages UHLA**.**

6.4 Oxalic Acid

6.4.1 Equilibrium time of ions removal

Precipitation experiments were performed to determine the equilibrium time of the precipitation. These experiments were conducted with bore water from Mt

Weld and synthetic water with a higher concentration of ion similar to sea water.
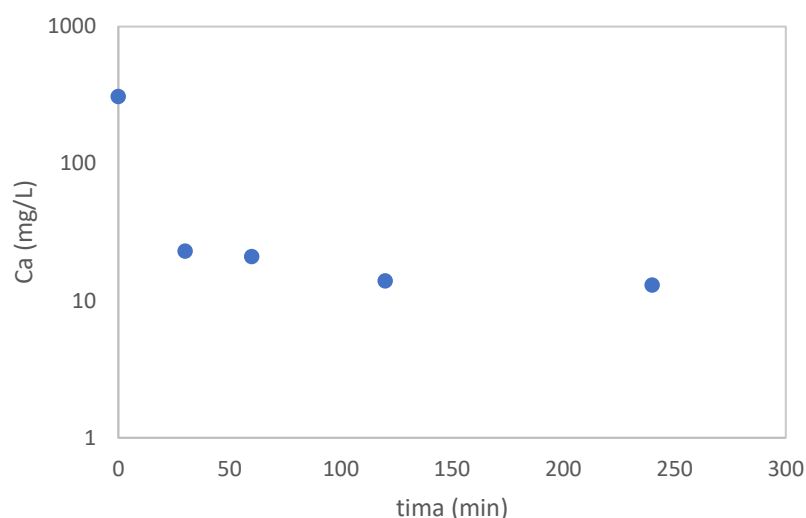
Figure 38 Equilibrium time of precipitation, oxalic acid/cation molar ratio (2:1)

A series of experiments to study the kinetics of the reaction and the removal of calcium and magnesium were conducted with synthetic water. Figure 38 shows the final concentration of calcium in solution at different reaction times. The results indicate that selective precipitation of calcium reach steady state of within 60 min which agrees with Tran et al., (2013) and Kennedy et al (2021) on the fact that the kinetics of calcium oxalate formation are extremely fast.

6.4.2 Effect of oxalic dose on selective precipitation

Different doses of oxalic acid were evaluated to determine if the reaction require more than the stoichiometric concentration to precipitate the ions. As can be seen in the figure 39 there is no appreciable impact on calcium and magnesium precipitation increasing the dose of oxalic acid. The removal of calcium achieved was above 95% for all the range of oxalic acid dose evaluated on the synthetic water (SW) and above 91.2% on the bore water (BW). Inversely, the magnesium precipitation was very limited even at high oxalic acid doses, this is due the pH required for the precipitation of magnesium oxalate.

112
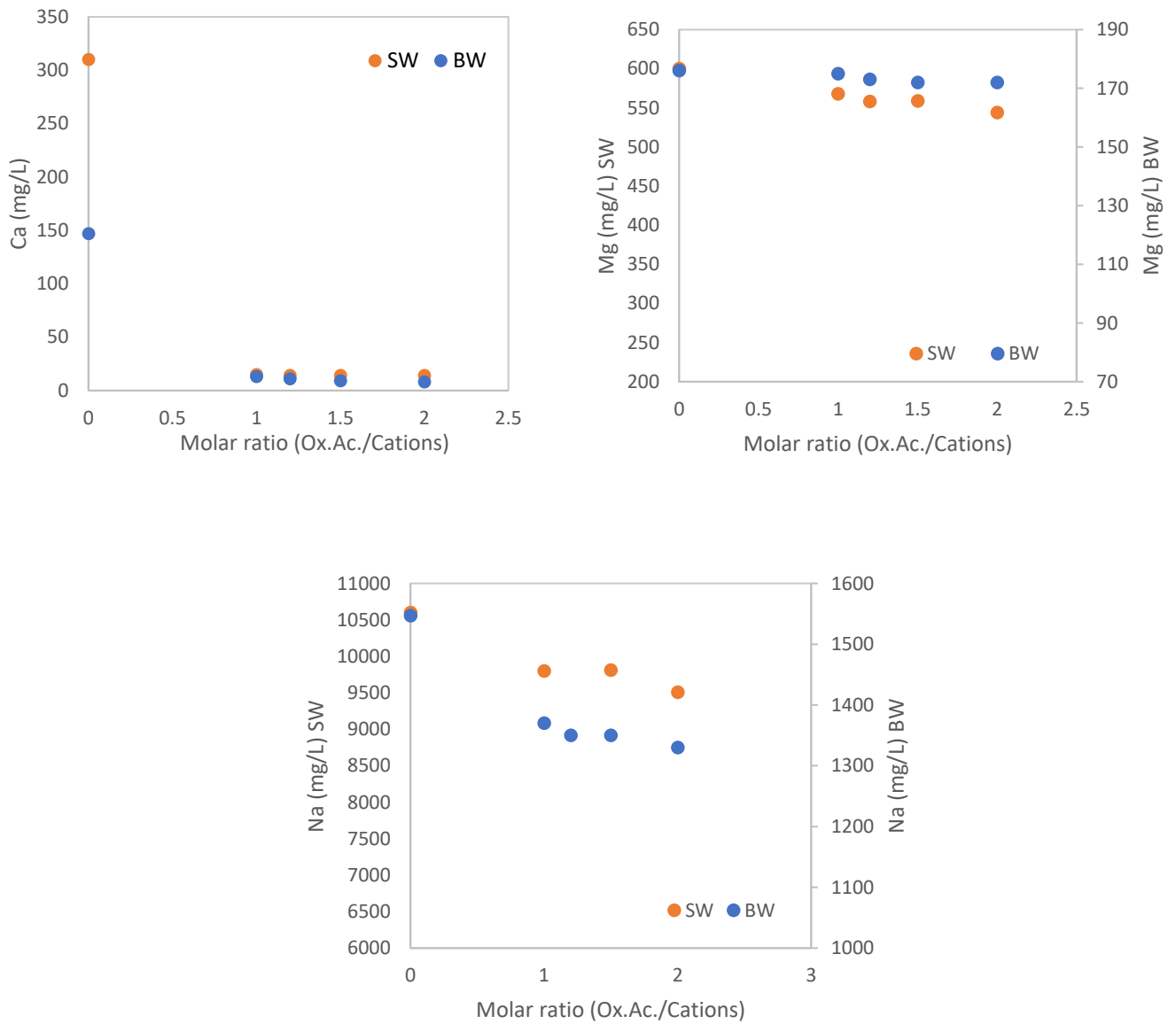
Figure 39 Effect of oxalic acid dose on cations precipitation

Figure 40, shows, the characterization by XRD of the final precipitate at molar ratio of 2:1. It can be seen that the only crystalline phase identified is the Whewellite which is the hydrate form of calcium oxalate $CaC_2O_4 \cdot H_2O$. which agrees with the results shown on figure 39 where the main ion precipitated is calcium.
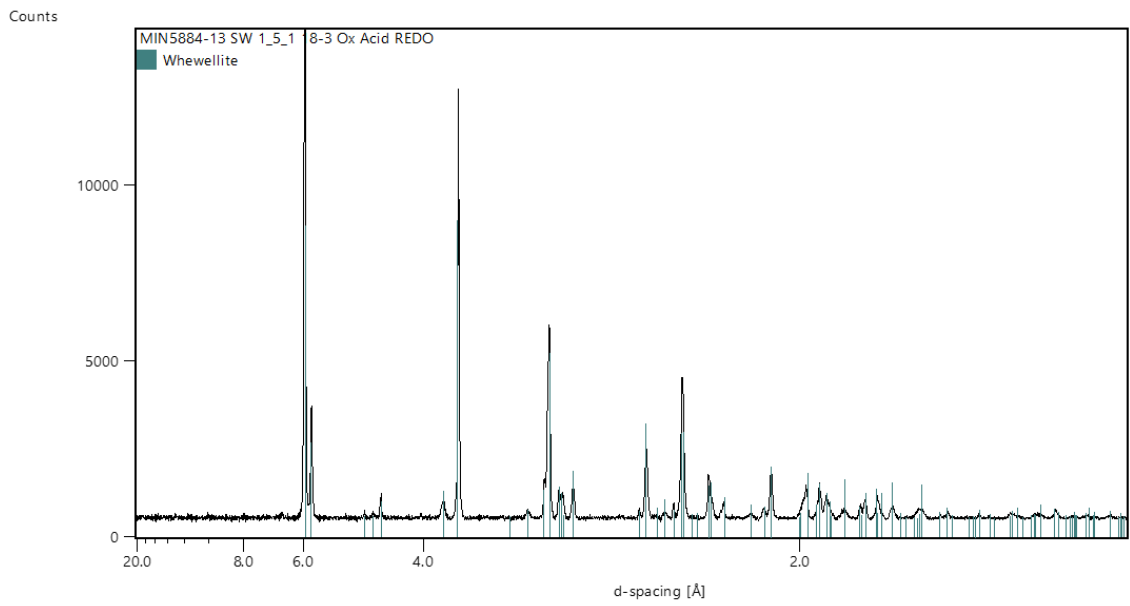
Figure 40 X-ray diffraction precipitate. Molar ratio 2:1. Natural pH

6.4.3 Selective magnesium precipitation by adjusting the pH.
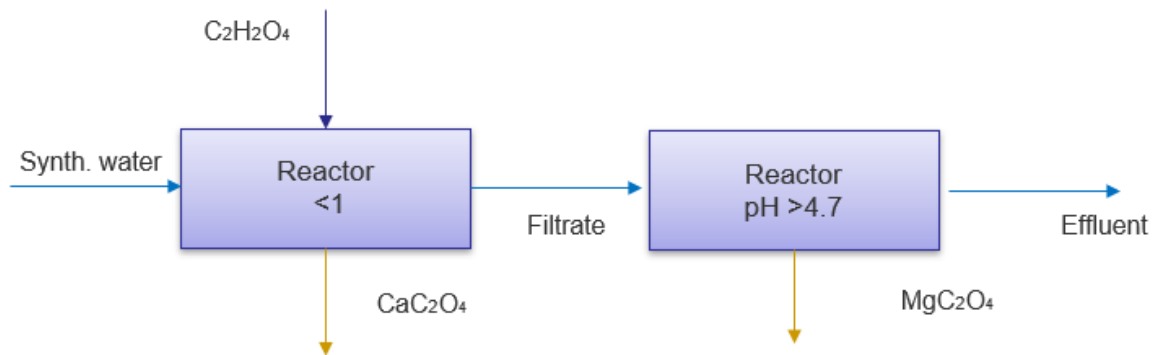
Figure 41 selective precipitation of Magnesium (synthetic sea water)
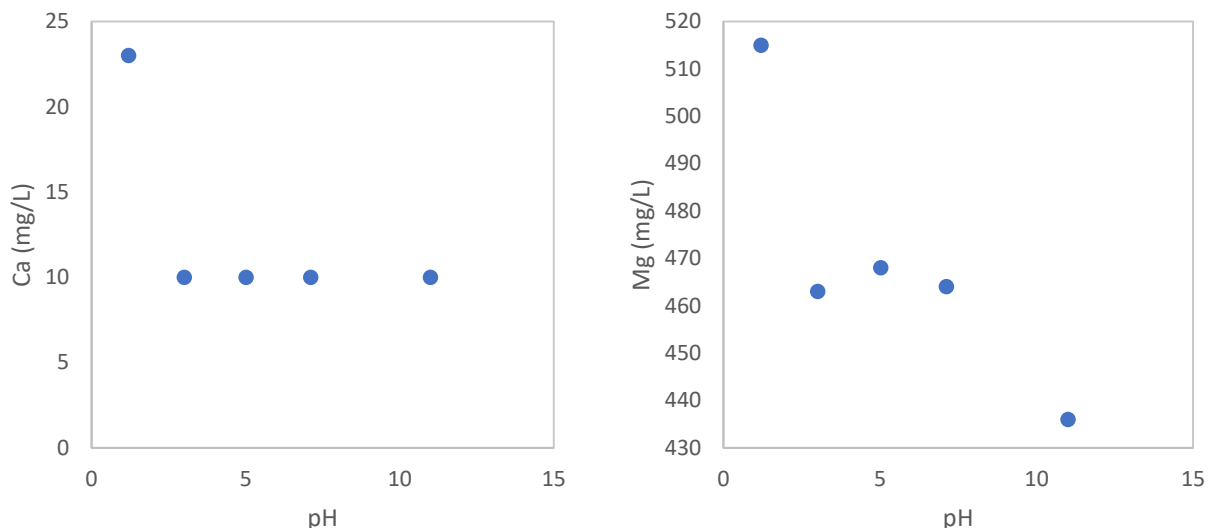
Figure 42 Selective precipitation of Magnesium. Molar ratio 2:1. 120 min. synthetic sea water.

Figure 42 show the calcium and magnesium concentration achieved at different pH. The results indicate that in comparison with precipitation at pH 1, magnesium precipitation at pH between 3 and 7 improve on 9% and an improvement of 13% at pH over 10. These results agree with the data reported in figure 10, where is displayed the conditions of pH and magnesium concentration to precipitate as magnesium oxalate and magnesium hydroxide. In this case from figure 10 it was expected to precipitate magnesium oxalate at pH approximately of 2 and precipitation of magnesium hydroxide at pH over 10, which agrees with the results obtained of precipitation at different pH.

6.5 Conclusions

The precipitation of critical ions through the UHLA and oxalic acid methods and the precipitation conditions that affect the process were investigated. Experimental results showed that the kinetics of both processes is faster, and the reaction time should not pose a challenge for industrial applications. From the oxalic acid results can be appreciated that that removal of calcium was above 95% however it was found that precipitation of magnesium and sodium were not adequate. Further tests on certain conditions such as high concentration of ions and a pH adjustment may be required to achieve high

115

precipitation. Poor magnesium and sodium precipitation were also confirmed from XRD analysis of the precipitates which showed only the presence of calcium oxalate. From the UHLA results, it was determined that increasing the concentration of $Ca(OH)_2$ and $NaAlO_2$ on dose improves the ions removal efficiency. Al/anions ratios over 2 did not strongly impact overall ion removal. On the other hand, increasing ratio of lime improves the anions removal. The maximum removal efficiency (68% of chloride and 99% of sulphate) was achieved when the Ca/anions ratio was (2:1) and the Al/anions ratio was 3:1. Removal of calcium and magnesium ions was over 97% in all the tests performed. The chloride and sulphate removals were proportional to the pH being the optimum over 12. Temperature over 40 ºC negatively impacts the removal of chloride as the stability of the calcium chloroaluminate is affected at higher temperatures. Removal of chloride and sulphate can be improved by implementing a two-stage process using half of the $Ca(OH)_2$ dose in the first stage to avoid the competition of chloride with other ions such as bicarbonate and aluminium.

The method of precipitation with oxalic acid was highly efficient to produce calcium oxalate, however, it has some drawbacks such as requirements of high concentrations of magnesium to precipitate. The method of UHLA explored in this study is highly efficient in reducing calcium magnesium, and sulphate. Furthermore, it showed considerable high efficiencies of chloride removal which depending on the standards of quality required by different mineral processing operations can be combined with other methods to refine the effluent and remove the residual concentration of chloride.

7 FURTHER WORK OF RESEARCH AND RECOMMENDATIONS

The following limitations and improvements can be addressed in the future:

- Implementation of NF and ED systems to recover valuable metals from tailings in mineral processing operations.
- Evaluate the effect of membrane polarization (ED and NF) and antiscalants to reduce it.
- Evaluate NF and ED units in continuous mode to determine changes in variables and results.
- Development of selective membranes (ED and NF) for recovery of specific ions.
- Study of temperature effect on ED and NF performance.
- Test different combinations of ED membranes to reduce energy consumption.
- ED reversal to investigate the use of raw water with ultra-high ions concentration (hundreds of g/L) to use the gradient concentration for the generation of energy.
- Asses a closed circuit of concentration of brines by ED and NF and reuse the brine to precipitate valuable salts.

8 REFERENCES

Abdel-Wahab, A. (2003). The ultra-high lime with aluminium process for removing chloride from recirculating cooling water. PhD. Civ. Eng. Thesis. Texas A&M University

Abdel-Wahab, A., & Batchelor, B. (2006). Interactions between chloride and sulfate or silica removal using advanced lime-aluminium softening process. Water environment research, 78, 13, 2474. https://doi.org/10.2175/106143006X102006

Ahmad, A., Ooi, B., Mohammad, A., and Choudhury, J. (2004). Development of a highly hydrophilic nanofiltration membrane for desalination and water treatment. *Desalination,* 168, 215-221. https://doi.org/10.1016/j.desal.2004.07.001

Aktas, O., Sahinkaya, E., Yutsever, A., Demir, S., Yuceyurt, M., Cakmak, A., Kulekci, C., Taahmaz, S., Uluda, M. (2017). Treatment of a chemical industry effluent by nanofiltration and reverse osmosis. *Desalination Water Treatment.* 75 274-283. doi: 10.5004/dwt.2017.20482Almasri, D. 2013.

Sulfate removal from reject brined in inland desalination with zero liquid discharge. MSc. Chem. Eng. Thesis. Texas A&M University,

Amshave, S., Yusri, M., Aziz, A., Geraint, D., Habib, I., Abu, H. (2020). Electrodialysis desalination for water and wastewater: a review. *Chemical Engineering.* 380, 122231.: https://doi.org/10.1016/j.cej.2019.122231

Australian bureau statistics. (2016). Water in mining. https://search.abs.gov.au/s/search.html?form=simple&collection=abs-search&query=water+in+mining

Bajpayee, A., Luo, T., Muto, A., & Chen, G. (2011). Very low temperature membrane-free desalination by directional solvent extraction. *Energy and environmental science,* 4, 1672-1675. https://doi.org/10.1039/C1EE01027A

Barnett, S., Harrington, N., Cook, P., & Simmons, C. (2020). Groundwater in Australia: Occurrence and Management Issues. *Sustainable Groundwater Management.* 24, 109-127. https://doi.org/10.1007/978-3-030-32766-8_6

Belessiotis, V., Kalogirou, S., & Delyannis, E. (2016). Chapter Four - Membrane Distillation, *Thermal Solar Desalination*, Academic Press, (pp. 191-251) https://doi.org/10.1016/B978-0-12-809656-7.00004-0.

Berk, Z. (2009). Chapter 10 - Membrane processes, In Food Science and Technology, *Food Process Engineering and Technology,* Academic Press, (pp. 233-257). https://doi.org/10.1016/B978-0-12-373660-4.00010-7.

Bo, S., Muxing, Z., Shifang, H., Wei, S., Junming, Z., & Xiaosong, Z. (2019). Performance evaluation on regeneration of high-salt solutions used in air conditioning systems by electrodialysis. *Journal of Membrane Science*. 582. 224-235. https://doi.org/10.1016/j.memsci.2019.04.004

Boo, C., Billinge, I., Chen, I., Shah, K., Yip, N. (2020). Zero Liquid Discharge of Ultrahigh-Salinity Brines with Temperature Swing Solvent Extraction. *Environmental science and technology*, 54, 9124-9131. https://dx.doi.org/10.1021/acs.est.0c02555?ref=pdf

Bowell, R., & Parshley, J. (2000). Sulphate and salt minerals: The problem of treating mine waste. *Mining environmenta management,* 11-13.

Bulut, G., & Yenial, U. (2016). Effects of major ions in recycled water on sulphide minerals flotation. *Minerals and metallurgical processing,* 33 (3), 137-143. https://doi.org/10.19150/mmp.6750

Casas, S. (2011). Valorization of brines in the chlor-alkali industry. Integration of precipitation and membrane processes. Doctoral Thesis. Universitat Politecnica de Catalunya, Spain.

Chakrabarty,T.. Giri, A., & Sarkar, S. (2022). Chapter 4 - Nanofiltration membrane technologies, *Advancement in Polymer-Based Membranes for Water Remediation*, Elsevier, (pp. 121-157) https://doi.org/10.1016/B978-0-323-88514-0.00012-7.

Cruz, C., Ramos, J., Robles, P., Leiva, W., Jeldres, R., Cisternas, L. (2020). Partial seawater desalination treatment for improving chalcopyrite floatability and tailing flocculation with clay content. *Minerals engineering*, 151. https://doi.org/10.1016/j.mineng.2020.106307

119

Dach, H. (2009). Comparing nanofiltration and reverse osmosis processes for selective desalination of brackish water feeds. PhD thesis (unpublished) Engineering science, University D Angers.

Davidson, R., Smith, W., & Hood, D. (1960). Structure and Amine-Water Solubility in Desalination by Solvent Extraction. *Journal of Chemical Engineering Data* , 5 (4), 420−423. https://doi.org/10.1021/je60008a005

Deepti, A., Sinha, P., Biswas. S., Sarkar, Bora., U & Purkait, M., (2020). Separation of chloride and sulphate ions from nanofiltration rejected wastewater of steel industry. *Journal of water process engineering,* 33, 101-108*.* https://doi.org/10.1016/j.jwpe.2019.101108

Derhy, M., Taha, Y., Hakkou., R & Benzaazoua, M. (2020). Review of the Main Factors Affecting the Flotation of Phosphate Ores. *Minerals,*10,1109. https://doi.org/10.3390/min10121109

Devora-Isiorida, G., Espinoza, A., Rangel, L., Guzman, M., Sanchez, R., Sanchez, J., Martinezm, M. (2021) , Effect of Temperature on DiluateWater in Batch Electrodialysis Reversal. *Separations*. 8, 229. https://doi.org/10.3390/separations8120229

Di Feo, A., Hill, C., Hart, B., Volchek, K., Morin, L., & Demeres, A., (2021). The effects of water recycling on flotation at a North American concentrator. *Minerals Engineering,* 170. 107037. https://doi.org/10.1016/j.mineng.2021.107037

Diawara, K., Lo, S., Rumeau, M., Pontie, A., & Sarr, O. (2003). Phenomenological mass transfer approach in nanofiltration of halide ions for a selective defluorination of brackish drinking water. *Journal of Membrane Science*. 219 (1-2), 103-112. https://doi.org/10.1016/S0376-7388(03)00189-3

Ding, W., Zhuo, H., Bao, M., Li, Y., & Lu, Y. (2017). Fabrication of organic-inorganic nanofiltration membrane using ordered stacking SiO2 thin film as rejection layer assisted with layer-by-layer method, *Journal of Chemical Engineering*, 330, 337-344. https://doi.org/10.1016/j.cej.2017.07.159

Dos Santo, M., Santana, R., Capponi, F., Ataide, C., & Barrozo, M. (2010). Effect of ionic species on the performance of apatite flotation. *Separation and*
120

purification technology, 76 (1), 15-20. https://doi.org/10.1016/j.seppur.2010.09.014

Eykamp, W. (1995). Chapter 1 Microfiltration and ultrafiltration, *Membrane Science and Technology*, Elsevier, 2, (pp. 1-43). https://doi.org/10.1016/S0927-5193(06)80003-3.

Galama, A. (2015). *Ion exchange membranes in seawater applications. Processes and characteristics.* [Doctorate dissertation, Wageningen University]

Grano, S., Wong, P., Skinner, W., Johnson, N., & Ralston, J. (1995). *Detection and control of calcium sulfate precipitation in the lead circuit of the hilton concentrator of mount isa mines limited*. Proceedings of the XIX IMPC. Australia.

Gennady E., & Haghi, A. (2016). *Analytical chemistry from laboratory to process line*. Apple academic press. Inc. Canada. ISBN-13: 978-1-77188-237-8

Generous, M., Qasem, N., Akbar, U., Zubair, S. (2021). Techno-economic assessment of electrodialysis and reverse osmosis desalination plants. *Separation and purification technology*, 272, 118875. https://doi.org/10.1016/j.seppur.2021.118875

Giacobbo, A., Bernanrdes, A., Rosa, M., De Pinho M. (2018). Concentration Polarization in Ultrafiltration/Nanofiltration for the Recovery of Polyphenols from Winery Wastewaters. *Membranes*, 8 (3), 46. doi: 10.3390/membranes8030046

Govardhan, B., Fatima, S., Madhumala, M., Sridhar, S. (2020). Modification of used commercial reverse osmosis membranes to nanofiltration modules for the production of mineral-rich packaged drinking water. *Applied Water Science.* 10, 230. https://doi.org/10.1007/s13201-020-01312-1

Guimares, R., & Peres, A. (1999). Interfering ions in the flotation of a phosphate ore in a batch column. *Minerals Engineering.* 12, 7. 757-768. https://doi.org/10.1016/S0892-6875(99)00062-X

121

Hidalgo, A., Leon, G., Gomez, M., Murcia, M., Gomez, E., & Gomez, J. (2013) Application of the Spiegler–Kedem–Kachalsky model to the removal of 4-chlorophenol by different nanofiltration membranes. *Desalination,* 315, 70-75. https://doi.org/10.1016/j.desal.2012.10.008

Ikumapayi, F., Makitalo, M., Johansson, B., Hanumantham K. (2012). Recycling of process water in sulphide flotation: Effect of calcium and sulphate ions on flotation of galena. *Minerals Engineering,* 39, 77-88. https://doi.org/10.1016/j.mineng.2012.07.016

Ismail, A., Khulbe, K., Matsuura, T. (2019). Chapter 1 - Introduction—Do RO Membranes Have Pores?, *Reverse Osmosis,* (pp. 1-24), Elsevier. https://doi.org/10.1016/B978-0-12-811468-1.00001-3

Jadhav, S., Marathe, K., Rathod, V. (2016) A pilot scale concurrent removal of fluoride, arsenic, sulfate and nitrate by using nanofiltration: Competing ion interaction and modelling approach. *Journal of Water and Process. Engineering* 13, 153–167 https://doi.org/10.1016/j.jwpe.2016.04.008

Jeldres, R., Bravo, M., Reyes, A., Aguirre, C., Cortes, C., & Cisternas, L. (2017). The impact of seawater with calcium and magnesium removal for the flotation of copper-molybdenum sulphide ores. *Minerals engineering,* 109,10-13. https://doi.org/10.1016/j.mineng.2017.02.003

Jung, M., Craig, D., Logan, A., Dyer, L., Albijanic, B., Tadesse, B. (2022). Influence of monovalent and divalent cations on monazite flotation. *Colloids. and Surfaces A: Physicochemical and Engineering Aspects.,* 653, 129975, https://doi.org/10.1016/j.colsurfa.2022.129975

Kabay, N., Demircioooglu M., Ersoz, E., & Kurucaovali, I. (2002). Removal of calcium and magnesium hardness by electrodialysis. *Desalination,* 149, 343-349. https://doi.org/10.1016/S0011-9164(02)00807-X

Kammeyer, C. (2017). *The World's Water Challenges 2017*. Pacific Institute. http://bcn.cl/246lp. (Marzo de 2018)

Karimi L., Ghaseemi, L., & Zamani, H. (2018). Quantitative studies of electrodialysis performance. *Desalination,* 445, 159-169. https://doi.org/10.1016/j.desal.2018.07.034

Kelewou, H., Lhassani, A., Merzouki, H., Drogui, P., & Sellamuthu, B. (2011). Salts retention by nanofiltration membranes: Physicochemical and hydrodynamic approaches and modelling. *Desalination,* 227(1-3) 106-112. https://doi.org/10.1016/j.desal.2011.04.010

Kennedy, S., Zijil, L., Rooyen, C., Bertossi, L., Shekede, B., Joos-Vandewalle, J., Smith, S., & Turton, A. (2021). Coordination and Precipitation of Calcium Oxalate: Computation to Kinetics. *Crystal Growth and design*, 21, 1249-1258. https://dx.doi.org/10.1021/acs.cgd.0c01536?ref=pdf

Kitchen, C., Wang, B. (2022). *International electricity prices: How does Australia compare? Australian Energy Council.* https://www.energycouncil.com.au/analysis/international-electricity-prices-how-does-australia-compare/

Koyuncu, I., Yazgan, M., Topacik, D., & Sarikaya, H. (2001). Evaluation of the low-pressure RO and NF membranes for an alternative treatment of Buyukcekmece Lake. *Water Science and technology: Water supply,* 1(1), 107-115. http://dx.doi.org/10.2166/ws.2001.0013

Krieg. M., Modise, J., Keizer, K., Neomagus, H. (2005) Salt rejection in nanofiltration for single and binary salt mixtures in view of sulfates removal, *Desalination*, 171. 205-215. https://doi.org/10.1016/j.desal.2004.05.005

Krol, J., Wessling, M., & Strathmann, H. (1999). Concentration polarization with monopolar ion exchange membranes: current - voltage curves and water dissociation. *Membranes* Sci.162. 145-154. https://doi.org/10.1016/S0376-7388(99)00133-7

Kundzewicz, Z. (2008). Hydrosphere. Sven Erik Jørgensen, Brian D. Fath (Eds). *Encyclopedia of Ecology*, Academic Press, (pp. 1923-1930). https://doi.org/10.1016/B978-008045405-4.00740-0.

Lhassani, A., Rumeau, M., Benjelloun, D., & Pontie, M. (2001). Selective demineralization of water by nanofiltration Application to the defluorination of brackish water. *Water. Research.* 35 3260-3264. https://doi.org/10.1016/S0043-1354(01)00020-3

Liu, Y., Zhang, Z., Li, W., Liu, R., Qiu, J., & Wang, S. (2020). Water purification performance and energy consumption of gradient nanocomposite membranes. *Composites Part B: Engineering*. 202. 108426. https://doi.org/10.1016/j.compositesb.2020.108426

Luo, J., Ding, L., Su, Z., Wei, S., Wan, Y. (2010). Concentration polarization in concentrated saline solution during desalination of iron dextran by nanofiltration. *Journal of Membrane Science*. 363 (1-2), 170-179. https://doi.org/10.1016/j.memsci.2010.07.033

Ma, J., Li, Z., Jiang, Y., Yang, X., Ma, J., Li, Z., Jiang, Y., & Yang, X. (2015). Synthesis, characterization and formation mechanism of Friedel's salt (FS: $3CaO \cdot Al_2O_3 \cdot CaCl_2 \cdot 10H_2O$) by the reaction of calcium chloride with sodium aluminate *Journal Wuhan University Technology*. 30. 76-83. https://doi.org/10.1007/s11595-015-1104-y

Mahaut, M. (1992). Aplicaciones de la osmosis inversa, ultrafiltracion y microfiltracion en la industrea lacteal. *Revista Argentina de lactologia*. 6: 19-44.

Manono, M.S., & Corin, K.C. (2022). Considering Specific Ion Effects on Froth Stability in Sulfidic Cu-Ni-PGM Ore Flotation. *Minerals*, 12(3), 321.

Martín, M. (2016). Chapter 4 – Water. *Industrial Chemical Process Analysis and Design*, Elsevier, (pp. 125-197). https://doi.org/10.1016/B978-0-08-101093-8.00004-5.

Membrain. (2019). *Technical documentation electrodialysis module EDR-Z/2 10-0.8 19*. https://www.membrain.cz/en/mic.html

Minnesota Rural Water Association. (1994). *Chapter 16 Lime softening. Water works operations manua*l. Minnesota. https://www.mrwa.com/mn-water-works-manual/

Montiel V., García-García V., Expósito E., Ortiz J.M., & Aldaz A. (2014) Membrane Processes, Electrodialysis. Kreysa G., Ota K., Savinell R.F. (eds) *Encyclopedia of Applied Electrochemistry.* Springer, https://doi.org/10.1007/978-1-4419-6996-5_123chrome-

Nayara, G., Sundararamana, P., O'Connorb, C., Schacherla, J., Heath, M., Orozco, M., Shaha, S., Wrighta, N., & Winter, A. (2016). Feasibility study of an electrodialysis system for in-home water desalination in urban India. *Development Engineering*. 2, 38-46. http://dx.doi.org/10.1016/j.deveng.2016.12.001

October, LL., Manono, M.S., Corin, K.C., Schreithofer, N., & Wiese, J.G (2021). The Influence of Specific Ions and Oxyhydroxo Species in Plant Water on the Bubble–Particle Attachment of Pyrrhotite. *ACS Omega*, 6, 43, 28496–28506

Olanrewaju, J., Newalkar, B.L., Mancino, C., & Komarneni, S. (2000) Simplified Synthesis of Nitrate Form of Layered Double Hydroxide, *Materials Letters*, 45 (6), 307-310. https://doi.org/10.1016/S0167-577X(00)00123-3

Ozkan, S., & Acar, A. (2004). Investigation of impact of water type on borate ore flotation. *Water research,* 38(7), 1773-1778. https://doi.org/10.1016/j.watres.2003.12.036

Patel, S., Qin, M., Walker, S., & Elimelech, M. (2020). Energy Efficiency of Electro-Driven Brackish Water Desalination: Electrodialysis Significantly Outperforms Membrane Capacitive Deionization. *Environmental science and technology*. 54, 3663-3667. https://dx.doi.org/10.1021/acs.est.9b07482

PCCell*. Complete lab. Scale systems, control and measurements*. Electrodialysis.de https://www.pccell.de/en/

Prosser, I., Wolf, L., & Littleboy. A. (2011*). Water: Science and Solutions for Australia. Chapter 10: Water in mining and industry*. CSIRO.. https://www.csiro.au/en/research/natural-environment/water/water-book/water-in-mining-and-industry

Ramdani, A., Deratanni, A., Taleb, S., Drouiche, N., & Lounici, H. (2021). Performance of NF90 and NF270 532 commercial nanofiltration membranes in the defluoridation of Algerian brackish water. *Desalination*. 212. 286-296. doi: 10.5004/dwt.2021.26680.

Rioyo, J. (2019). *Integrated treatment of brackish groundwater*. [Thesis Doctor of Philosophy. University of southern Queensland Australia].
125

Rives, V. (2001). *Layered Double Hydroxides: Present and Future*, Nova Science Publisher, Inc.: Huntington, New York. http://dx.doi.org/10.1016/S0169-1317(02)00112-6.

Spiegler, K., & Kedem, O. (1996). Thermodynamics of hyperfiltration (reverse osmosis): criteria for efficient membranes. *Desalination*, 1 (4), 311-326. https://doi.org/10.1016/S0011-9164(00)80018-1

Suhalim, N., Kasim, N., Mahmoudi, E., Shamsudin, I., Mohammad, A., Mohamed, & F., Jamari, N. (2022). Rejection Mechanism of Ionic Solute Removal by Nanofiltration Membranes: An Overview*. Nanomaterials*, 12, 437. https://doi.org/10.3390/nano12030437

Synder Filtration*. Tubular membranes.*

https://synderfiltration.com/learning-center/articles/module-configurations-process/tubular-membranes/

Tadesse, B. (2021). *Mineral processing of critical minerals.* Australia-Japan International Workshop on Critical Minerals. Curtin University.

Tanaka, Y. (2015). Chapter Six - Electrodialysis, *Progress in Filtration and Separation*, Academic Press, (pp. 207-284). https://doi.org/10.1016/B978-0-12-384746-1.00006-9.

Tanne, N., Xu, R., Zhou, M., Zhang, P., Wang, X., Wen, X. (2019) Influence of pore size and membrane surface properties on arsenic removal by nanofiltration membranes. *Frontiers Environmental Science Engineering.* 13,19. https://doi.org/10.1007/s11783-019-1105-8

Tapley, B. (2017). *Improving gold mining economic through the use of membrane technology – a study into the reduction of lime and cyanide consumption at WA gold mines*. MetFest 2017, Kalgoorlie Australia.

Tran, K., Luong, T., An, J., Kang, D., Kim, M., & Tran, T. (2013). Recovery of magnesium from Uyuni salar brine as high purity magnesium oxalate. *Hydrometallurgy.* 138 (2013) 93–99. http://dx.doi.org/10.1016/j.hydromet.2013.05.013

126

Ulbricht, M., (2006), Advanced functional polymer membranes, *Polymer*, 47 (7), 2217-2226. https://doi.org/10.1016/j.polymer.2006.01.084

Ulibarri, M., & Hermosin, M. (2001). Chapter 9. Layered Double Hydroxides in Water Decontamination. *Layered Double Hydroxides: Present and Future*; Vicente Rives. (pp. 251-284) Nova Science Publishers, Inc.: New York

UNESCO (2016): *Drought risk management. A strategic approach.* http://bcn.cl/247e2. (Marzo de 2018)

United States geological Survey (USGS). 2019. *The distribution of water on, in, and above the Earth*. The USGS water science school. https://pubs.er.usgs.gov/publication/70202434

Van der Bruggen, B., Schaep, J., Wilms D., & Vandecasteele C. (1999). Influence of molecular size, polarity and charge on the retention of organic molecules by nanofiltration. *Journal of Membrane Science*, 156 (1), 29-41. https://doi.org/10.1016/S0376-7388(98)00326-3

Vatanpour, V. Pasaoglu, M. Barzegar, H. Teber, O. Bastug, R. Khataee, A. Koyuncu, I. 2021. Cellulose acetate in fabrication of polymeric membranes: A review, Chemosphere, Volume 295, 133914, ISSN 0045-6535, https://doi.org/10.1016/j.chemosphere.2022.133914.

Walha, K., Amar, R., Firdaous, A., & Quemeneur, F. (2007). Brackish groundwater treatment by nanofiltration, reverse osmosis and electrodialysis in Tunisia: performance and cost comparison. *Desalination.* 207(1-3), 95-106. doi:10.1016/j.desal.2006.03.583

Wang, B., & Peng, Y. (2014). The effect of saline water on mineral flotation – A critical review, *Minerals Engineering,* 66-68, 13-24. https://doi.org/10.1016/j.mineng.2014.04.017

Wang, Y., Guo, X., Bai, Y., & Sun, X. (2019). Effective removal of calcium and magnesium sulfates from wastewater in the rare earth industry. *Royal society of chemistry*, 58, 33922-33930. https://doi.org/10.1039/C9RA05615G.

127

Wiesner, M., & Aptel, P. (1996). Mass Transport and Permeate Flux and Fouling in Pressure-DrivenProcesses. *Water Treatment Membrane Handbook* . McGraw-HillCom: New York.

Willem, R., Reig, P., & Schleifer, L. (2019). *17 Countries, Home to One-Quarter of the World's Population, Face Extremely High Water Stress*. World resources institute. World resources institute. https://www.wri.org/insights/17-countries-home-one-quarter-worlds-population-face-extremely-high-water-stress

Wing, H., & George, N. (1978). A kinetic study of the seeded growth of barium sulfate in the presence of additives. *Journal of Inorganic and Nuclear Chemistry,* 40(11), 1871-1875. https://doi.org/10.1016/0022-1902(78)80245-0

Winston, W., & Sirkar, K. (1992). *Membrane Handbook.* Springer Science+Business Media New York. https://doi.org/10.1007/978-1-4615-3548-5

Woo, Y., Kim, S., Shon, H., & Tijing, L. (2019). Introduction: Membrane Desalination Today, Past, and Future, Current Trends and Future Developments on (Bio-) Membranes. *Membrane desalination systems: The next generarion.* (pp. 24-46) Elsevier. https://doi.org/10.1016/B978-0-12-813551-8.00028-0.

Xiaofang, Y., Xiaodan, Z., Qiang, M., Jun, Z., Jiaming, G., Dongqi, S., Sheng, Z., Jie, X., & Zhen, Z. (2021). Process optimization to enhance utilization efficiency of precipitants for chloride removal from flue gas desulfurization wastewater via Friedel's salt precipitation. *Journal of environmental management.* 299, 113682. https://doi.org/10.1016/j.jenvman.2021.113682

Yammine, S., Rabagliato, R., & Vitrac, X. (2019). The use of nanofiltration membranes for the fractionation of polyphenols from grape pomace extracts. *Oeno one*, 53, 11-23. 10.20870/oeno-one.2019.53.1.2342

Yi, X., Zhen, Z., Qian, M., Dongqi, S., Jun, H., Xiaofang, Y., Shifend, D., Lu, J., Xiaodan, Z., and Ying, Z. (2020). A. A two-stage desalination process for zero liquid discharge of flue gas desulfurization wastewater by chloride precipitation. *Journal of hazardous materials*, 397, 122744. https://doi.org/10.1016/j.jhazmat.2020.122744
128

Yoshino, A. (2017). *Desalination of produced water with electrodialysis: ion exchange membrane fouling, system performance, and fate of organic constituents*. [Master of science thesis, Colorado Schoool of mines].

Zhang, W., Honaker, R., & Groppo, J. (2017). Flotation of monazite in the presence of calcite part I: Calcium ion effects on the adsorption of hydroxamic acid. *Minerals Engineering,* 100, 40-48. https://doi.org/10.1016/j.mineng.2016.09.020

9   APPENDICES

9.1   Appendix 1. Nanofiltration membrane NF90 4040

‹DUPONT›™

Product Data Sheet

FilmTec™ Membranes
FilmTec™ NF90 Nanofiltration Elements for Commercial Systems
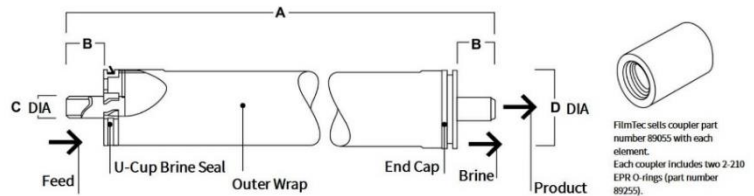
Description

The FilmTec™ NF90 Membrane Elements provide high productivity performance while removing a high percentage of salts, nitrate, iron and organic compounds such as pesticides, herbicides and THM precursors. The low net driving pressure of the NF90 membrane allows the removal of these compounds at low operating pressures.

Typical Properties

Product	Part Number	Applied Pressure psig (bar)	Permeate Flow Rate gpd (m^3/d)	Minimum Salt Rejection (%)
NF90-2540	149982	70 (4.8)	680 (2.6)	97.0
NF90-4040	149983	70 (4.8)	2,000 (7.6)	98.7

1. Permeate flow and salt rejection based on the following test conditions: 2,000 ppm MgSO$_4$, 77°F (25°C) and 15% recovery at the pressure specified above.
2. Permeate flows for individual NF90-2540 Elements may vary by -20% / +30%. NF90-4040 individual elements may vary -15% / +50%.
3. Developmental products available for sale.

Element Dimensions

FilmTec sells coupler part number 89055 with each element. Each coupler includes two 2-210 EPR O-rings (part number 89255).

	Dimensions – Inches (mm)			1 inch = 25.4 mm
Product	A	B	C	D
NF90-2540	40.0 (1,016)	1.19 (30)	0.75 (19)	2.4 (61)
NF90-4040	40.0 (1,016)	1.05 (27)	0.75 (19)	3.9 (99)

1. Refer to FilmTec™ Design Guidelines for multiple-element systems of midsize elements (Form No. 45-D01588-en).
2. NF90-2540 has a tape outer wrap. NF90-4040 has a fiberglass outer wrap.

130

Operating and Cleaning Limits

Membrane Type	Polyamide Thin-Film Composite
Maximum Operating Temperature	113°F (45°C)
Maximum Operating Pressure	600 psi (41 bar)
Maximum Feed Flow Rate	
4040 elements	16 gpm (3.6 m^3/hr)
2540 elements	6 gpm (1.4 m^3/hr)
Maximum Pressure Drop	
tape wrapped	13 psig (0.9 bar)
fiberglassed	15 psig (1.0 bar)
pH Range	
Continuous Operation[a]	2 – 11
Short-Term Cleaning (30 min.)[b]	1 – 12
Maximum Feed Silt Density Index	SDI 5
Free Chlorine Tolerance[c]	<0.1 ppm

a. Maximum temperature for continuous operation above pH 10 is 95°F (35°C).
b. Refer to Cleaning Guidelines (Form No. 45-D01696-en) for NF90.
c. Under certain conditions, the presence of free chlorine and other oxidizing agents will cause premature membrane failure. Since oxidation damage is not covered under warranty, DuPont Water Solutions recommends removing residual free chlorine by pretreatment prior to membrane exposure. Please refer to Dechlorinating Feedwater (Form No. 45-D01569-en) for more information.

9.2 Appendix 2. Electrodialysis anionic membrane

PRODUCT DATA SHEET
PDS-DMP/RALEX® MEMBRANE AMHPES; EN/19/10

RALEX® MEMBRANE
AMHPES

ANION-EXCHANGE MEMBRANE FOR **ELECTRODIALYSIS,**
ELECTRODEIONIZATION AND **MEMBRANE ELECTROLYSIS**.
COMES IN 3 VERSIONS: ROLLS, SHEET.

BASIC MATERIAL SPECIFICATION

Ion-exchange group	$R - (CH_3)_3N^+$	quaternary ammonium
Ionic form – counter ion	Cl^-	chloride
Basic binder on base	PE	polyethylene
Fitting fabrics	PES	polyester

MECHANICAL PROPERTIES

Thickness of dry membrane		tl_s [mm]	< 0.45
Thickness of swelled membrane		tl_z [mm]	< 0.75
Swelled differences Δ (in demi-water)	thickness	$\Delta\, tl$ [%]	< 60
	length	$\Delta\, l$ [%]	< 3
	width	$\Delta\, w$ [%]	< 4
	weight	$\Delta\, m$ [%]	< 65
Hydrodynamic permeability for water	$\Delta P = 1$ bar	[l/h.m²]	0

ELECTROCHEMICAL PROPERTIES

Resistance in 0.5 M NaCl	surface	R_A [Ω.cm²]	< 7.5
(measured under DC current)	specific	R_s [Ω.cm]	< 120
Transport number	0.5/0.1 M KCl	t^M	> 0.95
Permselectivity	0.5/0.1 M KCl	P_{STAT} [%]	> 90

OTHER PROPERTIES

Good thermal resistance:	
outside membrane stack (regeneration, sanitation)	up to 1 hour 90 °C, more than 1 hour 65 °C
inside membrane stack	under DC current 40 °C, for a short time 45 °C
Resistance against aggressive chemicals and fouling materials	
Long-term pH stability on a scale of 0 to 10, excluding oxidizing chemicals	
Possibility of a use of alkali up to pH 12 for a short time for regeneration	
High resistance against some industrial membrane poisons	
Long life cycle	

CERTIFICATES

MEGA is ISO-certified by TÜV.

Material is ROHS compliant (European Union Directive 2011/65/EU).

Material is REACH compliant (European Union Regulation No. 1907/2006).

AMHPES have Sanitary and Epidemiology Certificate for whey and drinking water.

ralex®

mega

www.mega.cz/membranes

132

PRODUCT DATA SHEET
PDS-DMP/RALEX® MEMBRANE CMHPES; EN/19/10

RALEX® MEMBRANE
CMHPES

CATION-EXCHANGE MEMBRANE FOR **ELECTRODIALYSIS, ELECTRODEIONIZATION** AND **MEMBRANE ELECTROLYSIS**. COMES IN 3 VERSIONS: ROLLS, SHEET.

BASIC MATERIAL SPECIFICATION

Ion-exchange group	$R - SO_3^-$	sulphon
Ionic form − counter ion	Na^+	sodium
Basic binder on base	PE	polyethylene
Fitting fabrics	PES	polyester

MECHANICAL PROPERTIES

Thickness of dry membrane		tl_s [mm]	< 0.45
Thickness of swelled membrane		tl_z [mm]	< 0.7
Swelled differences Δ (in demi-water)	thickness	Δtl [%]	< 65
	length	Δl [%]	< 3
	width	Δw [%]	< 4
	weight	Δm [%]	< 65
Hydrodynamic permeability for water	$\Delta P = 1$ bar	[l/h.m²]	0

ELECTROCHEMICAL PROPERTIES

Resistance in 0.5 M NaCl	surface	R_A [Ω.cm²]	< 8
(measured under DC current)	specific	R_S [Ω.cm]	< 120
Transport number	0.5/0.1 M KCl	t^M	> 0.95
Permselectivity	0.5/0.1 M KCl	P_{STAT} [%]	> 90

OTHER PROPERTIES

Good thermal resistance:

outside membrane stack (regeneration, sanitation)	up to 1 hour 90 °C, more than 1 hour 65 °C
inside membrane stack	under DC current 40 °C, for a short time 45 °C

Resistance against aggressive chemicals and fouling materials

Long-term pH stability on a scale of 0 to 10, excluding strong oxidizing chemicals

Possibility of a use of alkali up to pH 12 for a short time for regeneration

High resistance against some industrial membrane poisons

Long life cycle

CERTIFICATES

MEGA is ISO-certified by TÜV.

Material is ROHS compliant (European Union Directive 2011/65/EU).

Material is REACH compliant (European Union Regulation No. 1907/2006).

CMHPES have Sanitary and Epidemiology Certificate for whey and drinking water.

ralex®

m ga

9.4   Appendix 4. Electrodialysis module characteristics

LIST OF MODULE COMPONENTS

Table 1: List of module components

No.	EDR-Z module components	Pcs.	Material
1	EDR-Z end plate	2	PP
2	Electrode sealing	2	EPDM
3	Cathode	1	Ti / Pt
3	Anode	1	Ti / Pt
4	EDR-Z electrode spacer	2	PE
5	RALEX® EDR-Z membrane - cation exchange	11	Catex
6	EDR-Z spacer	20	PE
7	RALEX® EDR-Z membrane - anion exchange	10	Anex
8	Direct hose fitting	3	PP
9	90° hose fitting	5	PP
10	Screw φ 6-50	2	stainless steel
11	Washer φ 6,4	32	stainless steel
12	Nut M 6	16	stainless steel
13	Serrated lock washer φ 6,4	2	stainless steel
14	Tie rod φ 6-110	12	stainless steel
15	Countersink screw φ 4,8-13	2	stainless steel

TECHNICAL PARAMETERS OF COMPONENTS

Table 2: Specification of EDR-Z module end plates

Item		Value	
General size		100 × 260 × 30 mm (width, height, depth)	
Diluate piping diameter		Ø 12	
Concentrate piping diameter		Ø 12	
Electrode solution piping diameter		Ø 12	
Colour identification of ED module type solutions			
Diluate	D	Blue	
Concentrate	C	Red	
Electrode solution	E	Green	

OPERATING CHARACTERISTICS

Table 6: Unit operating limits

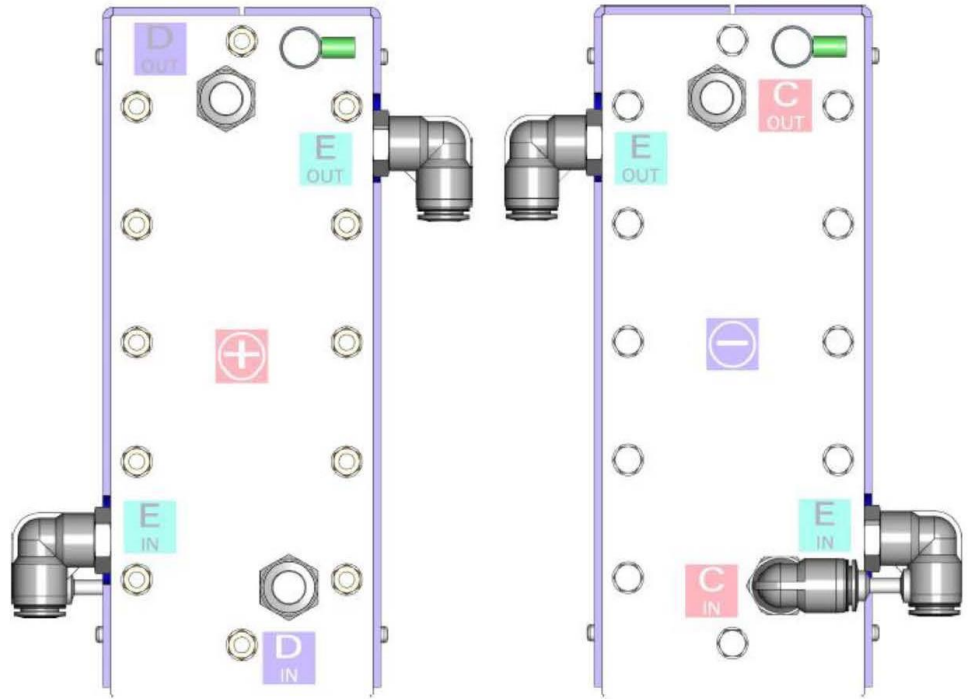| Description		Parameter
Electro U/I		Maximum 3A/30V
Operating flow rate	Diluate	45-65 L/h
	Concentrate	
	Electrode solution	50-60 L/h
Minimal flow rate	Diluate	25 L/h
	Concentrate	
	Electrode solution	20 L/h
Temperature	Operating	20-30 °C
	Minimal	10 °C
	Maximal	35 °C

Figure 2: EDR-Z end plate (in positive mode - anode),   *Figure 3: EDR-Z end plate (in positive mode - cathode)*

Table 3: EDR-Z module membrane and spacer specifications

| RALEX® EDR-Z ion-exchange membranes	Value
General size of the membrane	56 × 206 mm
Effective size of the membrane	40 × 160 mm
Effective surface of the membrane	64 cm²
Membrane channel size	Ø 6 mm
EDR-Z spacers	Value
Spacer thickness	0.8 mm for EDR-Z/2×10-0.8
Spacer size	60 × 210 mm
Channel size	Ø 6 mm
Distributor size	1 beam, width of 1.5 mm
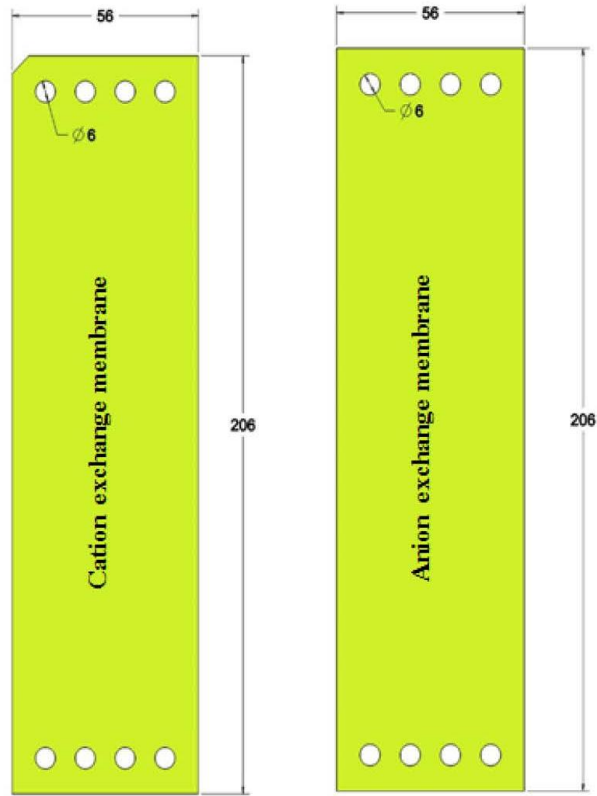
Figure 4: Cation and anion exchange membranes
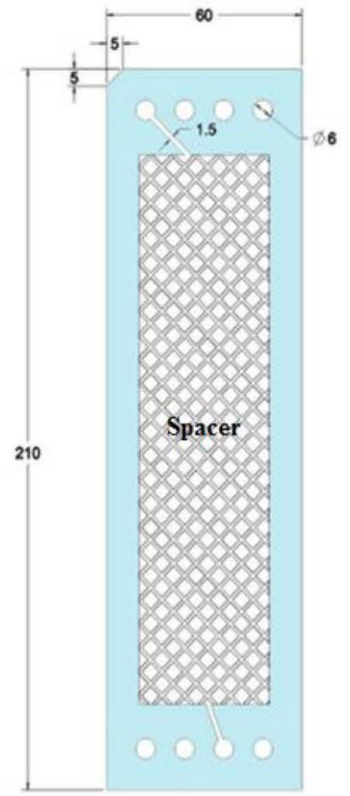
Figure 5: EDR-Z spacer

DIMENSIONS, SCHEMES, AND PICTURES – TECHNICAL PARAMETERS OF THE MODULE

Table 4: EDR-Z module specifications

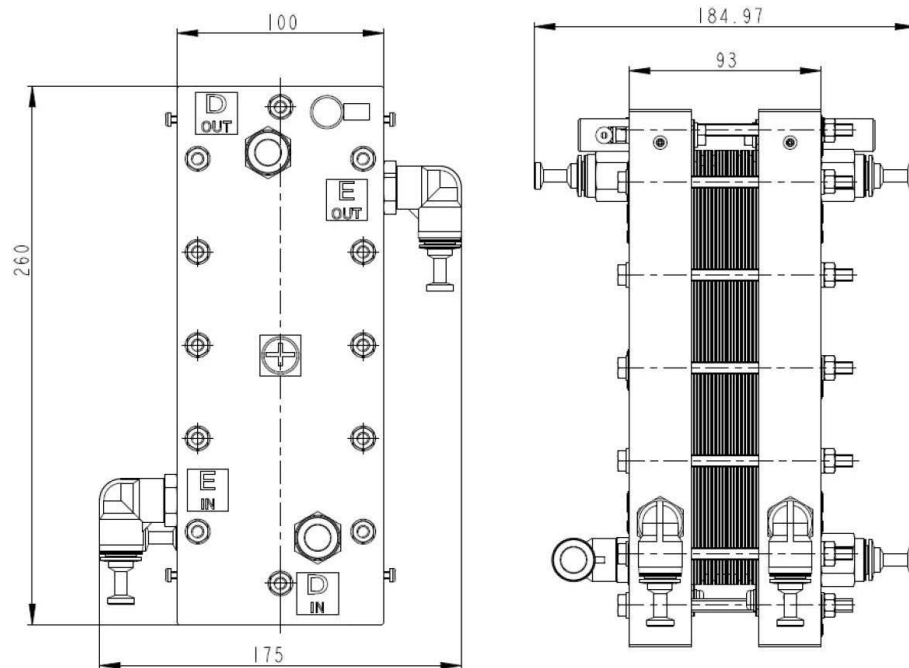| Parameter	EDR-Z/2×10-0.8
Total number of membrane pairs	10
Number of diluate chambers (D)	10
Number of concentrate chambers (C)	10
Number of electrode chambers (E)	2
Total installed surface of membranes	2646 cm²
Total effective surface of membranes	1344 cm²
Size of ED module (	144 × 260 × 175 mm

136

Figure 6: View of EDR-Z/2×10-0.8 module incl. dimensions with plugins

Table 5: EDR-Z module assembly scheme

No.	EDR-Z module components	pcs.	Comments
	EDR-Z end plate - cathode (complete)	1	
CATHODE (with EDR module in positive mode - MINUS)			
1	EDR-Z end plate	1	
2	Electrode sealing	1	
3	Electrode – cathode	1	
MEMBRANE STACK			
4	EDR-Z spacer – electrode	1	
5	RALEX® EDR-Z membrane – cation exchange	1-10	Upper left corner cut-off
6	EDR-Z spacer (diluate)	1-10	Bottom right corner cut-off
7	RALEX® EDR-Z membrane – anion exchange	1-10	
6	EDR-Z spacer (concentrate)	1-10	Bottom left corner cut-off
5	RALEX® EDR-Z membrane – cation exchange	1	Upper left corner cut-off
4	EDR-Z spacer – electrode	1	
	EDR-Z end plate – anode (complete)	1	
ANODE (with EDR module in positive mode – PLUS)			
3	Electrode – anode	1	
2	Electrode sealing	1	
1	EDR-Z end plate	1	

137

9.5 Appendix 5. Copyright license.